European Journal of Medicinal Chemistry 250 (2023) 115170

Contents lists available at ScienceDirect

European Journal of Medicinal Chemistry

journal homepage: www.elsevier.com/locate/ejmech

Research paper

Synthesis and structure-activity relationship of new nicotinamide phosphoribosyltransferase inhibitors with antitumor activity on solid and haematological cancer

Simone Fratta [a], Paulina Biniecka [b], Antonio J. Moreno-Vargas [a], Ana T. Carmona [a,**], Aimable Nahimana [b], Michel A. Duchosal [b,c], Francesco Piacente [d], Santina Bruzzone [d], Irene Caffa [e,f], Alessio Nencioni [e,f], Inmaculada Robina [a,*]

[a] Departamento de Química Orgánica, Facultad de Química, Universidad de Sevilla, Sevilla, 41012, Spain
[b] Central Laboratory of Hematology, Medical Laboratory and Pathology Department, Lausanne University Hospital, 1011, Lausanne, Switzerland
[c] Service of Hematology, Oncology Department, Lausanne University Hospital, 1011, Lausanne, Switzerland
[d] Department of Experimental Medicine, Section of Biochemistry, University of Genoa, 16132, Genoa, Italy
[e] Department of Internal Medicine and Medical Specialties, University of Genoa, 16132, Genoa, Italy
[f] IRCCS Ospedale Policlinico San Martino, 16132, Genoa, Italy

ARTICLE INFO

Keywords:
NAMPT inhibitors
Cytotoxic agents
Cancer
NAD^+
Cyanoguanidines
Furan

ABSTRACT

Cancer cells are highly dependent on Nicotinamide phosphoribosyltransferase (NAMPT) activity for proliferation, therefore NAMPT represents an interesting target for the development of anti-cancer drugs. Several compounds, such as FK866 and CHS828, were identified as potent NAMPT inhibitors with strong anti-cancer activity, although none of them reached the late stages of clinical trials. We present herein the preparation of three libraries of new inhibitors containing (pyridin-3-yl)triazole, (pyridin-3-yl)thiourea and (pyridin-3/4-yl)cyanoguanidine as cap/connecting unit and a furyl group at the tail position of the compound. Antiproliferative activity *in vitro* was evaluated on a panel of solid and haematological cancer cell lines and most of the synthesized compounds showed nanomolar or sub-nanomolar cytotoxic activity in MiaPaCa-2 (pancreatic cancer), ML2 (acute myeloid leukemia), JRKT (acute lymphobalistic leukemia), NMLW (Burkitt lymphoma), RPMI8226 (multiple myeloma) and NB4 (acute myeloid leukemia), with lower IC_{50} values than those reported for FK866. Notably, compounds **35a**, **39a** and **47** showed cytotoxic activity against ML2 with $IC_{50} = 18$, 46 and 49 pM, and IC_{50} towards MiaPaCa-2 of 0.005, 0.455 and 2.81 nM, respectively. Moreover, their role on the NAD^+ synthetic pathway was demonstrated by the NAMPT inhibition assay. Finally, the intracellular NAD^+ depletion was confirmed *in vitro* to induced ROS accumulation that cause a time-dependent mitochondrial membrane depolarization, leading to ATP loss and cell death.

1. Introduction

Nicotinamide phosphoribosyltransferase (NAMPT) is a key enzyme for the biosynthesis of nicotinamide adenine dinucleotide (NAD^+) in cells. NAD^+ is a cofactor in multiple redox reactions related to cell energy production and is used as a substrate by enzymes involved in protein chemical modifications (post-translational modifications) and modulation of intracellular Ca^{2+} homeostasis, thus regulating important functions, including metabolic pathways, DNA repair, and inflammatory responses. Due to these relevant redox and non-redox functions of NAD^+, NAMPT constitutes an attractive target in drug research [1]. Mammalian cells utilize three biosynthetic pathways to generate NAD^+. NAMPT controls the rate-limiting step of one of these pathways, the so-called salvage pathway, where nicotinamide (NAM) generates NAD^+, this being the preferred NAD^+ production route of many types of cancer (salvage-dependent tumors) [2]. In this type of cancer cells, NAMPT is typically over-expressed compared to normal tissues and helps enhancing NAD^+ synthesis. Overall, since many cancer cells are highly

* Corresponding author.
** Corresponding author.
E-mail addresses: anatere@us.es (A.T. Carmona), robina@us.es (I. Robina).

https://doi.org/10.1016/j.ejmech.2023.115170
Received 10 January 2023; Accepted 29 January 2023
Available online 31 January 2023

dependent on NAMPT activity for proliferation, NAMPT represents an interesting target for the development of anti-cancer drugs [3]. Over the last years, several compounds were identified as potent NAMPT inhibitors with strong anti-cancer activity [4]. FK866 (compound **1**, also known as APO866, Fig. 1) was the first compound that was co-crystallized in 2006 with NAMPT [5], therefore representing the most relevant reference for this class of anti-cancer drugs. Although this molecule entered phase II clinical trials in patients with advanced solid tumors, it failed due to limited antitumor activity and off-target toxicity (i.e., thrombocytopenia) [6]. Similar results in patients were obtained with Teglarinad, a prodrug of the known NAMPT inhibitor CHS828 (compound **2**, Fig. 1), that was found to induce thrombocytopenia and gastrointestinal symptoms while not achieving significant antitumor activity [7]. Besides, most NAMPT inhibitors are known to be associated with on-target hematological and retinal toxicities [8] which have limited their clinical development. Nevertheless, the inhibition of NAMPT still remains as a promising strategy for cancer therapy as it was demonstrated with compound **3** (KPT-9274), a dual inhibitor of NAMPT and of the serine/threonine-protein kinase PAK4 [9], that was successfully transited in phase I from advanced solid malignancies to acute myeloid leukemia [10]. OT-82 (compound **4**) was also identified as a new NAMPT inhibitor with marked efficacy against hematopoietic malignancies such as leukemia, lymphoma and myeloma and it is being currently evaluated in clinical studies [11].

Recently triazole-, cyanoguanidine- and urea derivatives **5**–**7** were identified as potent NAMPT inhibitors showing similar or improved anticancer activity with respect to FK866 and CHS828 [12–14].

As part of a program for the development of new NAMPT inhibitors with improved anticancer activity (the European 7th Framework Programme project PANACREAS – www.panacreas.eu), we have recently reported the preparation and biological evaluation of FK866 analogues that retain the (pyridin-3-yl)acrylamide moiety and vary the linker and tail group [15]. In the present work, we have also focused on modifications of the connecting unit and cap group. In addition to the triazolylpyridine and cyanoguanidino-pyridine cores present in inhibitors **5** and **6**, the incorporation of thiourea as connecting group has been explored. The substitution of the pyridine moiety by other aromatic ring as cap group was also considered (Fig. 2). A structure-based design was used for the preparation of the new inhibitors. The introduction of a furan moiety in the structure of the new NAMPT inhibitors could increase the polarity of the molecule and minimize retinal toxicity due to a reduced exposure in the retina, as previously reported [16]. Moreover recent publications have demonstrated that biologically relevant furan

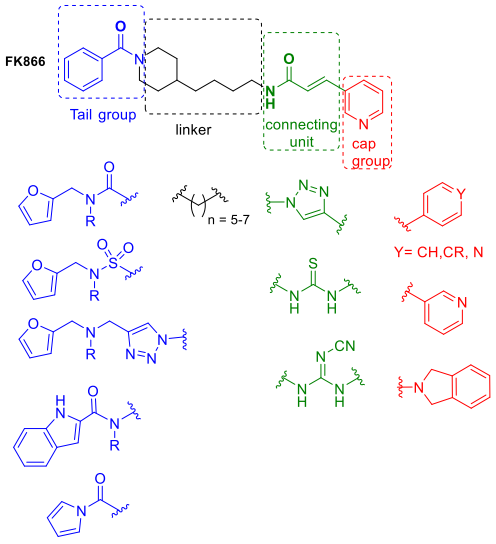

Fig. 2. Structural motifs for the new inhibitors prepared in this work.

containing cargos can be easily and selectively released in *in vivo* models in a novel strategy for target drug delivery [17,18]. As a consequence, furan has been chosen as a tail group for most of the newly prepared compounds.

2. Results and discussion

2.1. Chemistry

*Preparation of (pyridin-*3-yl*)triazole-based inhibitors*. This family of compounds (**8**–**12**, Scheme 1) is characterized by a 3-triazolylpyridine core connected to the piperidine alkyl chain of FK866 or to a flexible carbon chain. The phenyl group of FK866 was modified with different more hydrophilic heteroaromatic moieties (furan, pyrrole, indole), which could improve the water solubility of the resulting inhibitor. In this set of compounds, incorporation of the pyridine moiety into the inhibitor was carried out by copper-catalyzed alkyne azide cycloaddition (CuAAC) of commercial 3-ethynylpyridine with azide-functionalized derivatives **13**–**15** and **17**. The preparation of the target compounds is depicted in Scheme 1. The S_N2 reaction of commercial 8-

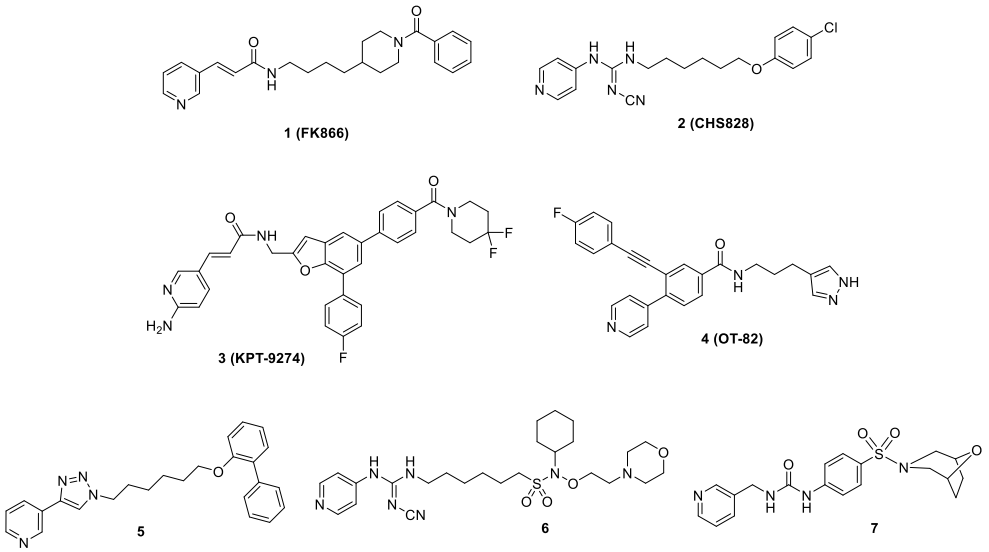

Fig. 1. Representative examples of known NAMPT inhibitors with relevant anticancer activity.

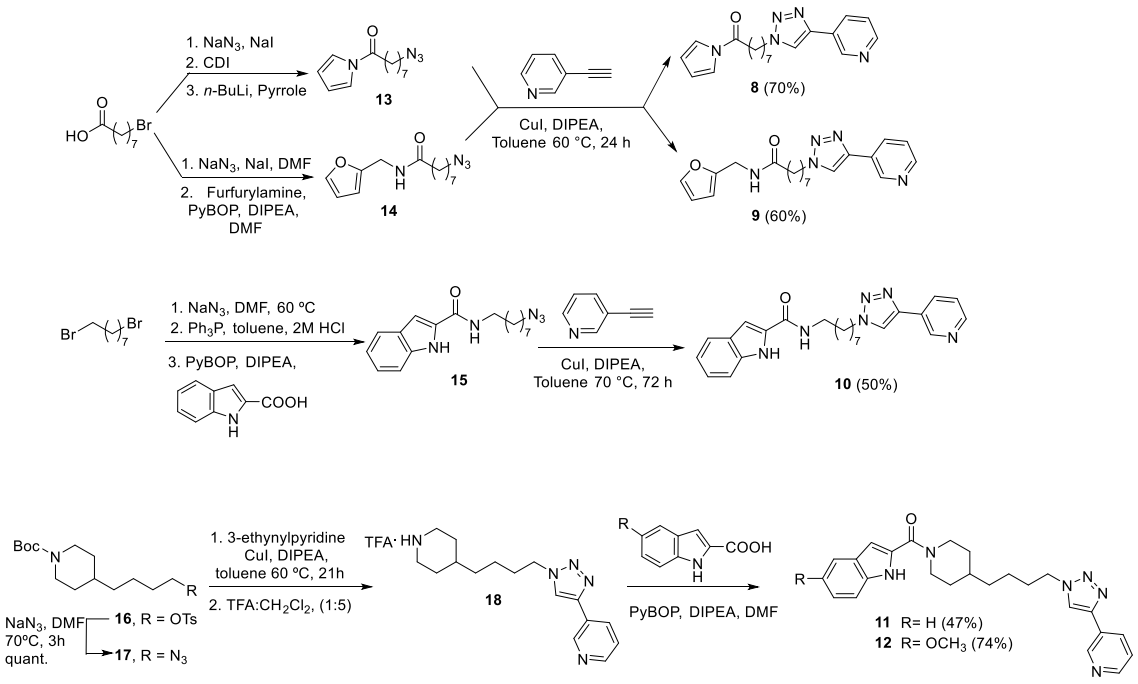

Scheme 1. Synthesis of (pyridin-3-yl)triazole-based inhibitors.

bromooctanoic acid with NaN_3, followed by coupling of the resulting intermediate with lithium pyrrolate in the presence of 1,1-carbonyldiimidazole (CDI), gave the azido-acylated pyrrole **13**. On its side, standard amide coupling of 8-azidooctanoic acid with furfurylamine afforded **14**. CuAAC reaction of azides **13** and **14** with 3-ethynylpyridine in the presence of catalytic amount of CuI and DIPEA in toluene led to

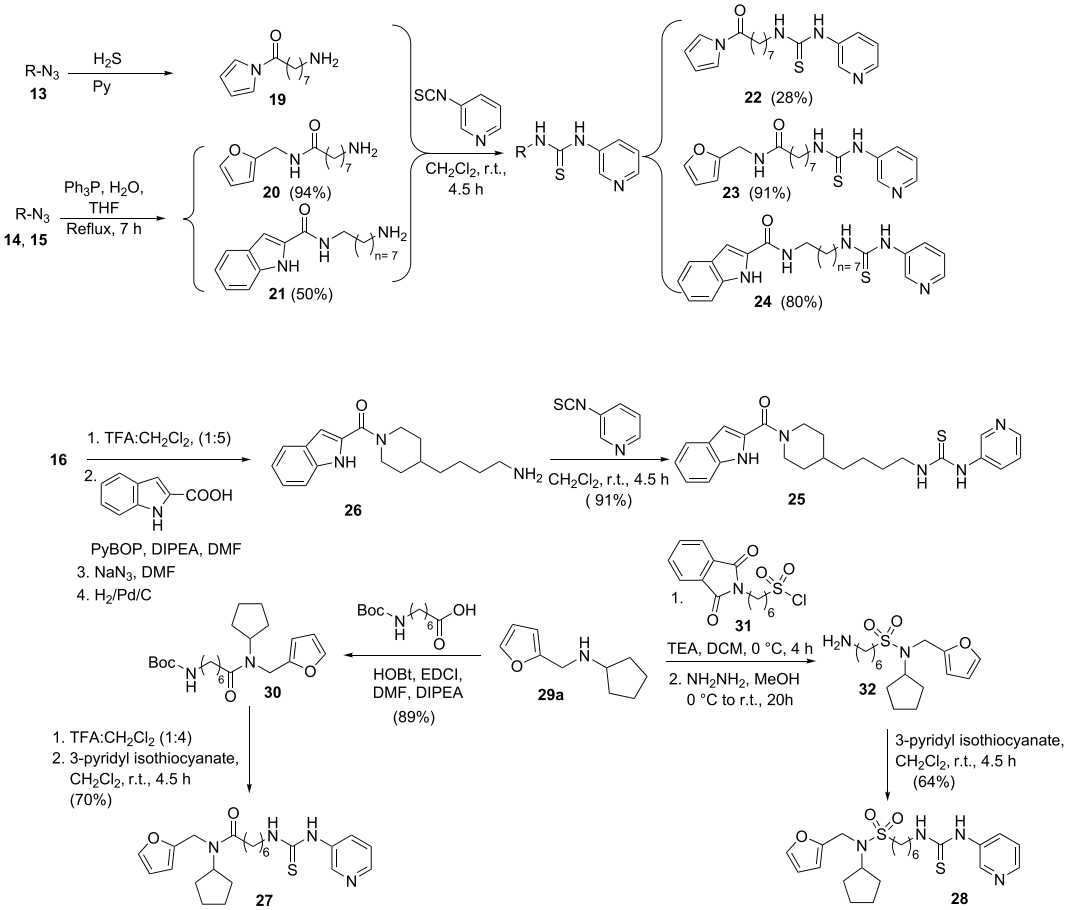

Scheme 2. Synthesis of (pyridin-3-yl)thiourea-based inhibitors.

triazoles **8** and **9** in moderate-to-good yield. On the other hand, starting from commercial 1,8-dibromooctane, S_N2 displacement with NaN_3 gave the corresponding diazido derivative. Monoreduction of one of the azido groups was feasible by the Staudinger reaction under biphasic media (toluene-aq. HCl). Standard coupling reaction of the resulting amino derivative with 1*H*-indole-2-carboxylic acid gave derivative **15**. Click reaction of **15** with 3-ethynylpyridine, as described above, gave **10** in 50% yield. The preparation of **11** and **12** was carried out from *tert*-butyl 4-(4-tosyloxybutyl)piperidine-1-carboxylate **16** [19] which was transformed into *N*-Boc-protected azide derivative **17** by displacement with NaN_3. Subsequent CuAAC click reaction with 3-ethynylpyridine, *N*-deprotection, and standard amide coupling with 1*H*-indole-2--carboxylic acid derivatives gave **11** and **12** in moderate-to good overall yield, respectively (3 steps).

Preparation of (pyridin-3-yl)thiourea-based inhibitors. The (thio)urea group is a well-established functional group in medicinal chemistry because of the ability of establishing stable hydrogen bonds with key elements of proteins and enzymes, enhancing the ligand–receptor interactions [20]. Regarding NAMPT inhibitors it has been reported the crystallographic data of the complex inhibitor-NAMPT enzyme. Thus Zheng et al. [21] studied the crystal structure of a thiourea-derived compound in complex with NAMPT and observed the interaction of Asp219 and Ser245 with the NH of the thiourea moiety through water-mediated hydrogen bonds. We envisioned that the substitution of the acrylamide group by a more powerful hydrogen-bond-donating group could enhance the interaction inhibitor/NAMPT. The preparation of these compounds is described in Scheme 2. Azido derivatives **13**, **14**, and **15** were reduced to the corresponding amino derivatives **19**–**21** through the Staudinger reaction. Subsequent coupling with commercial 3-pyridyl isothiocyanate gave thiourea analogues **22**, **23** and **24** in moderate-to-good yield. The preparation of **25** requires Boc-deprotection of **16** [16] followed by coupling with 1*H*-indole-2-carboxylic acid, displacement of the tosylate group with NaN_3 and subsequent azido reduction, affording amine **26**. Reaction of **26** with 3-pyridyl isothiocyanate gave compound **25** in excellent yield. The preparation of **27** and **28** followed a similar strategy using *N*-cyclopentylfurfurylamine **29a** as starting furan precursor. Conventional amide coupling of **29a** with *N*-Boc-7-aminoheptanoic acid followed by Boc-deprotection and reaction with 3-pyridyl isothiocyanate furnished **27** in good overall yield. The preparation of the thiourea-based inhibitor **28** involves the reaction of **29a** with (1, 3-dioxoisoindolin-2-yl)hexanesulfonyl chloride **31** [22] followed by hydrazinolysis and coupling with 3-pyridyl isothiocyanate.

Preparation of (pyridin-3/4-yl)cyanoguanidine based inhibitors. The preparation of this family of inhibitors (Scheme 3) was carried out starting from the amino-functionalized furan precursors **29a-f** (see Supporting Information for synthetic details). Reaction of **29a** and **29d** with sulfonyl chloride **31** followed by hydrazinolysis gave sulfonamides **32** and **33d**. Subsequent coupling with phenyl *N*-cyano-*N'*-(pyridin-4-yl) carbamimidate **34a**, easily prepared [23] from commercial diphenyl cyanocarbonimidate, gave compounds **35a** and **35d**, respectively in moderate-to-good yields. Similarly, deprotection of Boc derivatives **30**, **36a**, **36b**, **36d,** and **37b-e** and subsequent coupling with carbamimidate **34a** furnished derivatives **38a**, **38b**, **38d** and **39a-e** in moderate-to-good yields. Compound **40f** was obtained by reaction of **20** with **34a** under the same standard coupling conditions. Similar reaction conditions applied to indole derivatives **21** and **26** afforded indole-(pyridin-3-yl) cyanoguanidine derivatives **41** and **42**.

As this family of (pyridin-3/4-yl)cyanoguanidine-based inhibitors (compounds **35, 38–42**) showed excellent results in cytotoxicity assays (see Table 1), two new compounds were additionally prepared incorporating a triazole moiety to link the tunnel binder and the furan tail. Reaction of 1,6-dibromohexane with an excess of sodium azide gave the corresponding diazido derivative, which was further subjected to a

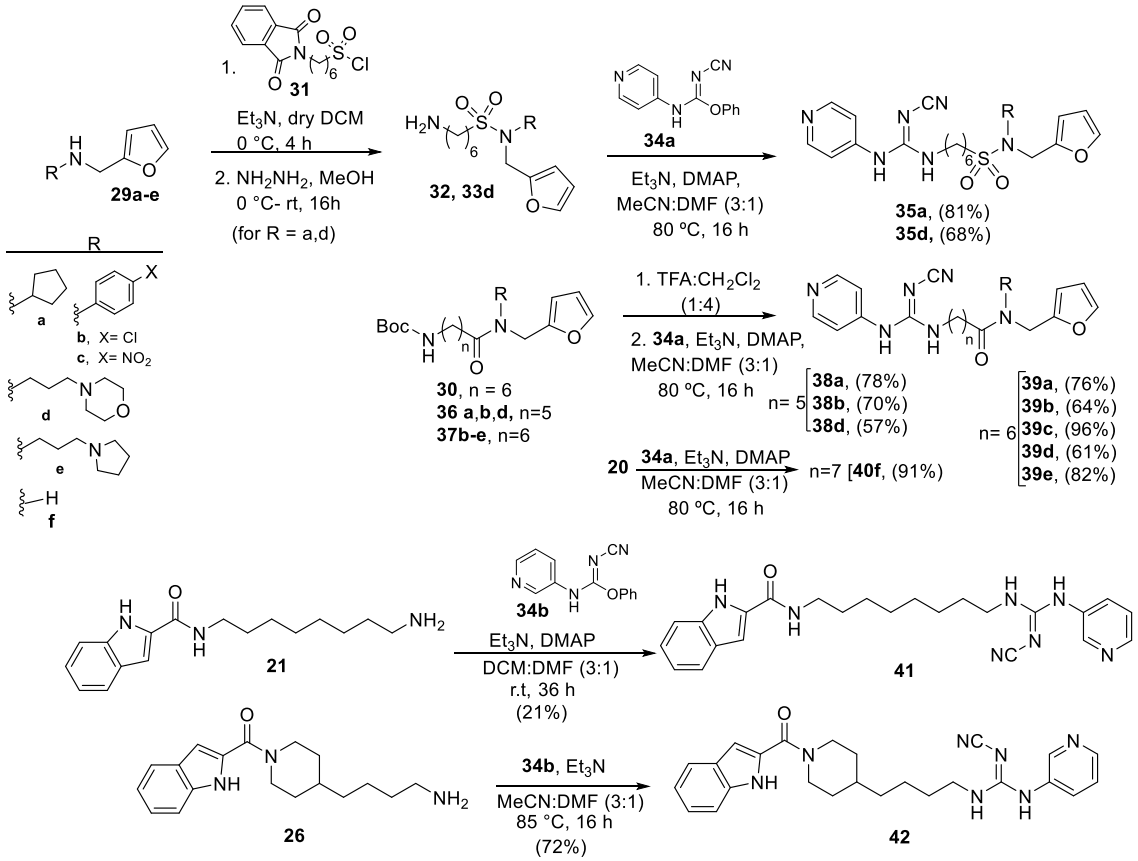

Scheme 3. Synthesis of (pyridin-3/4-yl)cyanoguanidine-based inhibitors (subfamily I).

Table 1
Evaluation of the cytotoxicity and iNAD $^{+}$ depletion on MiaPaCa-2 cells for the new compounds. NAMPT inhibition assays.

Entry	Compound	Viability MiaPaCa-2 cells (IC_{50} in nM)	iNAD^{+} depletion 24h on MiaPaCa-2 cells (IC_{50} in nM)	NAMPT inhibition assay (IC_{50} in nM)
1	**1 (FK866)**	2.4 ± 0.51	0.34 ± 0.08	3.27 ± 0.38
(pyridin-3-yl)triazoles				
2	**8**	494 ± 143	NA	NA
3	**9**	>1000	NA	NA
4	**10**	549 ± 101	NA	NA
5	**11**	727 ± 187	NA	NA
6	**12**	860 ± 191	NA	NA
(pyridin-3-yl)thioureas				
7	**22**	854 ± 188.5	NA	NA
8	**23**	>1000	NA	NA
9	**24**	605 ± 140.5	NA	NA
10	**25**	>1000	NA	NA
11	**27**	153 ± 17.4	NA	NA
12	**28**	16.4 ± 2.35	0.43 ± 0.11	69.1 ± 4.43
(pyridin-3/4-yl)cyanoguanidines				
13	**35a**	0.005 ± 0.001	0.25 ± 0.08	3.50 ± 0.77
14	**35d**	2. 26 ± 0.37	1.50 ± 0.62	NA
15	**38a**	3.0 ± 0.94	0.20 ± 0.05	NA
16	**38b**	6.3 ± 1.74	0.50 ± 0.12	NA
17	**38d**	16.3 ± 2.64	11.25 ± 0.65	NA
18	**39a**	0.45 ± 0.085	0.88 ± 0.32	12.45 ± 0.50
19	**39b**	1.7 ± 0.415	0.17 ± 0.05	NA
20	**39c**	2.1 ± 0.556	0.14 ± 0.04	NA
21	**39d**	3.0 ± 0.827	1.43 ± 0.49	NA
22	**39e**	4.5 ± 0.099	2.00 ± 0.78	NA
23	**40f**	>1000	NA	NA
24	**41**	81 ± 14.6	NA	NA
25	**42**	113 ± 14.4	NA	NA
26	**46**	25.8 ± 6.7	2.36 ± 0.75	NA
27	**47**	2.81 ± 0.761	1.48 ± 0.33	4.98 ± 0.46
Non pyridine-based inhibitors				
28	**51**	>1000	NA	NA
29	**52**	>1000	NA	NA
30	**53**	>1000	NA	NA
31	**54**	>1000	NA	NA
32	**55**	>1000	NA	NA
33	**57**	>1000	NA	NA
34	**58**	176 ± 11.7	4.70 ± 0.27	NA
35	**59**	738 ± 148	NA	NA
36	**60**	1000	NA	NA

NA = not available. Data are mean ± SD, n ≥ 3.

controlled Staudinger reduction in biphasic media that afforded the corresponding monoamino derivative. Subsequent coupling with **34a** gave azide **43** (Scheme 4) with an acceptable overall yield. CuAAC reactions of azide **43** and the furan-containing fragments **44** and **45** bearing a terminal alkyne yielded **46** and **47** in good yields.

Non pyridine-based inhibitors (non-substrate inhibitors). The pyridine moiety is present in the most potent NAMPT inhibitors reported so far, which could be explained considering that NAM is the substrate of NAMPT. The pyridine ring of FK866 is sandwiched between Tyr18 and Phe193 of the active site, making a π–π stacking interaction between the aromatic rings of two amino acids of the active site, mimicking the position of NAM. Simultaneously, pyridine nitrogen establishes a hydrogen bond with the OH group of Ser275 [24]. However, *in vitro* metabolic stability studies on previously reported pyridine-based NAMPT inhibitors have shown that pyridine nitrogen is prone to microsomal oxidation giving the corresponding *N*-oxide metabolite whose cytotoxicity is reduced with respect to the non-oxidized precursor [10]. This fact could be one of the reasons for the lack of efficacy of the inhibitors *in vivo*. Moreover, it has been recently demonstrated that phosphoribosylation of the pyridine nitrogen of NAMPT inhibitors is not required for *in vivo* antitumor efficacy [25] as it was previously postulated [26]. This evidence led to explore non pyridine-based structures as possible NAMPT inhibitors [27]. Therefore, in this paper we also report the preparation of some analogues of potent NAMPT inhibitors where the pyridine moiety has been replaced by other aromatic rings less prone to oxidation than pyridine. First, we focused on the preparation of isoindoline-based derivatives inspired by the interesting results previously obtained with NAMPT inhibitor **48** (A1293201) [21]. Thus, the reaction between commercial isoindoline and ethyl 4-isocyanobenzoate gave urea **49** (Scheme 5). Basic hydrolysis of **49** followed by standard amide coupling between the resulting acid **50** and furfurylamine afforded the furyl analogue of **48**, compound **51**. A similar strategy was followed for the preparation of **52**, except that *N*-cyclopentylfurfurylamine **29a** was used in the final coupling. Then, we turned to the substitution of pyridine by the isoindoline moiety in the subfamily I of cyanoguanidine derivatives. For this purpose, we focused on three of the most cytotoxic compounds prepared in this family (**39a**, **39b**, **39d**, Scheme 3, Table 1) and synthesized their isoindoline analogues **53**, **54** and **55**. A similar strategy to the above described in Scheme 3 was followed for the preparation of these compounds, except that phenyl *N*-cyanoisoindoline-2-carbimidate **56** (see Supporting Information for synthetic details) was used in the final coupling.

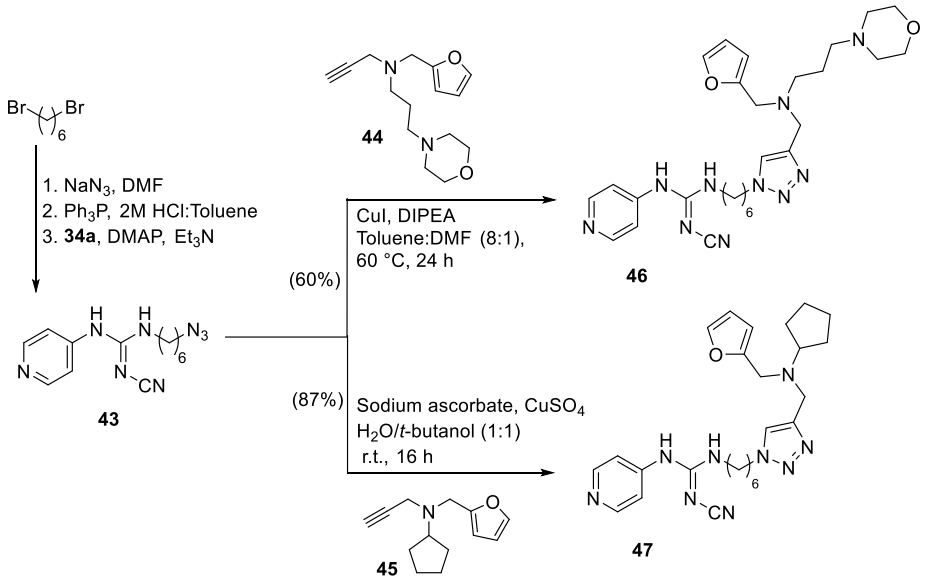

Scheme 4. Synthesis of (pyridin-4-yl)cyanoguanidine-based inhibitors (subfamily II).

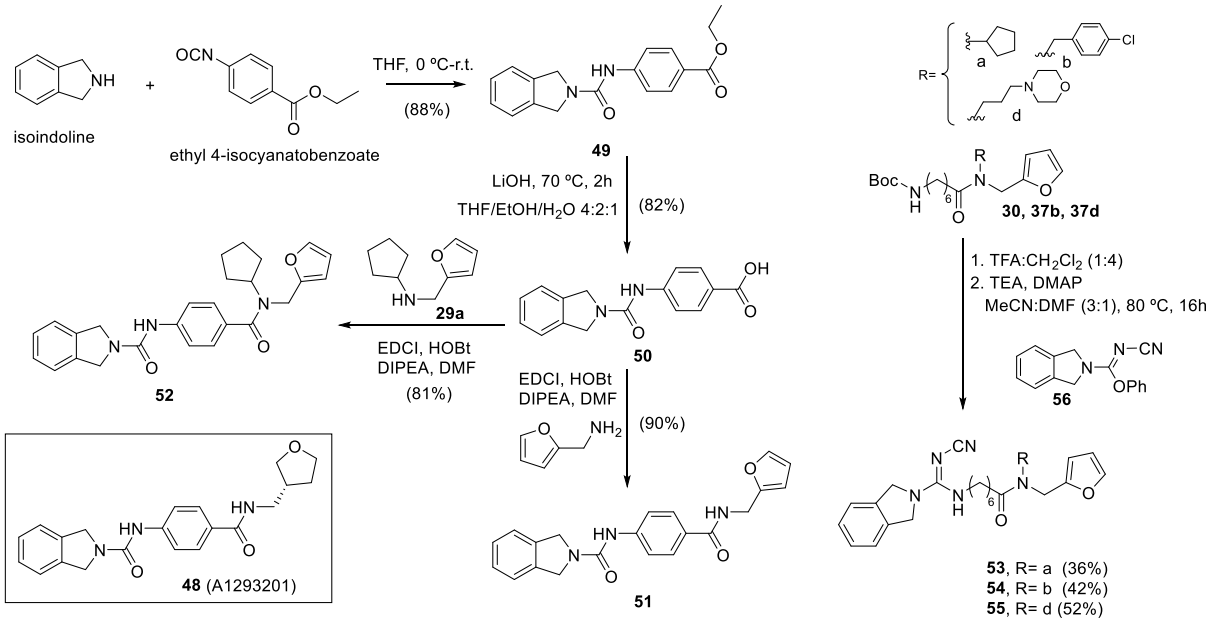

Scheme 5. Synthesis of isoindoline-based inhibitors.

Finally, we decided to replace the pyridin-4-yl moiety by a phenyl moiety in two highly cytotoxic cyanoguanidines, sulfonamide **35a** and its amide analogue **39a** (Scheme 3). For the synthesis of these new non-pyridine analogues **57**–**60** we followed a similar synthetic strategy than the one already described in Scheme 3, except that (*p*-substituted)phenyl *N*-cyano-*N*′-phenylcarbamimidates **61** instead of the pyridine analogues **34** were used in the synthesis (Scheme 6).

2.2. Biological evaluation

Cytotoxicity on MiaPaCa-2 cells, effect on intracellular NAD$^+$ concentration and NAMPT inhibition. The new compounds were tested *in vitro* for their anti-proliferative effects on a cancer cell line (Table 1). Human pancreatic MiaPaca-2 was used as model for cell lines sensitive to NAMPT inhibitors [28].

Triazoles **8**–**12** were much less cytotoxic than FK866 (Table 1, entries 2–6). FK866 analogues **11** and **12** were approximately 300-fold less cytotoxic than FK866, what indicates that the substitution of the acrylamide group by a triazole and the benzamido group by a more hydrophilic indole substituent was detrimental to biological activity. A similar modification was introduced in **25** (Scheme 2) and **42** (Scheme 3), with the exception that a thiourea and a cyanoguanidine groups were incorporated, respectively, instead of the triazole moiety of **11**.

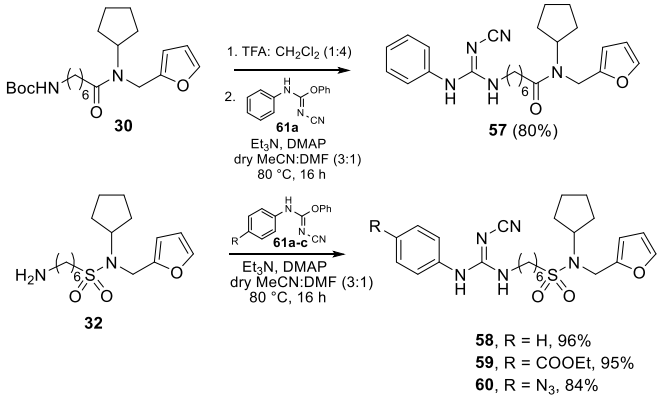

Scheme 6. Phenyl-based inhibitors prepared in this work.

Cyanoguanidine **42** (Table 1, entry 25) showed a cytotoxic effect 6.4 times greater than triazole **11** while the cytotoxicity of thiourea **25** (Table 1, entry 10) was even lower than that presented by compound **11**.

Other pyridine-3-yl thioureas were also prepared using a more flexible tunnel binder (C6 or C7 alkyl chain) to connect the thiourea and tail groups. One of the members of this family, sulfonamide **28**, showed a high cytotoxicity (IC_{50} = 16.4 nM, Table 1, entry 12). The comparison between the cytotoxicity data obtained for **28** and the amide counterpart **27** (IC_{50} = 153 nM, Table 1, entry 11) clearly showed the benefit having a sulfonamide group to connect the tail group (a furan moiety in both cases). The sulfonamide function is less prone to hydrolysis under biological conditions than the amide. Moreover, the sulfone can behave as a very good hydrogen bond acceptor for the interaction within the binding site.

The analysis of the cytotoxicity of (pyridin-3/4-yl)cyanoguanidine derivatives (**35a**, **35d**, **38a**, **38b**, **38d**, **39a-39e**, **41** and **42**) afforded several conclusions. Most cyanoguanidines (Table 1, entries 13–22) share a general structure which contains: i) a flexible alkyl C5 or C6 carbon chain as a tunnel binder connecting cyanoguanidine and tail groups through a tertiary amide/sulfonamide function and ii) a furan as a tail group. The cytotoxicity of the members of this first group (except for **41** and **42**) was excellent, with IC_{50} < 16 nM. In fact, in some cases, the IC_{50} values were lower than the one obtained with FK866 in this cell line (IC_{50} = 2.4 nM). The C5 alkyl chain was always found to lead to slightly higher IC_{50} values (less cytotoxicity) than the C6 alkyl chain in different analogues (entry 15 *vs* 18, entry 16 *vs* 19, entry 17 *vs* 21). In the series of tertiary amides, different N-substituents together with the 2-furyl group were used, but no high differences in cytotoxicity were observed, being the compounds with *N*-cyclopentyl group slightly better cytotoxic agents (entry 15 vs entries 16,17; entry 18 *vs* entries 19–22). As was already observed for the family of pyridine-3-yl thioureas, substituting the amide function in the *N*-cyclopentylamide **39a** with a *N*-cyclopentylsulfonamide led to a remarkable improvement of the cytotoxic activity (entry 18 *vs* 13), yielding the most potent compound of this study (**35a**, IC_{50} = 5 ρM). Another example where the above mentioned bioisosterism led to a compound with improved potency is represented by the non-substrate inhibitor **58** (Table 1, entry 34). Compared to the amide analogue **57** (entry 34 *vs* 33), the sulfonamide **58** showed an increase in potency of 40-fold. Amide **39e** and sulfonamide **35d** (entries 22 and 14), presented similar cytotoxicity. The NMR spectra of **35d**

showed signals corresponding to a mixture of rotamers, in contrast with the other sulfonamide derivatives where only one set of signals was observed in the ^{1}H and ^{13}C NMR spectra. Our hypothesis to explain the lower cytotoxicity of **35d** compared to other sulfonamide derivatives is that one of the rotamers could fit better than the other at the active site of NAMPT due to a more favorable binding pose, leading to a decrease in binding efficacy. In addition to amide and sulfonamide connecting groups, the triazole moiety was also explored in some of the compounds. The biological evaluation of **46** and **47** showed a decrease in their cytotoxicity compared to amides **39d** and **39a** or sulfonamides **35d** and **35a**, respectively (entry 26 *vs* entries 21,14; entry 27 *vs* entries 18 and 13).

Finally, the cytotoxicity of the series of non-pyridine-based compounds was also analyzed. Replacement of pyridine with an isoindoline group was detrimental to the antitumor activity of the compounds in all cases (entries 28–32 *vs.* entries 19–21). In addition, compounds **51** and **52**, which bear a 2-furyl moiety instead of the 2-tetrahydrofuryl group of the known analogue **48** (Scheme 5), showed cytotoxicity in the μM range (entries 28 and 29) as in the case of the other isoindoline analogues **53**–**55**. Replacement of the pyridine-4-yl moiety in the highly cytotoxic sulfonamide **35a** with a phenyl or with 4-substituted-phenyl moieties (compounds **57**–**60**) was detrimental in terms of cytotoxicity (entry 13 *vs* entries 34–36). Compound **58** was the most cytotoxic compound in this family of non pyridine-based inhibitors with an $IC_{50} = 176$ nM.

Next, we evaluated intracellular NAD^+ concentration ($iNAD^+$) in MiaPaCa-2 cells in response to the most cytotoxic compounds, in order to confirm that the observed antitumor effect was associated with NAD^+ depletion, which would be in line with these compounds being NAMPT inhibitors. Consistent with this hypothesis, all of the tested compounds reduced NAD^+ concentration in cells (Table 1). Some of the compounds **28**, **35a, 38a**, **39b**, **39a**, and **39c** reduced $iNAD^+$ to similar, or even higher extent compared to FK866. Compound **58**, a nonpyridine-based compound, reduced iNAD $^+$ when added in the nM range. Compounds **28**, **35a**, **39a** and **47**, which all effectively lowered $iNAD^+$ levels, were also assayed as NAMPT inhibitors on the recombinant enzyme. All these compounds exerted a strong inhibition of NAMPT activity ($IC_{50} < 70$ nM). Again, compound **35a** showed the highest potency, ($IC_{50} = 3.5$ nM), which was similar to the potency of the reference compound, FK866 ($IC_{50} = 3.3$ nM). Interestingly, the potency of **35a** in terms of inhibition of recombinant NAMPT did not exactly match its cytotoxic activity in MiaPaCa-2 cells, the latter being already clearly detectable in the low ρM range. For the other compounds, **28**, **39a**, and **47**, inhibiting NAMPT activity in the nM range, such a discrepancy was not observed. Therefore, these results suggest that the exceptional cytotoxic activity of **35a** may also reflect other mechanisms in addition to NAMPT inhibition in MiaPaCa-2 cells. Indeed, in MDA-MB-231 cells, the IC_{50}s obtained with **35a** for iNAD $^+$ reduction and for cell toxicity were similar (0.56 ± 0.15 and 0.47 ± 0.64 nM, respectively). By comparison, in these cells, the FK866 IC_{50}s for iNAD $^+$ depletion and cell toxicity were 0.54 ± 0.12 and 3.47 ± 0.412 nM, respectively, being similar values to those obtained in MiaPaCa-2 cells. The time-dependent decrease in NAD^+ and ATP levels in MiaPaCa-2 cells demonstrated that the high cytotoxic activity observed in the presence of **35a** is not due to a NAD^+ -unrelated intracellular ATP depletion, since NAD^+ decrease preceded the fall in ATP levels (Fig. S47 A). Cell death induced by FK866 analogues could be due to the triggering of apoptotic processes, as confirmed by the detection of PARP cleavage after 48 h of treatment with compound **47** and **35a** (Fig. S47 B).

Molecular Modeling. Docking analysis (Glide) was performed to investigate the potential role of the furan moiety of **35a** in the binding site of NAMPT (Crystal structure, PDB: 2GVJ). The binding pose of **1** (**FK866**) was mainly stabilized in the active site by a π−π stacking interaction of the pyridine ring with Phe193 and Tyr18' and H-bonding of the carbonyl group with Ser275 (Fig. 3A). On the other hand, the docked structure of compound **35a** (Fig. 3B) showed the π−π stacking interaction of the pyridine ring with Phe193, two hydrogen bonds between the cyanoguanidine moiety and Asp219 and a π-π stacking interaction of the furan tail group with Tyr188. As showed in recent publications, interactions of the tail group of NAMPT inhibitors have been reported to strongly enhance the inhibitory potency and to anchor the molecule to the enzyme [23].

Cytotoxicity on haematological cancer cells

To demonstrate the broad antitumor activity of novel compounds, a selection of the most promising ones was evaluated in cells from various haematological malignancies, including acute myeloid leukemia (AML; ML2 and NB4); acute lymphoblastic leukemia (ALL; Jurkat); Burkitt's lymphoma (BL; Namalwa) and multiple myeloma (MM; RPMI8226). As summarized in Table 2, **35a** showed the highest antitumor activity against acute myeloid leukemia (ML2), with IC_{50} in the picomolar range ($IC_{50} = 18$ ρM). Two other compounds **39a** and **47** also presented cytotoxicity in the picomolar range with IC_{50} of 46 and 49 ρM, respectively. Overall, these three molecules were the most potent and AML cells were the most sensitive cells to all tested inhibitors. Therefore, **35a**, **39a** and **47** together with FK866 as a positive control were further used to decipher their molecular mechanism of action in blood cancers.

To this end, the effect of the new NAMPT inhibitors, compounds **35a**, **39a** and **47,** on the intracellular NAD^+ content was assessed in several hematopoietic malignant cells [7c,29,30]. In agreement with data obtained on MiaPaCa-2 cells, all tested compounds led to a profound NAD^+ depletion in a time dependent manner (Fig. 4A, B, C). NAD^+ concentrations decreased by half already after 6 h and were completely depleted after 24 h. Moreover, compound **35a** was the most efficient to deplete $iNAD^+$ in haematological cancer cells, with the lowest $iNAD^+$ IC_{50} compared to FK866 (Table 3). As NAD^+ cell content plays an important role in ATP synthesis, the impact of these NAMPT inhibitors on intracellular ATP content was next evaluated. As expected, the drop in NAD^+ cell content was followed by that of ATP (Fig. 4D, E, F).

The intracellular content of $NAD(P)H/NAD(P)^+$ plays a crucial role in oxidative stress and thus, the depletion of NAD^+ upon exposure to NAMPT inhibitors is expected to result in an increased ROS production. To test this issue, mitochondrial (mO_2^-) and cytosolic (cO_2^-) superoxide anions, as well as intracellular hydrogen peroxide (H_2O_2) were

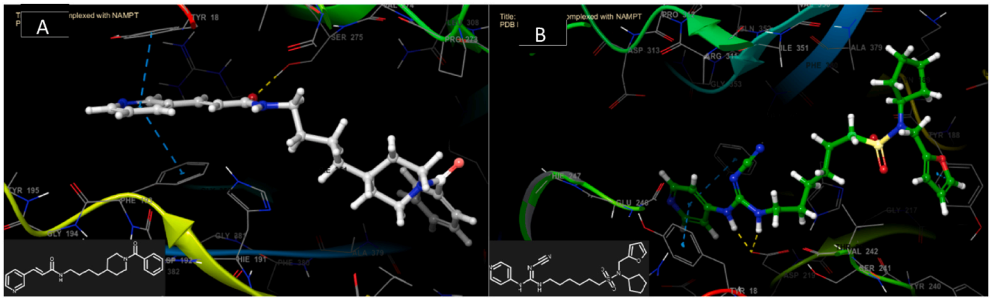

Fig. 3. Compounds **1** (FK866) (A) and **35a** (B) docked in the active site of NAMPT (Crystal structure, PDB: 2GVJ). The cyanoguanidine moiety of compound **35a** clearly forms two hydrogen bonds with Asp219 while the furan group is stabilized by a π-π stacking interaction with Tyr188.

Table 2
Evaluation of the cytotoxicity on MiaPaCa-2 and different haematological cancer cell lines for compounds **28**, **35a**, **38a**, **39a**, **39c**, **47** and **58** depicted as IC_{50} [nM].

Compound	MiaPaCa-2	ML2	JRKT	NMLW	RPMI8226	NB4
1 (FK866)	2.4 ± 0.51	0.24 ± 0.08	0.73 ± 0.04	0.37 ± 0.09	0.76 ± 0.08	2.0 ± 0.2
28	16.4 ± 2.35	3.1 ± 0.1	NA	4.23 ± 1	20.15 ± 2	NA
35a	0.005 ± 0.001	0.018 ± 0.001	0.15 ± 0.001	0.23 ± 0.08	0.16 ± 0.04	0.4 ± 0.08
38a	3.0 ± 0.94	0.36 ± 0.01	NA	1.77 ± 0.1	1.9 ± 0.1	NA
39a	0.45 ± 0.085	0.046 ± 0.01	0.2 ± 0.01	0.33 ± 0.006	0.27 ± 0.01	0.6 ± 0.03
39c	2.1 ± 0.556	0.32 ± 0.007	NA	1.39 ± 0.5	2.13 ± 0.2	NA
47	2.81 ± 0.761	0.049 ± 0.01	0.5 ± 0.01	0.36 ± 0.04	0.47 ± 0.09	0.7 ± 0.01
58	176 ± 11.7	nd	NA	nd	nd	NA

NA = not available. nd: not detected; ML2: acute myeloid leukemia; JRKT: acute lymphoblastic leukemia; NMLW: Burkitt lymphoma; RPMI8226: multiple myeloma; NB4: acute myeloid leukemia. Data are mean ± SD, n ≥ 3.

monitored in leukemic cells treated with new NAMPT inhibitors (FK866, **35a**, **39a** and **47**) using MitoSOX, DHE, and carboxy-H2DCFDA probes, respectively. The novel compounds caused a tremendous increase in ROS levels production in all treated cell types (Fig. 5A–F).

Excess ROS generation is known to lead to mitochondrial damage. Therefore, we evaluated whether these compounds could affect the mitochondrial membrane potential (MMP). Different hematopoietic malignant cells were exposed to NAMPT inhibitors and a time-dependent analysis of the MMP loss was measured using a fluorescent dye (TMRM) and flow cytometry analysis. As shown in Fig. 6A–C, treatment with the new NAMPT inhibitors induced a potent, time-dependent mitochondrial membrane depolarization at 72 h, but not at earlier time point (24-h; Fig. 6A–C). The timing of MMP loss correlates with that of cell death (Fig. 6D–F).

To provide evidence that NAD^+ depletion is the primary cause of cell death in malignant cells treated with the new NAMPT inhibitors, various hematopoietic malignant cells were incubated with inhibitors and with an excess of NAD^+ precursors (NAM, nicotinic acid [NA]) or NAD^+ itself. Cell death was monitored as described above. Indeed, supplementation with NAM, NA, or NAD^+ fully blunted the killing effect of all tested NAMPT inhibitors (Fig. 7A–C), supporting that NAD^+ depletion was responsible for cell death.

We previously reported that treatment with FK866 leads to the decrease in catalase (CAT), a powerful ROS scavenger enzyme, resulting in ROS accumulation, what ultimately leads to cell death. Therefore, we tested the ability of CAT to prevent the cell death mediated by the new NAMPT inhibitors. As shown in Fig. 8 the extracellular addition of CAT before **35a**, **39a** and **47** fully abrogated their cytotoxic effects, which is in line with our previous studies [31,32].

Altogether, these results indicate that the new NAMPT inhibitors are highly potent and promising antitumor agents. Mechanistically, these data demonstrate that, similarly to FK866, they deplete NAD^+ cell content, which induces ROS accumulation that damage mitochondria, leading to ATP loss, and ultimately to cell death. NAD^+ depletion was indeed responsible for cell death.

3. Conclusions

In summary, in this work we have prepared and evaluated several families of furan-containing NAMPT inhibitors. The compounds were designed by combining a furan-tail moiety with different structural motifs that had been successfully used in previously reported NAMPT

Table 3
Evaluation of $iNAD^+$ depletion after 24 h of drug treatment on different haematological cancer cell lines for compounds **FK866**, **35a**, and **47** depicted as IC_{50} [nM]. Data are mean ± SD, n ≥ 3.

Compound	ML2	JRKT	RPMI8226
1 (FK866)	0.11 ± 0.03	0.37 ± 0.003	0.1 ± 0.005
35a	0.05 ± 0.03	0.09 ± 0.009	0.05 ± 0.01
47	0.09 ± 0.01	0.2 ± 0.2	0.06 ± 0.04

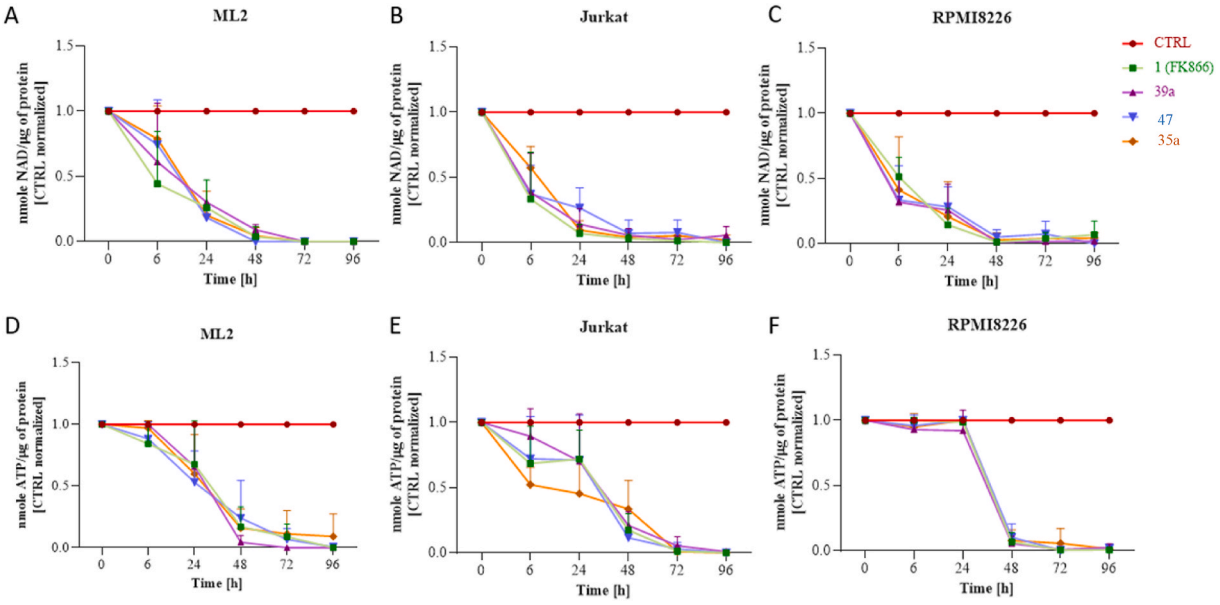

Fig. 4. NAMPT inhibitors induce the depletion of intracellular NAD^+ and ATP. ML2 (A, D), Jurkat (B, E) and RPMI8226 (C, F) cells were incubated with NAMPT inhibitors (FK866, **35a**, **39a** and **47**) for 96 h. Intracellular NAD^+ (A, B, C) and ATP (D, E, F) contents were measured every day. Both, NAD^+ and ATP concentrations were first normalized to the total protein and then to control at each time point. Data are ± SD, n = 4.

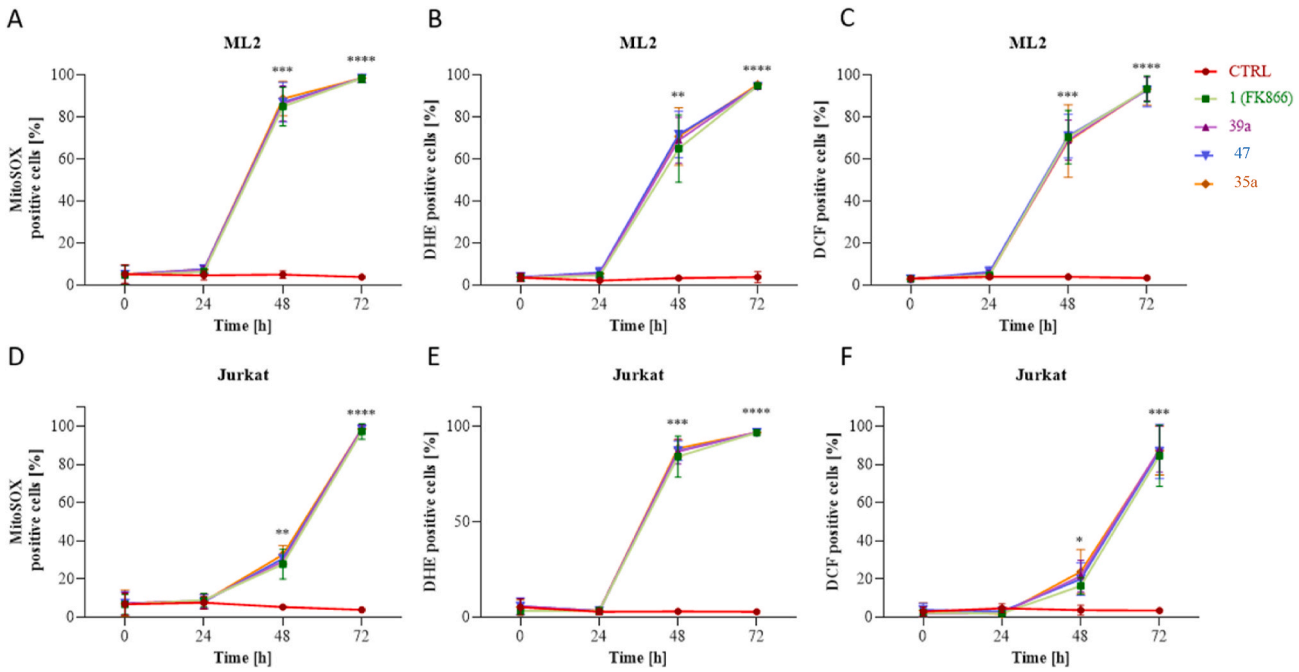

Fig. 5. NAMPT inhibitors induce ROS production upon cell death in malignant cells. ML2 (A, B, C) and Jurkat (D, E, F) cells were treated with compounds (FK866, **35a**, **39a** and **47**) for 72 h. Mitochondrial (A, D), cytosolic (B, E) superoxide anions, and hydrogen peroxide (C, F) were detected with MitoSOX, DHE and H2DCFDA probes, respectively, using flow cytometry. The percentage of positive cells is proportional to the amount of superoxide anions and hydrogen peroxide produced. Data are ± SD, n = 3, **P < 0.005, ***P < 0.001, ****P < 0.0001.

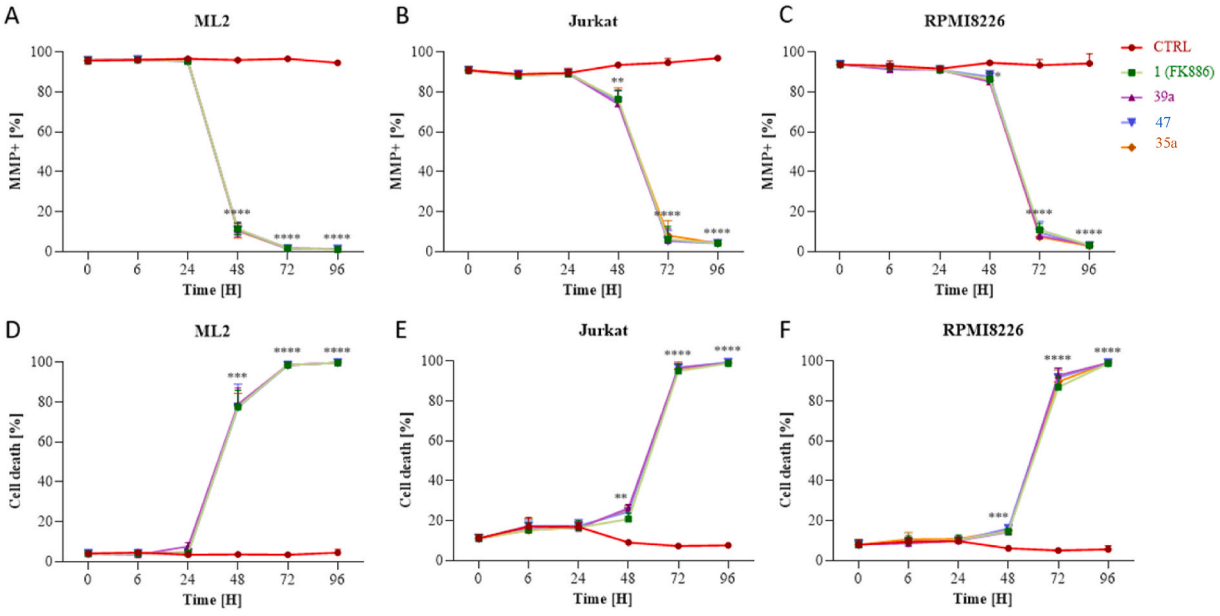

Fig. 6. NAMPT inhibitors induce the loss of MMP and cell death over time. ML2 (A, D), Jurkat (B, E) and RPMI8226 (C, F) cells were incubated with NAMPT inhibitors (FK866, **35a**, **39a** and **47**) for 96 h. MMP (A, B, C) and cell death (D, E, F) were measured every day over a period of 96 h. MMP was measured using TMRM staining, and cell death is depicted here as a total cell death consisting of annexin V (ANXN) and 7AAD stainings. Both were assessed with flow cytometry. Data are ± SD, n = 3. *P < 0.05, **P < 0.005, ***P < 0.001, ****P < 0.0001.

inhibitors. Compound **35a** was identified as the most potent NAMPT inhibitor with an IC_{50} = 3.5 nM, similar to that of FK866 (IC_{50} = 3.3 nM). However, **35a** was 500-fold more cytotoxic in the pancreatic cell line MiaPaCa-2 (IC_{50} of 5.0 ρM) than FK866 (IC_{50} of 2.4 nM), indicating that another mechanism in addition to NAMPT inhibition may be responsible for its antitumor effects. This compound was also moderately to slightly more cytotoxic than FK866 on other five different haematological cancer cell lines. Although further research is warranted and needed to elucidate the mechanism of action of these new inhibitors, **35a** can be considered as promising lead compound to develop more potent and efficient NAMPT inhibitors. The furan moiety on these compounds mimics the role of the benzamide group of FK866 while helping to anchor the molecule in the active site of NAMPT. Furthermore, the furan moiety can be used as a handle for bioconjugation strategies making these compounds amenable to linker chemistry for target drug delivery [14,15].

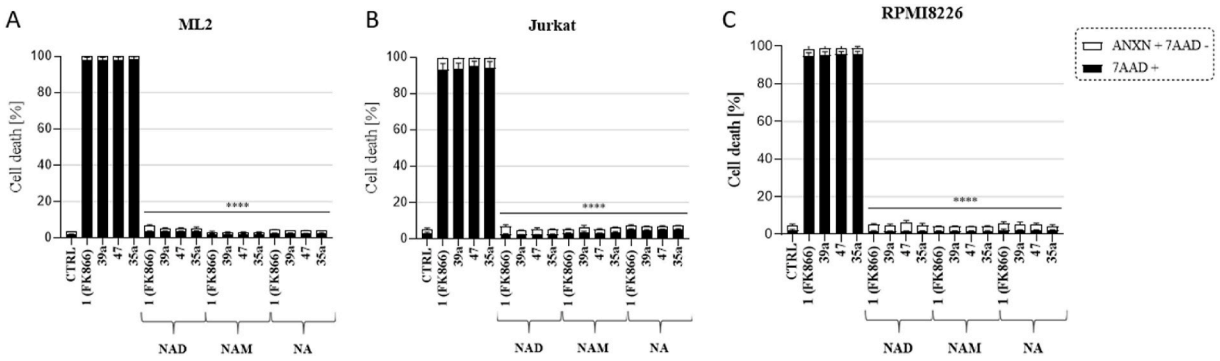

Fig. 7. The addition of NAD, NAM, and NA can reverse the cytotoxic effect of NAMPT inhibitors. ML2 (A), Jurkat (B) and RPMI8226 (C) cells were incubated for 96 h with NAMPT inhibitors (FK866, **35a**, **39a** and **47**) without or with NAD (0.5 mM), NAM (1 mM) or NA (10 μM). Cell death was assessed with flow cytometry by double staining with annexin V (ANXN) and 7AAD after 96 h of treatment. The percentages of early apoptotic cells (ANXN+ 7AAD-) are shown in white and the percentage of late apoptotic and dead cells (7AAD+) are shown in black. Data are ± SD, n = 3. ****P < 0.0001 (inhibitors treated vs. NAD, NAM, and NA groups).

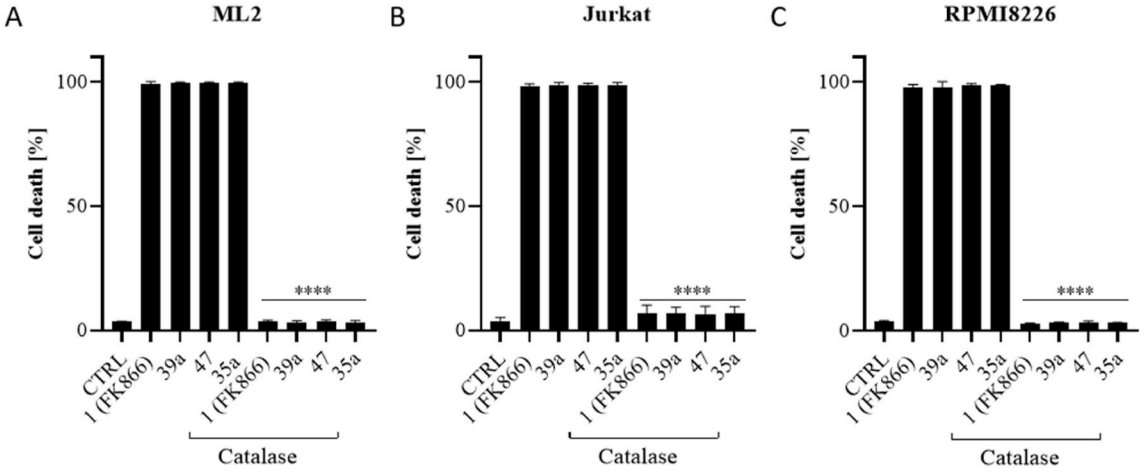

Fig. 8. Supplementation of catalase abrogates the killing effect of NAMPT inhibitors in tested cell lines. Catalase was added 1 h before the inhibitors. The cell death at 96 h was assessed on ML2 (A), Jurkat (B) and RPMI8226 (C). Cell death was determined as in Fig. 5 and is depicted here as total cell death. Data are ± SD, n = 3. ****P < 0.0001 (inhibitors treated vs. catalase treated groups).

4. Experimental section

4.1. Chemistry

General methods

^{1}H and ^{13}C NMR spectra were recorded with a Bruker AMX300 spectrometer for solutions in $CDCl_3$, DMSO-d_6, acetone-d_6 and CD_3OD. δ are given in ppm and J in Hz. Chemical shifts are calibrated using residual solvent signals. All the assignments were confirmed by 2D spectra (COSY and HSCQ). High resolution mass spectra were recorded on a Q-Exactive spectrometer. TLC was performed on silica gel 60 F_{254} (Merck), with detection by UV light charring with *p*-anisaldehyde, $KMnO_4$, ninhydrin, phosphomolybdic acid or with reagent [$(NH_4)_6MoO_4$, Ce$(SO_4)_2$, H_2SO_4, H_2O]. Purification by silica gel chromatography was carried out using either hand-packed glass columns (Silica gel 60 Merck, 40–60 and 63–200 μm) or Puriflash XS520 Plus Interchim system with prepacked cartridges. The purity of representative final compounds was assessed by HPLC and was >95%. The HPLC analysis were performed on a Thermo UltiMate 3000 instrument with Accucore C18 column (2.1 mm × 150 mm). Mobile phase consisted in solvent A (H_2O, 0.1% TFA) and solvent B (CH_3CN). The samples were eluted with a linear gradient from 70% A and 30% B to 0% A and 100% B, between 5 and 20 min. All chromatograms were registered at 254 nm wavelength.

8-Azido-1-(1H-pyrrol-1-yl*)octan-1-one (**13**)*. To a suspension of NaN_3 (1.0 g, 16 mmol) and NaI (0.1 g, 0.9 mmol) in DMF (50 mL), 8-bromooctanoic acid (2.0 g, 9.0 mmol) was added. The reaction mixture was stirred at r.t. for 16 h. Then, the reaction was cooled to 0 °C and 1 M HCl was added dropwise until the suspension became clear. The reaction mixture was extracted with EtOAc (2 × 50 mL). The organic layer was washed with brine, dried over $NaSO_4$, filtered, and concentrated in vacuo to give 8-azidooctanoic acid [33] that was used in the next step without further purification. A solution of 8-azidooctanoic acid (1.6 g, 8.4 mmol) and 1,1′-carbonyldiimidazole (1.4 g, 8.6 mmol) were dissolved in dry THF (20 mL) and the reaction was stirred under Ar at r.t. for 16 h. Pyrrole (0.7 mL, 9.5 mmol) was taken up in dry THF (5.0 mL) and the solution was cooled to −78 °C. *n*-Butyllithium (2.5 M in hexanes; 5.0 mL, 13 mmol) was added and the mixture was stirred at −78 °C for 3 h under Ar. Then, the activated compound was added quickly via syringe and the reaction was slowly warmed to r.t. and stirred overnight. A sat. aq. soln. of NH_4Cl was added and the mixture extracted with EtOAc. The organic phases were dried over $NaSO_4$, filtered, and concentrated in vacuo. Purification was performed by chromatography column on silica gel (EtOAc:Cyclohexane, 1:15) to yield **13** (800 mg, 40%) as a white solid. ^{1}H NMR (300 MHz, $CDCl_3$, δ ppm) 7.37–7.25 (m, 2H, pyrrole), 6.33–6.24 (m, 2H, pyrrole), 3.26 (t, J = 6.9 Hz, 2H, CH_2–N_3), 2.82 (t, J = 7.4 Hz, 2H, CH_2–C═O), 1.84–1.73 (m, 2H, CH_2), 1.67–1.54 (m, 2H, CH_2), 1.43–1.35 (m, 6H, 3 CH_2). ^{13}C NMR (75.4 MHz, $CDCl_3$, δ ppm) 170.6 (C═O), 119.1 (2 CH, pyrrole), 113.1 (2 CH, pyrrole), 51.5 (CH_2–N_3), 34.6 ($\underline{CH_2}$–C═O), 29.1 (CH_2), 29.0 (CH_2), 28.9 (CH_2), 26.6 (CH_2), 24.5 (CH_2). ESI-HRMS *m/z* calcd for $C_{12}H_{18}N_4ONa$ $[M+Na]^+$,

257.1373; found, 257.1373.

*8-Azido-*N*-(furan-2-ylmethyl)octanamide* ***(14)***. A solution of 8-azidooctanoic acid (1.7 g, 9.0 mmol), furfurylamine (1.2 mL, 13 mmol) and PyBOP (7.9 g, 15 mmol) in DMF (36 mL) was cooled to 0 °C. DIPEA (7.5 mL, 43 mmol) was slowly added at 0 °C, and the reaction mixture was stirred at r.t. for 16 h. The reaction mixture was dried under vacuum and diluted with EtOAc (50 mL) and washed with 1 M HCl (x3) and brine (x3), dried over Na_2SO_4, filtered, and concentrated in vacuo. The crude was purified by chromatography column on silica gel (EtOAc:Cyclohexane 1:2) to yield **14** (1.9 g, 81%) as a white solid. ^{1}H NMR (300 MHz, $CDCl_3$, δ ppm) 7.37–7.29 (m, 1H, furan), 6.30 (dd, J = 3.1, 1.9 Hz, 1H, furan), 6.20 (d, J = 3.2 Hz, 1H, furan), 5.92 (br s, 1H, NH–C═O), 4.41 (d, J = 5.3 Hz, 2H, C$\underline{H}_2$–NH), 3.23 (t, J = 6.9 Hz, 2H, CH_2–N_3), 2.17 (t, J = 7.2 Hz, 2H, CH_2–C$\underline{O}$), 1.69–1.50 (m, 4H, 2 CH_2), 1.39–1.26 (m, 6H, 3 CH_2). ^{13}C NMR (75.4 MHz, $CDCl_3$, δ ppm) 172.9 (C═O), 151.5 (qC, furan), 142.3 (CH, furan), 110.6 (CH, furan), 107.5 (CH, furan), 51.5 (CH_2–N_3), 36.6 (2C, CH_2–NH, C$\underline{H}_2$–C═O), 29.1 (CH_2), 28.9 (CH_2), 28.8 (CH_2), 26.6 (CH_2), 25.6 (CH_2). ESI-HRMS *m/z* calcd. for $C_{13}H_{20}N_4O_2Na$ $[M+Na]^+$, 287.1479; found, 287.1478.

N-*(8-Azidooctyl)-1H-indole-2-carboxamide* ***(15)***. NaN_3 (977 mg, 15.0 mmol) was added to a solution of 1,8-dibromooctane (1.0 mL, 5.4 mmol) in DMF (25 mL) and the mixture was stirred at 60 °C for 10 h. Then, water was added (125 mL) and the product was extracted with Et_2O (3 × 20 mL). The organic phase was washed with water (3 × 20 mL), dried, filtered and the solvent was evaporated to afford 1,8-diazidooctane. To a solution of this compound (930 mg, 4.70 mmol) in toluene:HCl 2 M (1:1, 80 mL), Ph_3P (1.24 g, 4.74 mmol) was slowly added, and the mixture was vigorously stirred at r.t. for 16 h. The aqueous phase was separated and washed three times with Et_2O and dried under vacuum to obtain 8-azidooctan-1-amine hydrochloride [34]. A solution of this compound (720 mg, 3.50 mmol), 1H-indole-2-carboxylic acid (842 mg, 5.20 mmol) and PyBOP (3.1 g, 5.9 mmol) in DMF (16 mL) was cooled to 0 °C. DIPEA (2.9 mL, 17 mmol) was slowly added at 0 °C, and the reaction mixture was stirred at r.t. overnight. The reaction mixture was diluted with EtOAc (160 mL) and washed with 1 M HCl (x3) and brine (x3), dried over Na_2SO_4, filtered, and concentrated in vacuo. The crude was purified by chromatography column on silica gel (EtOAc:Toluene 1:9) to yield **15** (860 mg, 80%) as a white solid. ^{1}H NMR (300 MHz, $CDCl_3$, δ ppm) 10.00 (s, 1H, NH indole), 7.64 (d, J = 8.0 Hz, 1H, indole), 7.45 (t, J = 7.0 Hz, 1H, indole), 7.32–7.23 (m, 1H, indole), 7.13 (t, J = 7.2 Hz, 1H, indole), 6.85 (d, J = 1.4 Hz, 1H, indole), 6.36 (s, 1H, NH–C═O), 3.57–3.45 (m, 2H, CH_2–N_3), 3.24 (t, J = 6.9 Hz, 2H, C$\underline{H}_2$–NH), 1.77–1.49 (m, 4H, 2 CH_2), 1.46–1.25 (m, 8H, 4 CH_2). ^{13}C NMR (75.4 MHz, $CDCl_3$, δ ppm) 162.0 (C═O), 136.6 (qC, indole), 130.9 (qC, indole), 127.7 (qC, indole), 124.5 (CH, indole), 121.9 (CH, indole), 120.7 (CH, indole), 112.2 (CH, indole), 101.9 (CH, indole), 51.5 (CH_2–N_3), 39.9 (CH_2–NH), 29.9 (CH_2), 29.3 (CH_2), 29.1 (CH_2), 28.9 (CH_2), 27.0 (CH_2), 27.7 (CH_2). ESI-HRMS *m/z* calcd for $C_{17}H_{23}N_5ONa$ $[M+Na]^+$, 336.1793; found, 336.1795.

*8-(4-(Pyridin-*3*-yl)-1H-1,2,3-triazol-*1*-yl)-1-(1H-pyrrol-*1*-yl)octan-1-one* ***(8)***. To a solution of **13** (50.0 mg, 0.21 mmol) in toluene (3 mL), 3-ethynylpyridine (45.0 mg, 0.43 mmol), DIPEA (0.14 mL, 0.81 mmol) and CuI (8.0 mg, 40 μmol) were added, and the solution was stirred at 60 °C for 24 h. Quadrasil® resin (150 mg) was added and the mixture stirred for 1 h at r.t. Then, it was filtrated through a Celite pad, and the solvent evaporated. The resulting residue was dissolved in EtOAc and a sat. aq. soln. of $NaHCO_3$ was added. The aq. phase was extracted with EtOAc (x2) and the organic layers were dried over Na_2SO_4, filtered and evaporated. The resulting residue was purified by chromatography column on silica gel (EtOAc:Cyclohexane, 7:1) to obtain **8** (50 mg, 70%) as a white solid. ^{1}H NMR (300 MHz, $CDCl_3$, δ ppm) 9.00 (br s, 1H, Py), 8.56 (br s, 1H, Py), 8.25–8.14 (m, 1H, Py), 7.84 (s, 1H, triazole), 7.41–7.32 (m, 1H, Py), 7.31–7.25 (m, 2H, pyrrole), 6.32–6.22 (m, 2H, pyrrole), 4.41 (t, J = 7.2 Hz, 2H, C$\underline{H}_2$-triazole), 2.80 (t, J = 7.3 Hz, 2H, CH_2–C═O), 2.03–1.90 (m, 2H, CH_2), 1.83–1.69 (m, 2H, CH_2), 1.44–1.34 (m, 6H, 3 CH_2). ^{13}C NMR (75.4 MHz, $CDCl_3$, δ ppm) 170.5 (C═O), 149.2 (qC, Py), 147.1 (CH, Py), 144.8 (qC, triazole), 133.1 (CH, Py), 127.0 (CH, Py), 123.9 (2CH, pyrrole), 119.9 (CH, Py), 119.1 (CH, triazole), 113.2 (2CH, pyrrole), 50.6 (CH_2-triazole), 34.5 (C$\underline{H}_2$–C═O), 30.3 (CH_2), 28.9 (CH_2), 28.8 (CH_2), 26.4 (CH_2), 24.4 (CH_2). ESI-HRMS *m/z* calcd for $C_{19}H_{24}N_5O$ $[M+H]^+$, 338.1975; found, 338.1975.

N-*(Furan-2-ylmethyl)-8-(4-(pyridin-*3*-yl)-1H-1,2,3-triazol-*1*-yl)octanamide* ***(9)***. CuAAC reaction of **14** (50.0 mg, 0.21 mmol) and 3-ethynylpyridine (40.0 mg, 0.4 mmol) followed the same procedure as that used to prepare **8**. Chromatography column (MeOH:EtOAc:CH_2Cl_2, 0.4:5:1). Yield: 60%, white solid. ^{1}H NMR (500 MHz, $CDCl_3$, δ ppm) 8.99 (s, 1H, Py), 8.57 (d, J = 3.6 Hz, 1H, Py), 8.21 (dd, J = 6.1, 1.8 Hz, 1H, Py), 7.84 (s, 1H, triazole), 7.41–7.29 (m, 2H, 1H Py, 1H furan), 6.35–6.26 (m, 1H, furan), 6.21 (d, J = 2.9 Hz, 1H, furan), 5.79 (s, 1H, NH), 4.47–4.36 (m, 4H, C$\underline{H}_2$–NH, C$\underline{H}_2$-triazole), 2.24–2.11 (m, 2H, C$\underline{H}_2$–C═O), 2.01–1.89 (m, 2H, CH_2), 1.68–1.57 (m, 2H, CH_2), 1.43–1.28 (m, 6H, 3 CH_2). ^{13}C NMR (125.7 MHz, $CDCl_3$, δ ppm) 172.7 (C═O), 151.6 (qC, furan), 149.3 (CH, Py), 147.2 (CH, Py), 144.9 (qC, triazole), 142.3 (CH, furan), 133.2 (CH, Py), 127.0 (qC, Py), 123.9 (CH, Py), 119.9 (CH, triazole), 110.6 (CH, furan), 107.5 (CH, furan), 50.6 (CH_2–NH), 36.6 (C$\underline{H}_2$-triazole), 36.5 (C$\underline{H}_2$–C═O), 30.3 (CH_2), 28.9 (CH_2), 28.6 (CH_2), 26.3 (CH_2), 25.4 (CH_2). ESI-HRMS *m/z* calcd for $C_{20}H_{26}N_5O_2$ $[M+H]^+$, 368.2076; found, 368.2081.

N-*(8-(4-(Pyridin-*3*-yl)-1H-1,2,3-triazol-*1*-yl)octyl)-1H-indole-2-carboxamide* ***(10)***. CuAAC reaction of **15** (50.0 mg, 0.16 mmol) and 3-ethynylpyridine (50.0 mg, 0.48 mmol) in toluene:DMF 3:1) followed the same procedure as that used to prepare **8**. Chromatography column (MeOH:EtOAc:CH_2Cl_2, 1:5:1). Yield: 50%, white solid.^{1}H NMR (300 MHz, DMSO-d_6, δ ppm) 11.51 (s, 1H, NH indole), 9.05 (d, J = 1.5 Hz, 1H, Py), 8.70 (s, 1H, triazole), 8.53 (dd, J = 4.8, 1.5 Hz, 1H, Py), 8.45–8.38 (m, 1H, N$\underline{H}$–C═O), 8.24–8.16 (m, 1H, Py), 7.62–7.56 (m, 1H, Py), 7.48 (dd, J = 8.0, 4.8 Hz, 1H, indole), 7.42 (d, J = 8.2 Hz, 1H, indole), 7.20–7.12 (m, 1H, indole), 7.09 (d, J = 1.4 Hz, 1H, indole), 7.06–6.98 (m, 1H, indole), 4.40 (t, J = 7.1 Hz, 2H, C$\underline{H}_2$-triazole), 3.26 (q, J = 6.7 Hz, 2H, C$\underline{H}_2$–NH), 1.94–1.80 (m, 2H, CH_2), 1.60–1.46 (m, 2H, CH_2), 1.34–1.26 (m, 8H, 4 CH_2). ^{13}C NMR (75.4 MHz, DMSO-d_6, δ ppm) 160.9 (C═O), 148.7 (CH, Py), 146.3 (CH, Py), 143.4 (qC, triazole), 136.3 (qC, indole), 132.4 (qC, Py), 131.9 (qC, indole), 127.1 (CH, Py), 126.8 (qC, indole), 124.0 (CH, indole), 123.1 (CH, Py), 121.9 (CH, triazole), 121.4 (CH, indole), 119.6 (CH, indole), 112.2 (CH, indole), 102.1 (CH, indole), 49.6 (CH_2-triazole), 39.0 (CH_2–NH), 29.6 (CH_2), 29.2 (CH_2), 28.6 (CH_2), 28.4 (CH_2), 26.4 (CH_2), 25.8 (CH_2). ESI-HRMS *m/z* calcd for $C_{24}H_{29}N_6O$ $[M+H]^+$, 417.2392; found, 417.2397.

*3-(1-(4-(Piperidin-*4*-yl)butyl)-1H-1,2,3-triazol-*4*-yl)pyridine 2,2,2-trifluoroacetate* ***(18)***. Compound **16** [16] (636 mg, 1.60 mmol) was dissolved in DMF (10 mL), NaN_3 (302 mg, 4.60 mmol) was added. The mixture was stirred at 70 °C for 3 h and then was evaporated under vacuum and the residue dissolved in CH_2Cl_2. The organic layer was washed with water and brine, dried over $NaSO_4$, filtered, and concentrated in vacuo to give **17** as a colourless oil. CuAAC reaction of **17** (192 mg, 0.68 mmol) and 3-ethynylpyridine (175 mg, 1.70 mmol) followed the same procedure as that described for **8**. Chromatography column (CH_2Cl_2:Acetone: 1:0 to 5:1). Yield: 88%, white solid. This compound was dissolved in 20% TFA/CH_2Cl_2 (5 mL) at 0 °C and the mixture was stirred at r.t. for 3.5 h. The solvent was evaporated in vacuo and the solvent was co-evaporated with toluene to yield **18** as a white solid that was used in the next step without further purification.

*(1H-Indol-*2*-yl)(4-(4-(4-(pyridin-*3*-yl)-1H-1,2,3-triazol-*1*-yl)butyl) piperidin-*1*-yl)methanone* ***(11)***. A solution of **18** (112.0 mg, 0.28 mmol), 1H-Indole-2-carboxylic acid (68.0 mg, 0.42 mmol) and PyBOP (248 mg, 0.48 mmol) in dry DMF (2.5 mL) was cooled to 0 °C. DIPEA (0.24 mL, 1.35 mmol) was slowly added at 0 °C, and the reaction mixture was stirred at r.t. for 16 h. The solvent was evaporated under reduced pressure and the crude was diluted with EtOAc (20 mL) and washed with sat. aq. soln. of NH_4Cl (x3), dried over Na_2SO_4, filtered and concentrated. The residue was purified by chromatography column on silica gel (MeOH:EtOAc, 1:20 → 1:10) to yield **11** (56 mg, 47%) as a white solid.

^{1}H NMR (300 MHz, DMSO-d_6, δ ppm) 11.51 (s, 1H, NH indole), 9.11–8.99 (m, 1H, Py), 8.72 (s, 1H, triazole), 8.54 (dd, J = 4.8, 1.5 Hz, 1H, Py), 8.21 (dt, J = 7.9, 1.9 Hz, 1H, Py), 7.59 (d, J = 7.9 Hz, 1H, indole), 7.52–7.44 (m, 1H, Py), 7.40 (d, J = 7.9 Hz, 1H, indole), 7.23–7.10 (m, 1H, indole), 7.09–6.98 (m, 1H, indole), 6.75–6.67 (m, 1H, indole), 4.53–4.31 (m, 4H, C$\underline{H}_2$-triazole, 2H piperidine), 2.96 (br s, 2H, piperidine), 1.96–1.81 (m, 2H, piperidine), 1.78–1.66 (m, 2H, piperidine), 1.62–1.44 (m, 1H, piperidine), 1.39–1.19 (m, 4H, 2 CH_2), 1.18–1.00 (m, 2H, CH_2). ^{13}C NMR (75.4 MHz, DMSO-d_6, δ ppm) 161.8, 148.8, 146.3, 143.5, 135.8, 132.3, 130.3, 126.8, 124.0, 123.0, 122.0, 121.2, 119.6, 112.0, 103.4, 49.6, 35.4, 35.3, 32.2, 32.1, 27.7, 22.1. ESI-HRMS m/z calcd for $C_{25}H_{29}N_6O$ $[M+H]^+$, 429.2391; found, 429.2397.

*(5-Methoxy-1H-indol-*2-yl*)(4-(4-(4-(pyridin-*3-yl*)-1H-1,2,3-triazol-*1-yl*)butyl)piperidin-*1-yl*)methanone **(12)***. Reaction of **18** (112.0 mg, 0.28 mmol) and 5-methoxy-1H-indole-2-carboxylic acid (80.0 mg, 0.42 mmol) was performed according to the same procedure as that used to prepare **11**. Chromatography column (MeOH:EtOAc, 1:20 → 1:10). Yield: 74%, white solid.^{1}H NMR (300 MHz, DMSO-d_6, δ ppm) 11.37 (s, 1H, NH, indole), 9.06 (d, J = 1.7 Hz, 1H, Py), 8.72 (s, 1H, triazole), 8.58–8.50 (m, 1H, Py), 8.28–8.15 (m, 1H, Py), 7.55–7.41 (m, 1H, Py), 7.29 (d, J = 8.9 Hz, 1H, indole), 7.06 (d, J = 2.3 Hz, 1H, indole), 6.82 (dd, J = 8.9, 2.4 Hz, 1H, indole), 6.63 (d, J = 1.6 Hz, 1H, indole), 4.54–4.29 (m, 4H, C$\underline{H}_2$-triazole, 2H piperidine), 3.74 (s, 3H, OCH_3), 2.96 (br s, 2H, piperidine), 1.96–1.81 (m, 2H, piperidine), 1.79–1.64 (m, 2H, piperidine), 1.63–1.44 (m, 1H, piperidine), 1.40–1.20 (m, 4H, CH_2), 1.19–0.98 (m, 2H, CH_2). ^{13}C NMR (75.4 MHz, DMSO-d_6, δ ppm) 161.8, 153.7, 148.8, 146.3, 143.5, 132.3, 131.1, 130.7, 127.1, 126.8, 124.0, 122.0, 114.0, 112.8, 103.2, 101.9, 55.2, 49.6, 35.2, 35.1, 32.1, 29.7, 22.1. ESI-HRMS m/z calcd for $C_{26}H_{31}N_6O_2$ $[M+H]^+$, 459.2495; found, 459.2503.

*1-(8-Oxo-8-(1H-pyrrol-*1-yl*)octyl)-3-(pyridin-*3-yl*)thiourea **(22)***. To a solution of **13** (0.50 g, 2.1 mmol) in pyridine (15 mL), H_2S was bubbled. After stirring at r.t. overnight the mixture was evaporated under vacuum. The crude product **19** was used directly in the next step without any further purification. ESI-HRMS m/z calcd for $C_{12}H_{21}N_2O$ $[M+H]^+$, 209.1647; found, 209.1648. To a solution of **19** (60.0 mg, 0.3 mmol) in dry CH_2Cl_2 (5 mL), 3-pyridyl isothiocyanate (40 μL, 0.4 mmol) was added. After stirring at r.t. for 6 h, the solvent was removed under vacuo and the resulting residue was purified by chromatography column on silica gel (EtOAc:Cyclohexane 4:1) to give **22** (25.0 mg, 28%) as a white solid. ^{1}H NMR (300 MHz, $CDCl_3$, δ ppm) 8.54 (d, J = 2.0 Hz, 1H, Py), 8.44 (d, J = 3.9 Hz, 1H, Py), 8.32 (br s, 1H, N$\underline{H}$-Py), 7.85 (d, J = 7.9 Hz, 1H, Py), 7.37 (dd, J = 8.1, 4.8 Hz, 1H, Py), 7.29 (br s, 2H, pyrrole), 6.44–6.31 (m, 1H, N$\underline{H}$–CH_2), 6.31–6.24 (m, 2H, pyrrole), 3.60 (q, J = 6.4 Hz, 2H, C$\underline{H}_2$–NH), 2.81 (t, J = 7.3 Hz, 2H, CH_2–C═O), 1.82–1.68 (m, 2H, CH_2), 1.68–1.52 (m, 2H, CH_2), 1.44–1.30 (m, 6H, 3 CH_2). ^{13}C NMR (75.4 MHz, $CDCl_3$, δ ppm) 181.3 (C═S), 170.8 (C═O), 147.4 (qC, Py), 146.1 (CH, Py), 134.2 (CH, Py) 132.6 (CH, Py), 124.3 (CH, Py), 119.1 (2CH, pyrrole), 113.2 (2CH, pyrrole), 45.5 (CH_2–NH), 35.5 (C$\underline{H}_2$–C═O), 29.8 (CH_2), 29.0 (CH_2), 28.8 (CH_2), 26.6 (CH_2), 24.4 (CH_2). ESI-HRMS m/z calcd for $C_{18}H_{25}N_4OS$ $[M+H]^+$, 345.1737; found, 345.1744.

N-*(Furan-2-ylmethyl)-8-(3-(pyridin-*3-yl*)thioureido)octanamide **(23)***. To a solution of **14** (100 mg, 0.38 mmol) in THF (1 mL), H_2O (40 μL) and Ph_3P (150 mg, 0.60 mmol) were added. The reaction mixture was stirred on reflux for 7 h. The resulting residue was evaporated under vacuum and purified by chromatography column on silica gel (MeOH: CH_2Cl_2: NH_4OH, 1:10:0.1) to yield **20** (85 mg, 94%) as a white solid. Reaction of **20** (70.0 mg, 0.3 mmol) and 3-pyridyl isothiocyanate (80 μL, 0.8 mmol) was performed according to the same procedure as that used to prepare **22**. Chromatography column (MeOH:EtOAc:CH_2Cl_2, 0.4:5:1). Yield: 91%, white solid. ^{1}H NMR (300 MHz, CD_3OD, δ ppm) 8.57 (dd, J = 2.5, 0.6 Hz, 1H, Py), 8.28 (dd, J = 4.8, 1.3 Hz, 1H, Py), 8.10–7.89 (m, 1H, Py), 7.44–7.36 (m, 2H, 1H Py, 1H, furan), 6.33 (dd, J = 3.2, 1.9 Hz, 1H, furan), 6.22 (dd, J = 3.2, 0.7 Hz, 1H, furan), 4.34 (s, 2H, C$\underline{H}_2$–NH), 3.68–3.44 (m, 2H, C$\underline{H}_2$-thiourea), 2.21 (t, J = 7.4 Hz, 2H, CH_2–C═O), 1.71–1.54 (m, 4H, 2 CH_2), 1.44–1.29 (m, 6H, 3 CH_2). ^{13}C NMR (75.4 MHz, CD_3OD, δ ppm) 183.1 (C═S), 176.1 (C═O), 153.2 (qC, furan), 145.8 (2CH, Py), 143.3 (CH, furan), 138.3 (qC, Py), 133.3 (CH, Py), 124.9 (CH, Py), 111.3 (CH, furan), 108.0 (CH, furan), 45.6 (CH_2-thiourea), 37.1 (CH_2–NH), 36.9 (C$\underline{H}_2$–C═O), 30.04 (CH_2), 30.02 (CH_2), 27.8 (CH_2), 26.8 (CH_2), 25.7 (CH_2). ESI-HRMS m/z calcd for $C_{19}H_{27}N_4O_2S$ $[M+H]^+$, 375.1845; found, 375.1849.

N-*(8-(3-(Pyridin-*3-yl*)thioureido)octyl)-1H-indole-2-carboxamide **(24)***. To a solution of **15** (100 mg, 0.32 mmol) in THF (1 mL), H_2O (30 μL) and Ph_3P (126 mg, 0.50 mmol) were added. The reaction mixture was stirred on reflux for 30 h. The resulting residue was evaporated under vacuum and purified by chromatography column on silica gel (MeOH:CH_2Cl_2:NH_4OH, 1:10:0.1) to yield **21** (45 mg, 50%) as a white solid. Reaction of **21** (37.0 mg, 0.1 mmol) and 3-pyridyl isothiocyanate (36 μL, 0.3 mmol) was performed according to the same procedure as that used to prepare **22**. Chromatography column (MeOH:EtOAc: CH_2Cl_2, 0.4:5:1). Yield: 80%, white solid. ^{1}H NMR (300 MHz, DMSO-d_6, δ ppm) 11.52 (s, 1H, NH indole), 9.53 (s, 1H, N$\underline{H}$-Py), 8.55 (t, J = 2.2 Hz, 1H, Py), 8.43 (t, J = 5.7 Hz, 1H, NH–C═O), 8.28 (dd, J = 4.7, 1.4 Hz, 1H, Py), 8.03–7.86 (m, 1H, Py), 7.60 (d, J = 7.9 Hz, 1H, indole), 7.42 (dd, J = 8.2, 0.7 Hz, 1H, indole), 7.33 (dd, J = 8.2, 4.7 Hz, 1H, Py), 7.20–7.12 (m, 1H, indole), 7.09 (s, 1H, indole), 7.07–6.98 (m, 1H, indole), 3.51–3.39 (m, 2H, C$\underline{H}_2$-thiourea), 3.28 (q, J = 6.4 Hz, 2H, C$\underline{H}_2$-amide), 1.60–1.49 (m, 4H, 2 CH_2), 1.40–1.26 (m, 8H, 4 CH_2). ^{13}C NMR (75.4 MHz, DMSO-d_6, δ ppm) 180.9 (C═S), 161.0 (C═O), 144.6 (CH, Py), 144.4 (CH, Py), 136.3 (qC, indole), 131.9 (qC, indole), 131.8 (qC, Py), 130.2 (CH, Py), 127.1 (qC, indole), 123.1 (2CH, Py, indole), 121.4 (CH, indole), 119.6 (CH, indole), 112.2 (CH, indole), 102.1 (CH, indole), 43.9 (C$\underline{H}_2$-thiourea), 38.7 (C$\underline{H}_2$-amide), 29.3 (CH_2), 28.8 (2(CH_2)), 28.4 (CH_2), 26.5 (CH_2), 26.4 (CH_2). ESI-HRMS m/z calcd for $C_{23}H_{30}N_5OS$ $[M+H]^+$, 424.2162; found, 424.2166.

*(4-(4-Aminobutyl)piperidin-*1-yl*)(1H-indol-*2-yl*)methanone **(26)***. Compound **16** [19] (483 mg, 1.2 mmol) was dissolved in 20% TFA/CH_2Cl_2 (9 mL) and the mixture was stirred at r.t. for 4.5 h. The mixture was evaporated under vacuum and the crude product (257 mg, 0.60 mmol) was dissolved in DMF (3.5 mL), cooled to 0 °C and 1H-indole-2-carboxylic acid (146 mg, 0.91 mmol), PyBOP (534 mg, 1.00 mmol) and DIPEA (0.51 mL, 2.90 mmol) were slowly added. After stirring at r.t. for 16 h, the reaction mixture was diluted with EtOAc (35 mL) and washed with 1 M HCl (x3) and brine (x3), dried over Na_2SO_4, filtered, and concentrated in vacuo. The crude was purified by chromatography column on silica gel (EtOAc:Toluene, 1:2) to yield the corresponding *N*-acylated intermediate (193 mg, 70%) as a white solid. This compound (170 mg, 0.37 mmol) was dissolved in DMF (2.5 mL), sodium azide (73.0 mg, 1.10 mmol) was added and the mixture was stirred at 120 °C for 32 h. The mixture was evaporated under vacuum and the residue dissolved in CH_2Cl_2. The organic layer was washed with water and brine, dried over Na_2SO_4, filtered, and concentrated in vacuo. The residue thus obtained (113 mg, 0.35 mmol) in MeOH (10 mL), Pd/C 10% (50 mg) was added, and the reaction mixture was stirred under H_2 (1 atm) at r.t. overnight. The mixture was filtered through a Celite pad and concentrated in vacuo. The crude product **26** was used in the next step without further purification.

*1-(4-(1-(1H-Indole-2-carbonyl)piperidin-*4-yl*)butyl)-3-(pyridin-*3-yl*) thiourea **(25)***. Reaction of **26** (22.0 mg, 0.1 mmol) and 3-pyridyl isothiocyanate (18 μL, 0.2 mmol) was performed according to the same procedure as that used to prepare **22**. Chromatography column (MeOH: EtOAc:CH_2Cl_2, 0:5:1 to 1:5:1). Yield: 91%, white solid. ^{1}H NMR (300 MHz, Acetone-d_6, δ ppm) 10.63 (s, 1H, NH indole), 8.91 (s, 1H, N$\underline{H}$-Py), 8.65–8.53 (m, 1H, Py), 8.31 (dd, J = 4.7, 1.3 Hz, 1H, Py), 8.07–7.94 (m, 1H, Py), 7.68–7.58 (m, 1H, indole), 7.57–7.39 (m, 2H, 1H indole, N$\underline{H}$–CH_2), 7.31 (dd, J = 8.1, 4.6 Hz, 1H, Py), 7.27–7.15 (m, 1H, indole), 7.15–7.00 (m, 1H, indole), 6.80 (d, J = 1.3 Hz, 1H, indole), 4.71–4.51 (m, 2H, piperidine), 3.72–3.54 (m, 2H, C$\underline{H}_2$–NH), 3.00 (br s, 2H, piperidine), 1.90–1.75 (m, 2H, piperidine), 1.75–1.55 (m, 3H, 1H piperidine, CH_2), 1.52–1.10 (m, 2H piperidine, 2 CH_2). ^{13}C NMR (75.4 MHz, Acetone-d_6, δ ppm) 181.8, 161.8, 145.3, 136.1, 136.0, 130.4,

127.5, 123.3, 122.9, 121.3, 119.8, 111.8, 111.7, 103.8, 103.7, 44.9, 44.2, 35.9, 32.4, 28.8, 23.6. ESI-HRMS *m/z* calcd for $C_{24}H_{30}N_5OS$ $[M+H]^+$, 436.2158; found, 436.2166.

tert-*Butyl (7-(cyclopentyl(furan-2-ylmethyl)amino)-7-oxoheptyl)carbamate* ***(30)***. A solution of **29a** [35] (80.0 mg, 0.48 mmol), 7-((*tert*-Butoxycarbonyl)amino)heptanoic acid [36] (178 mg, 0.73 mmol) and PyBOP (428 mg, 0.82 mmol) in DMF (2.5 mL) was cooled to 0 °C. DIPEA (0.21 mL, 1.21 mmol) was slowly added at 0 °C, and the reaction mixture was stirred at r.t. for 16 h. The reaction mixture was concentrated in vacuo and diluted with EtOAc (20 mL) and washed with 1 M HCl (x3) and brine (x3), dried over Na_2SO_4 and concentrated in vacuo. Chromatography column (EtOAc:Cyclohexane, 1:4 → 1:1) yielded **30** (170 mg, 89%) as a colourless oil. ^{1}H NMR (300 MHz, $CDCl_3$, δ ppm, mixture of rotamers) 7.46–7.10 (m, 2H, furan), 6.39–6.23 (m, 2H, furan), 6.23–6.07 (m, 2H, furan), 4.86–4.63 (m, 1H, CH cyclopentyl rotamer A), 4.58–4.28 (m, 6H, 2 C$\underline{H}_2$-furan, 2 NH), 4.28–4.10 (m, 1H, CH cyclopentyl rotamer B), 3.08 (br s, 4H, 2 C$\underline{H}_2$–NH), 2.50–2.26 (m, 4H, 2 CH_2–C═O), 1.91–1.21 (m, 46H, 8 CH_2, 8 CH_2 cyclopentyl, 2C $(CH_3)_3$). ^{13}C NMR (75.4 MHz, $CDCl_3$, δ ppm, mixture of rotamers) 173.9, 173.2, 156.2, 152.3, 152.3, 142.1, 141.0, 110.6, 107.6, 107.0, 79.2, 77.6, 77.2, 76.7, 60.5, 58.8, 56.2, 41.9, 38.4, 30.1, 29.8, 29.2, 28.6, 26.7, 25.4, 23.9, 14.3. ESI-HRMS *m/z* calcd for $C_{22}H_{36}N_2O_4Na$ $[M+Na]^+$, 415.2564; found, 415.2567.

N-*Cyclopentyl-N-(furan-2-ylmethyl)-7-(3-(pyridin*-3-yl*)thioureido)heptanamide* ***(27)***. Compound **30** (156 mg, 0.40 mmol) was dissolved in 20% TFA/CH_2Cl_2 (2.5 mL) at 0 °C and the mixture was stirred at r.t. for 3 h. The solvent was evaporated in vacuo and the residue was azeotropically dried with toluene (2 × 5 mL). After drying under high vacuum, the unprotected compound (110 mg, 0.27 mmol) was dissolved in dry CH_2Cl_2 (6 mL) and 3-pyridyl isothiocyanate (75 μL, 0.7 mmol) was added. After stirring at r.t. for 3 h, the solvent was removed under vacuo and the resulting residue was purified by chromatography column on silica gel (MeOH:EtOAc, 1:9) to give **27** (80.0 mg, 70%) as a white solid. ^{1}H NMR (300 MHz, $CDCl_3$, δ ppm, mixture of rotamers) 8.92–8.72 (m, 2H, Py), 8.55–8.41 (m, 2H, Py), 8.41–8.26 (m, 2H, Py), 8.18–8.00 (m, 2H, Py), 7.41–7.07 (m, 6 h, 2H furan, 2 N$\underline{H}$-Py, 2 N$\underline{H}$–CH_2), 6.40–6.16 (m, 2H, furan), 6.18–6.02 (m, 2H, furan), 4.69 (quint, J = 8.3 Hz, 1H, CH cyclopentyl rotamer A), 4.40 (br d, 4H, 2 C$\underline{H}_2$-furan), 4.29–4.09 (m, 1H, CH cyclopentyl rotamer B), 3.72–3.51 (m, 4H, 2 C$\underline{H}_2$–NH), 2.67–2.31 (m, 4H, 2 CH_2–C═O), 1.94–1.23 (m, 32H, 8 CH_2 cyclopentyl, 8 CH_2). ^{13}C NMR (75.4 MHz, $CDCl_3$, δ ppm, mixture of rotamers) 181.8, 174.5, 173.9, 152.0, 151.6, 145.8, 145.6, 145.0, 142.3, 141.4, 136.0, 132.2, 123.6, 123.6, 110.6, 107.3, 77.6, 77.2, 76.7, 59.0, 56.5, 45.2, 44.9, 41.8, 38.8, 33.6, 33.3, 30.0, 29.1, 28.3, 27.6, 27.1, 26.8, 24.6, 24.4, 23.9, 23.8. ESI-HRMS *m/z* calcd for $C_{23}H_{33}N_4O_2S$ $[M+H]^+$, 429.2316; found, 429.2319.

6-Amino-N-cyclopentyl-N-(furan-2-ylmethyl)hexane-1-sulfonamide ***(32)***. To a suspension of **29a** (1.1 g, 6.7 mmol) in dry CH_2Cl_2 (38 mL) was added Et_3N (2.6 mL, 19 mmol) under argon at 0 °C and stirred over 3 Å MS. Compound **31** [37] (5.3 g, 16 mmol) in dry CH_2 Cl_2 (40 mL) was added over 1 h and the resulting mixture stirred for 3 h at 0 °C. The reaction mixture was quenched with water and extracted with CH_2Cl_2. The combined organic layers were washed with water, brine, dried over anh. Na_2SO_4 and concentrated in vacuo. The crude product was purified by flash chromatography on silica gel (toluene:EtOAc, 20:1 → 12:1) to give the protected sulfonamide (1.8 g, 62%) as a white solid. To a stirred solution of this compound (1.9 g, 4.2 mmol) in dry MeOH (20 mL), was added NH_2NH_2 (1.2 mL, 25 mmol) at 0 °C and stirred for 3 h at 0 °C and at r.t. overnight. The white precipitate was filtered off and washed with MeOH (20 mL). The solvent was evaporated in vacuo and the crude product was dissolved in 2 N HCl (90 mL) and washed with Et_2O (90 mL x 3). The aqueous layer was basified with sat. aq. soln. of NaOH to pH = 8 and extracted with EtOAc (90 mL x 3). The organic layers were collected and dried over anh. Na_2SO_4 and concentrated in vacuo to yield **32** as a sticky solid that was carried forward to the next step without purification.

N-*Cyclopentyl*-N-*(furan-2-ylmethyl)-6-(3-(pyridin*-3-yl*)thioureido)hexane-1-sulfonamide* ***(28)***. Reaction of **32** (115 mg, 0.35 mmol) and 3-pyridyl isothiocyanate (100 μL, 0.90 mmol) was performed according to the same procedure as that used to prepare **22**. Chromatography column (EtOAc:Cyclohexane, 9:1). Yield: 64%, white solid. ^{1}H NMR (300 MHz, $CDCl_3$, δ ppm) 8.62–8.51 (m, 1H, Py), 8.50–8.37 (m, 1H, Py), 8.17 (br s, 1H, N$\underline{H}$-Py), 7.96–7.76 (m, 1H, Py), 7.42–7.30 (m, 2H, Py, furan), 6.45–6.22 (m, 3H, 2H furan, N$\underline{H}$–CH_2), 4.36 (s, 2H, CH_2-furan), 4.24–4.04 (m, 1H, CH cyclopentyl), 3.60 (q, J = 6.6 Hz, 2H, C$\underline{H}_2$–NH), 2.88–2.67 (m, 2H, CH_2SO_2), 1.98–1.47 (m, 12H, 8H cyclopentyl, 2 CH_2), 1.47–1.21 (m, 4H, 2 CH_2). ^{13}C NMR (75.4 MHz, $CDCl_3$, δ ppm) 181.5 (C═S), 151.4 (qC, furan), 147.0 (CH, Py), 145.7 (CH, Py), 142.3 (CH, furan), 134.6 (qC, Py), 132.7 (CH, Py), 124.3 (CH, Py), 110.8 (CH, furan), 109.2 (CH, furan), 59.3 (CH, cyclopentyl), 53.2 (CH_2SO_2), 45.2 (CH_2–NH), 40.1 (CH_2-furan), 30.0 (2CH_2, cyclopentyl), 28.5 (CH_2), 27.9 (CH_2), 26.3 (CH_2), 23.6 (2CH_2, cyclopentyl), 23.3 (CH_2). ESI-HRMS *m/z* calcd for $C_{22}H_{33}N_4O_3S_2$ $[M+H]^+$, 465.1982; found, 465.1989.

1-(Furan-2-yl*)-N-(4-nitrobenzyl)methanamine* ***(29c)***. A solution of furfuryl amine (0.73 mL, 8.20 mmol) and 4-nitrobenzaldehyde (1.24 g, 8.20 mmol) were stirred in dry CH_2Cl_2 (20.0 mL) over 3 Å MS at r.t. for 24 h. Then the reaction mixture was concentrated in *vacuo* and the residue was dissolved in MeOH (20 mL). $NaBH_4$ (623 mg, 16.5 mmol) was added in small portion to the mixture at 0 °C. The reaction was warmed to r.t. and stirred for 16 h. The solvent was removed under reduce pressure and the residue was dissolved in water (100 mL) and extracted with EtOAc (3 × 100 mL). The organic phases were extracted with 3% HCl (3 × 100 mL), and the pH of the obtained acidic aqueous solution was raised to pH 10 with sat. aq. soln. of NaOH. The aqueous phase was extracted with EtOAc (3 × 100 mL), and the organic phases were washed with water (100 mL), brine (100 mL), and dried over Na_2SO_4. The solvent was evaporated in vacuo to give **29c** (1.42 g, 75%) as a red oil. ^{1}H NMR (300 MHz, $CDCl_3$, δ ppm) 8.17 (d, J = 8.7 Hz, 2H, Ph), 7.51 (d, J = 8.8 Hz, 2H, Ph), 7.42–7.32 (m, 1H, furan), 6.37–6.25 (m, 1H, furan), 6.24–6.12 (m, 1H, furan), 3.89 (s, 2H, C$\underline{H}_2$-Ph), 3.80 (s, 2H C$\underline{H}_2$-furan), 1.85 (s, 1H, NH). ^{13}C NMR (75.4 MHz, $CDCl_3$, δ ppm) 153.3 (qC, Furan), 147.7 (qC, Ph), 147.3 (qC, Ph), 142.2 (CH, furan), 128.9 (2 CH, Ph), 123.8 (2 CH, Ph), 110.4 (CH, furan), 107.6 (CH, furan), 52.0 (C$\underline{H}_2$-furan), 45.5 (C$\underline{H}_2$-Ph). ESI-HRMS *m/z* calcd for $C_{12}H_{13}N_2O_3$ $[M+H]^+$, 233.0922; found, 233.0921.

N-*(Furan-2-ylmethyl)-3-morpholinopropan-1-amine* ***(29d)***. Reaction of furfural (3.5 mL, 42 mmol) and 3-morpholinopropan-1-amine (6.1 mL, 42 mmol) as indicated for the synthesis of **29c** afforded **29d** (8.0 g, 86%) as a yellow oil. ^{1}H NMR (300 MHz, $CDCl_3$, δ ppm) 7.34 (dd, J = 1.8, 0.8 Hz, 1H, furan), 6.30 (dd, J = 3.2, 1.8 Hz, 1H, furan), 6.17 (dd, J = 3.2, 0.8 Hz, 1H, furan), 3.77 (s, 2H, C$\underline{H}_2$-furan), 3.73–3.63 (m, 4H, morpholine), 2.67 (t, J = 6.8 Hz, 2H, CH_2), 2.48–2.34 (m, 6H, morpholine, CH_2), 2.16 (s, 1H, NH), 1.76–1.62 (m, 2H, CH_2). ^{13}C NMR (75,4 MHz, $CDCl_3$, δ ppm) 153.9 (qC, furan), 141.9 (CH, furan), 110.2 (CH, furan), 107.0 (CH, furan), 67.1 (2C, morpholine), 57.5 (CH_2), 53.9 (2C, morpholine), 47.9 (CH_2), 46.3 (C$\underline{H}_2$-furan), 26.6 (CH_2). ESI-HRMS *m/z* calcd for $C_{12}H_{21}N_2O_2$ $[M+H]^+$, 225.1596; found, 225.1598.

N-*(Furan-2-ylmethyl)-3-(pyrrolidin*-1-yl*)propan-1-amine* ***(29e)***.Reaction of furfural (0.34 mL, 4.20 mmol) and 3-(pyrrolidin-1-yl)propan-1-amine (0.53 mL, 4.20 mmol) as indicated for the synthesis of **29c** afforded **29e** (630 mg, 73%) as a colourless oil. ^{1}H NMR (300 MHz, $CDCl_3$, δ ppm) 7.34 (dd, J = 1.9, 0.9 Hz, 1H, furan), 6.29 (dd, J = 3.2, 1.9 Hz, 1H, furan), 6.18–6.12 (m, 1H, furan), 3.81–3.72 (m, 2H, C$\underline{H}_2$-furan), 2.66 (t, J = 7.0 Hz, 2H, CH_2), 2.55–2.43 (m, 6H, CH_2, 2 CH_2 pyrrolidine), 2.05 (s, 1H, NH), 1.83–1.65 (m, 6H, CH_2, 2 CH_2 pyrrolidine). ^{13}C NMR (75.4 MHz, $CDCl_3$, δ ppm) 154.1 (qC, furan), 141.8 (CH, furan), 110.1 (CH, furan), 106.8 (CH, furan), 54.8 (CH_2), 54.3 (2C, pyrrolidine), 47.9 (CH_2), 46.3 (C$\underline{H}_2$-furan), 29.3 (CH_2), 23.5 (2C, pyrrolidine). ESI-HRMS *m/z* calcd for $C_{12}H_{21}N_2O$ $[M+H]^+$, 209.1649; found, 209.1648.

6-Amino-N-*(furan-2-ylmethyl)-N-(3-morpholinopropyl)hexane-1-sulfonamide* ***(33d)***. To a suspension of **29d** (643 mg, 1.95 mmol) in dry

CH_2Cl_2 (12.0 mL) was added Et_3N (0.76 mL, 5.5 mmol) at 0 °C under argon. Compound **31** (643 mg, 1.95 mmol) in dry CH_2Cl_2 (5 mL) was added dropwise over 30 min at 0 °C and the resulting mixture was stirred at r.t. for 16 h. The reaction mixture was quenched with water (45 mL) and extracted with CH_2Cl_2 (50 mL x 3). The combined organic layers were washed with water, brine, dried over anh. Na_2SO_4 and concentrated in vacuo. Chromatography column (MeOH:CH_2Cl_2, 1:20) afforded protected sulfonamide (630 mg, 62%) as a white solid. This compound (610 mg, 1.18 mmol) in dry MeOH (6 mL), was added NH_2NH_2 (0.35 mL, 7.2 mmol) at 0 °C and stirred for 3 h at 0 °C and at r.t. overnight. The white precipitate was filtered off and washed with MeOH (6 mL). The solvent was evaporated in vacuo and the crude product was dissolved in 2 N HCl (30 mL) and washed with diethyl ether. The aqueous layer was basified with sat. aq. soln. of NaOH to pH = 8 and extracted with EtOAc. The combined organic layers were dried over anh. Na_2SO_4 and concentrated in vacuo to yield **33d** as a sticky solid that was carried forward to the next step without purification.

*(E)-6-(2-Cyano-3-(pyridin-4-yl)guanidino)-N-cyclopentyl-N-(furan-2-ylmethyl)hexane-1-sulfonamide (**35a**)*. Compound **34a** [23] (920.0 mg, 3.86 mmol) was dissolved in dry MeCN:DMF (48 mL, 3:1), **32** (1.65 g, 5.02 mmol), Et_3N (1.51 mL, 10.8 mmol) and DMAP (100 mg, 0.81 mmol) were added, and the mixture was heated and stirred at 80 °C under argon for 16 h. The reaction mixture was concentrated in vacuo and the residue was purified by flash chromatography on silica gel (MeOH:EtOAc, 1:12) to yield **35a** (1.48 g, 81%) as a white solid. ^{1}H NMR (300 MHz, $CDCl_3$, δ ppm) 8.50–8.33 (m, 2H, Py), 7.41–7.30 (m, 1H, furan), 7.30–7.16 (m, 2H, Py), 6.37–6.22 (m, 2H, furan), 6.10 (t, J = 5.6 Hz, 1H, N<u>H</u>–CH_2), 4.34 (s, 2H, CH_2-furan), 4.11 (quint, J = 8.5 Hz, 1H, CH cyclopentyl), 3.36 (q, J = 6.7 Hz, 2H, C<u>H</u>$_2$–NH), 2.82–2.67 (m, 2H, CH_2SO_2), 1.94–1.45 (m, 12H, 8H cyclopentyl, 2 CH_2), 1.45–1.23 (m, 4H, 2 CH_2). ^{13}C NMR (75.4 MHz, $CDCl_3$, δ ppm) 157.7 (C═N), 151.3 (qC, furan), 150.5 (2CH, Py), 145.4 (qC, Py), 142.3 (CH, furan), 117.1 (CN), 115.8 (CH, Py), 110.8 (CH, furan), 109.2 (CH, furan), 59.3 (CH, cyclopentyl), 53.1 (CH_2SO_2), 42.5 (CH_2–NH), 40.1 (CH_2-furan), 30.0 (2CH_2, cyclopentyl), 28.9 (CH_2), 27.8 (CH_2), 26.1 (CH_2), 23.6 (2CH_2, cyclopentyl), 23.2 (CH_2). ESI-HRMS *m/z* calcd for $C_{23}H_{33}N_6O_3S$ $[M+H]^+$, 473.2328; found, 473.2329.

*(E)-6-(2-Cyano-3-(pyridin-4-yl)guanidino)-N-(furan-2-ylmethyl)-N-(3-morpholinopropyl)hexane-1-sulfonamide (**35d**)*. Reaction of **34a** (73.0 mg, 0.31 mmol) and **33d** (130.0 mg, 0.34 mmol) followed the procedure described for **35a**. Chromatography column (MeOH:EtOAc, 1:6). Yield: 68%, white solid. ^{1}H NMR (300 MHz, $CDCl_3$, δ ppm, mixture of rotamers) 8.56–8.33 (m, 2H, Py), 7.62–7.34 (m, 4H, 2H furan, 2 N<u>H</u>-Py), 7.31–7.16 (m, 2H, Py), 6.88 (t, J = 5.7 Hz, 1H, N<u>H</u>–CH_2 rotamer A), 6.41–6.23 (m, 4H, furan), 5.94 (t, J = 5.5 Hz, 1H, N<u>H</u>–CH_2 rotamer B), 4.40 (s, 4H, 2 C<u>H</u>$_2$-furan), 3.77–3.60 (m, 8H, 4 CH_2 morpholine), 3.43–3.31 (m, 4H, 2 C<u>H</u>$_2$–NH), 3.24 (t, J = 7.3 Hz, 4H, 2 CH_2–NSO_2), 2.95–2.81 (m, 4H, 2 CH_2SO_2), 2.51–2.28 (m, 12H, 4 CH_2 morpholine, 2 CH_2), 1.82–1.67 (m, 8H, 4 CH_2), 1.67–1.50 (m, 4H, 2 CH_2), 1.50–1.29 (m, 8H, 4 CH_2). ^{13}C NMR (75.4 MHz, $CDCl_3$, δ ppm, mixture of rotamers) 169.5, 157.6, 150.8, 150.1, 150.0, 145.0, 143.0, 143.0, 134.9, 130.4, 128.4, 115.8, 110.8, 110.7, 110.0, 109.9, 67.0, 66.9, 55.7, 55.7, 53.7, 52.2, 52.0, 50.9, 45.4, 45.3, 43.2, 42.4, 40.1, 29.2, 28.9, 28.1, 27.8, 26.5, 26.1, 25.5, 25.4, 23.3. ESI-HRMS *m/z* calcd for $C_{25}H_{38}N_7O_4S$ $[M+H]^+$, 532.2693; found, 532.2700.

tert-*Butyl (6-(cyclopentyl(furan-2-ylmethyl)amino)-6-oxohexyl)carbamate (**36a**)*. Reaction of **29a** (80.0 mg, 0.48 mmol) and 6-((*tert*-butoxycarbonyl)amino)hexanoic acid [32] (168 mg, 0.73 mmol) followed the procedure described for **30**. Chromatography column (EtOAc:Cyclohexane, 1:1). Yield: 90%, yellow oil. ^{1}H NMR (300 MHz, $CDCl_3$, δ ppm, mixture of rotamers) 7.40–7.19 (m, 2H, furan), 6.38–6.23 (m, 2H, furan), 6.23–6.05 (m, 2H, furan), 4.88–4.30 (m, 7H, 2 C<u>H</u>$_2$-furan, CH cyclopentyl rotamer A, 2 NH), 4.29–4.03 (m, 1H, CH cyclopentyl rotamer B), 3.22–2.94 (m, 4H, 2 C<u>H</u>$_2$–NH), 2.49–2.26 (m, 4H, 2 CH_2–C═O), 1.88–1.17 (m, 46H, 6 CH_2, 8 CH_2 cyclopentyl, 2C$(CH_3)_3$). ^{13}C NMR (75.4 MHz, $CDCl_3$, δ ppm, mixture of rotamers) 173.1, 156.1, 152.7, 152.3, 142.1, 141.0, 110.6, 107.6, 107.0, 79.2, 58.7, 56.2, 41.9, 40.7, 38.4, 33.8, 33.6, 30.0, 29.2, 28.6, 26.7, 25.1, 23.9. ESI-HRMS *m/z* calcd for $C_{21}H_{34}N_2O_4Na$ $[M+Na]^+$, 401.2407; found, 401.2411.

tert-*Butyl (6-((4-chlorobenzyl)(furan-2-ylmethyl)amino)-6-oxohexyl)carbamate (**36b**)*. The same procedure to that described for the synthesis of **36a** but starting from **29b** (80.0 mg, 0.36 mmol). Chromatography column (EtOAc:Cyclohexane, 1:2 → 1:1). Yield: 83%, colorless oil. ^{1}H NMR (300 MHz, $CDCl_3$, δ ppm, mixture of rotamers) 7.45–7.20 (m, 6H, 2H furan, 4H Ph), 7.20–7.00 (m, 4H, Ph), 6.38–6.23 (m, 2H, furan), 6.23–6.09 (m, 2H, furan), 4.60–4.29 (m, 10H, 2 NH, 2 C<u>H</u>$_2$-furan, 2 C<u>H</u>$_2$-Ph), 3.21–2.99 (m, 4H, 2 C<u>H</u>$_2$–NH), 2.53 (t, J = 7.6 Hz, 2H, CH_2–C═O rotamer A), 2.32 (t, J = 7.3 Hz, 2H, CH_2–C═O rotamer B) 1.80–1.60 (m, 4H, 2 CH_2), 1.57–1.20 (m, 26H, 2C$(CH_3)_3$, 4 CH_2). ^{13}C NMR (75.4 MHz, $CDCl_3$, δ ppm, mixture of rotamers) 173.2, 156.2, 151.0, 150.1, 142.9, 142.4, 136.1, 135.4, 133.5, 133.3, 129.8, 129.2, 128.8, 127.8, 110.5, 109.0, 108.4, 79.1, 50.1, 47.6, 43.7, 41.6, 40.7, 33.2, 30.0, 28.6, 26.7, 25.0. ESI-HRMS *m/z* calcd for $C_{23}H_{31}ClN_2O_4Na$ $[M+Na]^+$, 457.1860; found, 457.1865.

tert-*Butyl (6-((furan-2-ylmethyl)(3-morpholinopropyl)amino)-6-oxohexyl)carbamate (**36d**)*. The same procedure to that described for the synthesis of **36a** but starting from **29d** (80.0 mg, 0.48 mmol). Chromatography column (MeOH:EtOAc, 1:12 → 1:6).Yield: 80%, yellow oil. ^{1}H NMR (300 MHz, $CDCl_3$, δ ppm, mixture of rotamers) 7.40–7.33 (m, 1H, furan rotamer A), 7.34–7.28 (m, 1H, furan rotamer B), 6.35–6.25 (m, 2H, furan), 6.25–6.15 (m, 2H, furan), 4.65–4.47 (m, 4H, C<u>H</u>$_2$-furan rotamer A, 2 NH), 4.43 (s, 2H, C<u>H</u>$_2$-furan rotamer B), 3.82–3.62 (m, 8H, morpholine), 3.49–3.24 (m, 4H, 2 CH_2), 3.13–3.05 (m, 4H, 2 CH_2), 2.61–2.21 (m, 16H, 8H morpholine, 4 CH_2), 1.76–1.56 (m, 12H, 6 CH_2), 1.56–1.26 (m, 24H, 2C$(CH_3)_3$, 2 NH, 2 CH_2). ^{13}C NMR (75.4 MHz, $CDCl_3$, δ ppm, mixture of rotamers) 173.2, 172.9, 156.1, 151.6, 150.6, 142.7, 142.0, 110.6, 110.5, 108.5, 108.1, 79.1, 77.6, 77.2, 76.7, 66.9, 66.4, 56.2, 55.6, 53.7, 53.4, 45.3, 45.1, 44.2, 41.5, 34.4, 33.2, 33.0, 30.0, 29.8, 28.5, 26.7, 25.5, 25.0, 24.9, 24.1. ESI-HRMS *m/z* calcd for $C_{23}H_{40}N_3O_5$ $[M+H]^+$, 438.2959; found, 438.2962.

tert-*Butyl (7-((4-chlorobenzyl)(furan-2-ylmethyl)amino)-7-oxoheptyl)carbamate (**37b**)*. To a solution of **29b** (80.0 mg, 0.36 mmol) and 7-((*tert*-butoxycarbonyl)amino)heptanoic acid [32] (106 mg, 0.43 mmol) in CH_2Cl_2 (2 mL), DMAP (4.0 mg, 40 μmol) and DCC (112 mg, 0.54 mmol) in CH_2Cl_2 (1 mL) were added at 0 °C. The reaction mixture was stirred overnight at r.t., filtered through Celite, washed with EtOAc (20.0 mL) and concentrated under vacuum, and the residue was purified by chromatography column on silica gel (EtOAc:Cyclohexane, 1:2 → 1:1) to obtain **37b** (130 mg, 80%) as a colourless oil. ^{1}H NMR (300 MHz, $CDCl_3$, δ ppm, mixture of rotamers) 7.40–7.20 (m, 6H, 2H furan, 4H Ph), 7.19–6.98 (m, 4H, Ph), 6.36–6.22 (m, 2H, furan), 6.22–6.08 (m, 2H, furan), 4.98–3.99 (m, 10H, 2 NH, 2 C<u>H</u>$_2$-furan, 2 C<u>H</u>$_2$-Ph), 3.18–2.96 (m, 4H, 2 C<u>H</u>$_2$–NH), 2.60–2.22 (m, 4H, 2 CH_2–C═O), 2.00–1.53 (m, 8H, 4 CH_2), 1.53–1.19 (m, 26H, 2C$(CH_3)_3$, 4 CH_2). ^{13}C NMR (75.4 MHz, $CDCl_3$, δ ppm, mixture of rotamers) 173.7, 173.3, 156.1, 154.2, 151.0, 150.1, 142.8, 142.3, 136.1, 135.4, 133.4, 133.2, 129.7, 129.1, 128.8, 127.8, 110.5, 108.9, 108.3, 79.1, 77.6, 77.2, 76.7, 56.0, 50.0, 49.8, 47.5, 43.7, 41.5, 35.7, 33.2, 33.1, 32.8, 31.0, 30.0, 30.0, 29.1, 29.0, 28.9, 28.5, 26.7, 26.6, 26.4, 25.6, 25.4, 25.2, 25.1, 24.8. ESI-HRMS *m/z* calcd for $C_{24}H_{33}ClN_2O_4Na$ $[M+Na]^+$, 471.2016; found, 471.2021.

tert-*Butyl (7-((furan-2-ylmethyl)(4-nitrobenzyl)amino)-7-oxoheptyl)carbamate (**37c**)*. The same procedure to that described for the synthesis of **37b** but starting from **29c** (80.0 mg, 0.35 mmol). Yield: 76%, yellow oil. ^{1}H NMR (300 MHz, $CDCl_3$, δ ppm, mixture of rotamers) 8.23–7.94 (m, 4H, Ph), 7.35–7.14 (m, 6H, 2H furan, 4H Ph), 6.29–6.18 (m, 2H, furan), 6.18–6.06 (m, 2H, furan), 4.69–4.22 (m, 10H, 2 NH, 2 C<u>H</u>$_2$-furan, 2 C<u>H</u>$_2$-Ph), 3.13–2.88 (m, 4H, 2 C<u>H</u>$_2$–NH), 2.60–2.15 (m, 4H, 2 CH_2–C═O), 1.93–1.49 (m, 6H, 3 CH_2), 1.49–0.96 (m, 28H, 2C$(CH_3)_3$, 5 CH_2). ^{13}C NMR (75.4 MHz, $CDCl_3$, δ ppm, mixture of rotamers) 173.4, 173.1, 156.0, 154.1, 150.5, 149.6, 147.5, 147.2, 145.3, 144.5, 142.9, 142.3, 128.6, 127.0, 124.1, 123.7, 110.5, 110.4, 109.2, 108.6, 79.0, 77.5, 77.1, 76.7, 50.3, 49.3, 48.2, 44.4, 41.8, 35.6, 33.7, 33.1, 33.0,

32.7, 30.9, 29.9, 29.0, 28.9, 28.8, 28.4, 26.6, 26.5, 26.3, 25.6, 25.5, 25.3, 25.0, 25.0, 24.9, 24.7. ESI-HRMS *m/z* calcd for $C_{24}H_{33}N_3O_6Na$ $[M+Na]^+$, 482.2259; found, 482.2262.

tert-*Butyl (7-((furan-2-ylmethyl)(3-morpholinopropyl)amino)-7-oxoheptyl)carbamate* (***37d***). The same procedure to that described for the synthesis of **37b** but starting from **29d** (80.0 mg, 0.36 mmol). Chromatography column (MeOH:EtOAc, 1:10 → 1:6). Yield: 67%, colourless oil. ^{1}H NMR (300 MHz, $CDCl_3$, δ ppm, mixture of rotamers) 7.36–7.31 (m, 1H, furan rotamer A), 7.31–7.27 (m, 1H, furan rotamer B), 6.36–6.23 (m, 2H, furan), 6.23–6.10 (m, 2H, furan), 4.68–4.45 (m, 4H, C$\underline{H}_2$-furan rotamer A, 2 NH), 4.40 (s, 2H, C$\underline{H}_2$-furan rotamer B), 3.76–3.54 (m, 8H, 4 CH_2), 3.46–3.22 (m, 4H, 2 CH_2), 3.13–2.92 (m, 4H, 2 CH_2), 2.53–2.12 (m, 16H, morpholine), 1.77–1.54 (m, 8H, 4 CH_2), 1.54–1.21 (m, 30H, 2C$(CH_3)_3$, 2 NH, 5 CH_2). ^{13}C NMR (75.4 MHz, $CDCl_3$, δ ppm, mixture of rotamers) 173.0, 172.9, 156.1, 151.6, 150.7, 142.6, 141.9, 110.5, 110.4, 108.4, 107.8, 79.0, 77.6, 77.2, 76.7, 67.0, 56.2, 55.5, 53.7, 53.6, 45.2, 45.1, 44.4, 41.4, 33.2, 33.0, 30.0, 29.7, 29.2, 29.1, 28.5, 26.7, 26.6, 25.5, 25.3, 25.1, 24.5.

tert-*Butyl (7-((furan-2-ylmethyl)(3-(pyrrolidin-1-yl)propyl)amino)-7-oxoheptyl)carbamate* (***37e***). The same procedure to that described for the synthesis of **37b** but starting from **29e** (80 mg, 0.4 mmol). Chromatography column (MeOH:DCM:NH_4OH, 1:20:0.1 → 1:10:0.1). Yield: 44%, colourless oil. ^{1}H NMR (300 MHz, $CDCl_3$, δ ppm, mixture of rotamers) 7.36–7.21 (m, 2H, furan), 6.31–6.20 (m, 2H, furan), 6.20–6.11 (m, 2H, furan), 4.59 (s, 2H, 2 NH), 4.49 (s, 2H, C$\underline{H}_2$-furan rotamer A), 4.39 (s, 2H, C$\underline{H}_2$-furan rotamer B), 3.44–3.22 (m, 4H, 2 C$\underline{H}_2$–NH), 3.09–2.97 (m, 4H, C$\underline{H}_2$–N–C═O), 2.84–2.70 (m, 4H, 2 C$\underline{H}_2$–N), 2.69–2.22 (m, 12H, 4 CH_2 pyrrolidine, 2 CH_2–C═O), 1.92–1.77 (m, 6H, 2 CH_2 pyrrolidine, CH_2), 1.77–1.65 (m, 4H, 2 CH_2 pyrrolidine), 1.65–1.49 (m, 4H, 2 CH_2), 1.49–1.11 (m, 30H, 2C$(CH_3)_3$, 6 CH_2). ^{13}C NMR (75.4 MHz, $CDCl_3$, δ ppm, mixture of rotamers) 173.4, 172.9, 156.0, 151.5, 150.3, 142.6, 141.8, 110.4, 110.4, 108.3, 108.2, 78.9, 77.6, 77.2, 76.7, 54.0, 53.8, 53.5, 53.0, 45.4, 44.8, 43.6, 41.4, 33.0, 32.8, 30.1, 29.9, 29.6, 29.3, 29.0, 28.9, 28.4, 27.6, 26.6, 26.5, 25.7, 25.2, 25.0, 23.3. ESI-HRMS *m/z* calcd for $C_{24}H_{42}N_3O_4$ $[M+H]^+$, 436.3165; found, 436.3170.

*(*E*)-6-(2-Cyano-3-(pyridin-4-yl)guanidino)*-N-*cyclopentyl*-N-*(furan-2-ylmethyl)hexanamide* (***38a***). Compound **36a** (144 mg, 0.38 mmol) was dissolved in 20% TFA/CH_2Cl_2 (0.5 mL TFA, 2 mL CH_2Cl_2) at 0 °C and the mixture was stirred at r.t. for 2.5 h. The solvent was evaporated in vacuo and the residue was azeotropically dried with toluene (2 × 5 mL). Finally, the residue was dried under high vacuum to yield a colourless oil that was used in the next step without further purification. This compound (149.0 mg, 0.38 mmol) was dissolved in dry MeCN:DMF (4 mL, 3:1) and **34a** (82.0 mg, 0.35 mmol), Et_3N (0.23 mL, 1.70 mmol) and DMAP (9.0 mg, 70 μmol) were added, and the mixture was heated and stirred at 80 °C under argon for 16 h. The reaction mixture was concentrated under vacuum and the residue was purified by chromatography column on silica gel (MeOH:EtOAc:CH_2Cl_2, 0.8:5:1) to give **38a** (113.0 mg, 78%) as white sticky solid. ^{1}H NMR (300 MHz, $CDCl_3$, δ ppm, mixture of rotamers) 8.50–8.30 (m, 4H, Py), 7.40–7.20 (m, 4H, 2H Py, 2H furan), 6.49 (br s, 2H, 2 N$\underline{H}$-Py), 6.39–6.21 (m, 2H, furan), 6.15–6.03 (m, 2H, furan), 4.72–4.53 (m, 1H, CH cyclopentyl rotamer A), 4.38 (s, 4H, 2 C$\underline{H}_2$-furan), 4.28–4.09 (m, 1H, CH cyclopentyl rotamer B), 3.52–3.40 (m, 4H, 2 C$\underline{H}_2$–NH), 2.52–2.31 (m, 4H, 2 CH_2–C═O), 1.91–1.21 (m, 30H, 6 CH_2, 8 CH_2 cyclopentyl, 2 N$\underline{H}$–CH_2). ^{13}C NMR (75.4 MHz, $CDCl_3$, δ ppm, mixture of rotamers) 173.6, 157.7, 152.1, 151.6, 150.4, 150.2, 145.7, 142.3, 141.4, 117.0, 115.5, 115.3, 110.7, 107.2, 58.9, 56.3, 42.2, 41.6, 38.8, 33.4, 33.1, 30.0, 29.8, 29.1, 28.3, 28.1, 26.0, 25.8, 23.8. ESI-HRMS *m/z* calcd for $C_{23}H_{31}N_6O_2$ $[M+H]^+$, 423.2497; found, 423.2503.

*(*E*)*-N-*(4-Chlorobenzyl)-6-(2-cyano-3-(pyridin-4-yl)guanidino)*-N-*(furan-2-ylmethyl)hexanamide* (***38b***). Same procedure as described for **38a** starting from **36b**. Chromatography column (NH_4OH:MeOH:EtOAc, 0.1:0.5:10). Yield: 70%, colourless sticky solid. ^{1}H NMR (300 MHz, $CDCl_3$, δ ppm, mixture of rotamers) 8.51–8.25 (m, 4H, Py), 7.43–7.18 (m, 10H, 2H furan, 4H Ph, 4H Py), 7.16–6.94 (m, 4H, Ph), 6.51–6.36 (m, 2H, 2 N$\underline{H}$-Py), 6.36–6.24 (m, 2H, furan), 6.19–6.10 (m, 2H, furan), 4.55–4.28 (m, 8H, 2 C$\underline{H}_2$-Ph, 2 C$\underline{H}_2$-furan), 3.51–3.41 (m, 4H, 2 C$\underline{H}_2$–NH), 2.58 (t, J = 6.7 Hz, 2H, CH_2–C═O rotamer A), 2.35 (t, J = 6.7 Hz, 2H, CH_2–C═O rotamer B), 1.80–1.30 (m, 14H, 6 CH_2, 2 N$\underline{H}$–CH_2). ^{13}C NMR (75.4 MHz, $CDCl_3$, δ ppm, mixture of rotamers) 173.6, 157.7, 150.4, 150.2, 149.6, 145.7, 145.7, 143.0, 142.6, 135.6, 134.9, 133.7, 133.4, 129.3, 128.9, 127.8, 117.1, 115.6, 110.6, 109.1, 108.8, 50.8, 50.1, 47.9, 43.9, 42.2, 41.8, 32.8, 32.7, 28.5, 28.4, 26.2, 26.0, 23.5, 23.4. ESI-HRMS *m/z* calcd for $C_{25}H_{28}ClN_6O_2$ $[M+H]^+$, 479.1949; found, 479.1957.

*(*E*)-6-(2-Cyano-3-(pyridin-4-yl)guanidino)*-N-*(furan-2-ylmethyl)*-N-*(3-morpholinopropyl)hexanamide* (***38d***). Same procedure as described for **38a** starting from **36d**. Chromatography column (MeOH:Acetone:CH_2Cl_2, 0.4:1:1). Yield: 57%, white sticky solid. ^{1}H NMR (300 MHz, $CDCl_3$, δ ppm, mixture of rotamers) 8.43–8.31 (m, 4H, Py), 7.40–7.18 (m, 6H, 4H Py, 2H furan), 6.62–6.42 (m, 2H, 2 NH-Py), 6.36–6.22 (m, 2H, furan), 6.22–6.10 (m, 2H, furan), 4.49–4.37 (m, 4H, 2 CH_2-furan), 3.70–3.57 (m, 8H, 4 CH_2 morpholine), 3.48–3.26 (m, 8H, 4 CH_2), 2.61–2.12 (m, 18H, 2 NH, 4 CH_2 morpholine, 4 CH_2), 1.72–1.50 (m, 12H, 6 CH_2), 1.45–1.28 (m, 4H, 2 CH_2). ^{13}C NMR (75.4 MHz, $CDCl_3$, δ ppm, mixture of rotamers) 173.1, 157.7, 150.3, 150.3145.5, 142.7, 142.1, 117.1, 115.4, 110.5, 108.4, 108.1, 66.9, 66.8, 55.0, 55.3, 53.6, 53.5, 45.3, 45.1, 44.5, 42.2, 42.0, 41.7, 32.7, 32.4, 28.5, 28.4, 26.1, 26.0, 25.3, 24.4, 23.6, 23.5. ESI-HRMS *m/z* calcd for $C_{25}H_{36}N_7O_3[M+H]^+$, 482.2868; found, 482.2874.

*(*E*)-7-(2-Cyano-3-(pyridin-4-yl)guanidino)*-N-*cyclopentyl*-N-*(furan-2-ylmethyl)heptanamide* (***39a***). Same procedure as described for **38a** starting from **30**. Chromatography column (MeOH:EtOAc:CH_2Cl_2, 0.8:5:1). Yield: 76%, white sticky solid. ^{1}H NMR (300 MHz, $CDCl_3$, δ ppm, mixture of rotamers) 8.50–8.30 (m, 4H, Py), 7.40–7.20 (m, 6H, 4H Py, 2H furan), 6.49 (br s, 2H, N$\underline{H}$-Py), 6.39–6.21 (m, 2H, furan), 6.15–6.03 (m, 2H, furan), 4.82–4.64 (m, 1H, CH cyclopentyl rotamer A), 4.53–4.30 (m, 4H, 2 C$\underline{H}_2$-furan), 4.26–4.08 (m, 1H, CH cyclopentyl rotamer B), 3.52–3.40 (m, 4H, 2 C$\underline{H}_2$–NH), 2.52–2.31 (m, 4H, 2 CH_2–C═O), 1.91–1.21 (m, 32H, 8 CH_2, 8 CH_2 cyclopentyl, 2 N$\underline{H}$–CH_2). ^{13}C NMR (75.4 MHz, $CDCl_3$, δ ppm, mixture of rotamers) 174.3, 173.6, 157.7, 152.1, 151.6, 150.4, 150.2, 145.7, 142.3, 141.4, 117.0, 115.5, 115.3, 110.7, 110.7, 107.2, 77.6, 77.2, 76.7, 58.9, 56.3, 42.2, 41.6, 38.8, 33.4, 33.0, 30.0, 29.8, 29.1, 28.3, 26.1, 26.0, 23.8, 23.3. ESI-HRMS *m/z* calcd for $C_{24}H_{33}N_6O_2$ $[M+H]^+$, 437.2656; found, 437.2660.

*(*E*)*-N-*(4-Chlorobenzyl)-7-(2-cyano-3-(pyridin-4-yl)guanidino)*-N-*(furan-2-ylmethyl)heptanamide* (***39b***). Same procedure as described for **38a** starting from **37b**. Chromatography column (MeOH:EtOAc:CH_2Cl_2, 0.8:5:1). Yield: 64%, white sticky solid. ^{1}H NMR (300 MHz, $CDCl_3$, δ ppm, mixture of rotamers) 8.46–8.30 (m, 4H, Py), 7.42–7.20 (m, 10H, 2H furan, 4H Ph, 4H Py), 7.16–6.99 (m, 4H, Ph), 6.37–6.23 (m, 4H, 2H furan, 2 N$\underline{H}$-Py), 6.21–6.09 (m, 2H, furan), 4.58–4.30 (m, 8H, 2 C$\underline{H}_2$-Ph, 2 C$\underline{H}_2$-furan), 3.49–3.35 (m, 4H, 2 C$\underline{H}_2$–NH), 2.57 (t, J = 6.9 Hz, 2H, CH_2–C═O rotamer A), 2.35 (t, J = 6.9 Hz, 2H, CH_2–C═O rotamer B), 1.77–1.23 (m, 18H, 8 CH_2, 2 N$\underline{H}$–CH_2). ^{13}C NMR (75.4 MHz, $CDCl_3$, δ ppm, mixture of rotamers) 173.6, 157.5, 150.5, 149.9, 149.7, 145.9, 143.0, 142.5, 135.7, 135.0, 133.4, 129.4, 129.3, 128.9, 127.8, 116.9, 115.6, 110.6, 109.1, 108.7, 77.6, 77.2, 76.7, 50.1, 47.9, 43.9, 42.4, 41.8, 32.9, 28.6, 28.5, 28.3, 28.1, 26.1, 24.3. ESI-HRMS *m/z* calcd for $C_{26}H_{30}ClN_6O_2$ $[M+H]^+$, 493.2107; found, 493.2113.

*(*E*)-7-(2-Cyano-3-(pyridin-4-yl)guanidino)*-N-*(furan-2-ylmethyl)*-N-*(4-nitrobenzyl)heptanamide* (***39c***). Same procedure as described for **38a** starting from **37c**. Chromatography column (MeOH:EtOAc:CH_2Cl_2, 0.8:5:1). Yield: 96%, yellow sticky solid. ^{1}H NMR (300 MHz, $CDCl_3$, δ ppm, mixture of rotamers) 8.44–8.33 (m, 4H, Py), 8.24–8.04 (m, 4H, Py), 7.40–7.18 (m, 8H, 2H furan, 4H Ph), 6.41–6.23 (m, 4H, 2H furan, 2 N$\underline{H}$-Py), 6.23–6.11 (m, 2H, furan), 4.75–4.35 (m, 8H, 2 C$\underline{H}_2$-Ph, 2 C$\underline{H}_2$-furan), 3.45–3.31 (m, 4H, 2 C$\underline{H}_2$–NH), 2.69–2.25 (m, 4H, 2 CH_2–C═O), 1.82–1.29 (m, 18H, 8 CH_2, 2 N$\underline{H}$–CH_2). ^{13}C NMR (75.4 MHz, $CDCl_3$, δ ppm, mixture of rotamers) 173.9, 173.7, 157.5, 150.1, 149.9, 149.3,

147.7, 147.4, 146.0, 145.0, 143.1, 142.7, 128.5, 127.1, 124.3, 123.9, 116.9, 116.8, 115.7, 110.7, 109.5, 109.1, 77.6, 77.4, 77.2, 76.7, 50.9, 48.5, 44.7, 42.5, 42.2, 33.0, 28.7, 28.5, 28.2, 26.2, 24.5. ESI-HRMS *m/z* calcd for $C_{26}H_{30}N_7O_4$ $[M+H]^+$, 504.2346; found, 504.2354.

(E)-7-(2-Cyano-3-(pyridin-4-yl)guanidino)-N-*(furan-2-ylmethyl)*-N-*(3-morpholinopropyl)heptanamide* ***(39d)***. Same procedure as described for **38a** starting from **37d**. Chromatography column (MeOH:EtOAc:NH_4OH, 1:10:0.1 → 1:6:0.1). Yield: 61%, white sticky solid. ^{1}H NMR (300 MHz, $CDCl_3$, δ ppm, mixture of rotamers) 8.49–8.34 (m, 4H, Py), 7.42–7.22 (m, 6H, 4H Py, 2H furan), 6.36–6.26 (m, 2H, furan), 6.26–6.12 (m, 4H, furan, 2 NH-Py), 4.53 (s, 2H, CH_2-furan rotamer A), 4.45 (s, 2H, CH_2-furan rotamer B), 3.75–3.58 (m, 8H, 4 CH_2 morpholine), 3.52–3.28 (m, 8H, 4 CH_2), 2.53–2.22 (m, 16H, 4 CH_2 morpholine, 4 CH_2), 1.77–1.52 (m, 12H, 6 CH_2), 1.52–1.22 (m, 10H, 2 NH, 4 CH_2). ^{13}C NMR (75.4 MHz, $CDCl_3$, δ ppm, mixture of rotamers) 173.4, 173.4, 157.6, 151.0, 150.6, 150.5, 150.3, 145.4, 142.8, 142.3, 117.0, 115.6, 115.6, 110.6, 110.6, 108.5, 108.2, 77.6, 77.2, 76.7, 67.0, 66.8, 56.1, 55.5, 53.8, 53.6, 50.8, 45.5, 45.2, 44.5, 42.4, 42.3, 41.9, 32.9, 32.6, 28.5, 28.2, 28.0, 26.0, 25.9, 25.5, 24.4, 24.2, 24.0. ESI-HRMS *m/z* calcd for $C_{26}H_{38}N_7O_3$ $[M+H]^+$, 496.3021; found, 496.3031.

(E)-7-(2-Cyano-3-(pyridin-4-yl)guanidino)-N-(furan-2-ylmethyl)-N-*(3-(pyrrolidin*-1-yl*)propyl)heptanamide* ***(39e)***. Same procedure as described for **38a** starting from **37e**. Chromatography column (MeOH:DCM:NH_4OH, 1:10:0.1 → 1:6:0.1). Yield: 82%, white sticky solid. ^{1}H NMR (300 MHz, $CDCl_3$, δ ppm, mixture of rotamers) 8.36–8.23 (m, 4H, Py), 7.36–7.24 (m, 6H, 4H Py, 2H furan), 6.50 (br s, 2H, 2 NH-Py), 6.32–6.28 (m, 2H, furan), 6.24–6.20 (m, 2H, furan), 4.54–4.33 (m, 4H, 2 CH_2-furan), 3.51–3.28 (m, 8H, 2 CH_2–NH, 2 CH_2–N–C═O), 3.12–2.59 (m, 12H, 2 CH_2–N, 4 CH_2 pyrrolidine), 2.52–2.24 (m, 4H, 2 CH_2–C═O), 2.04–1.89 (m, 6H, 3 CH_2), 1.89–1.70 (m, 6H, 3 CH_2), 1.69–1.47 (m, 8H, 4 CH_2), 1.42–1.20 (m, 8H, 4 CH_2). ^{13}C NMR (75.4 MHz, $CDCl_3$, δ ppm, mixture of rotamers) 174.3, 173.2, 162.7, 157.2, 150.2, 149.7, 145.8, 142.9, 142.1, 116.9, 114.9, 110.6, 108.7, 77.5, 77.0, 76.6, 54.0, 53.8, 53.1, 52.8, 45.1, 43.2, 42.3, 41.8, 32.7, 31.5, 30.1, 29.7, 29.2, 28.8, 28.2, 26.0, 24.9, 24.4, 23.4, 23.2, 22.7, 14.1. ESI-HRMS *m/z* calcd for $C_{26}H_{38}N_7O_2$ $[M+H]^+$, 480.3075; found, 480.3081.

(E)-8-(2-Cyano-3-(pyridin-4-yl)guanidino)-N-*(furan-2-ylmethyl)octanamide* ***(40f)***. Reaction of **34a** (63.6 mg, 0.27 mmol) and **20** (70.0 mg, 0.3 mmol) followed the procedure described for **35a**. Chromatography column (MeOH:EtOAc, 1:10 → 1:5). Yield: 91%, white solid. ^{1}H NMR (300 MHz, CD_3OD, δ ppm) 8.43–8.35 (m, 2H, Py), 7.46–7.39 (m, 1H, furan), 7.39–7.31 (m, 2H, Py), 6.33 (dd, J = 3.1, 1.9 Hz, 1H, furan), 6.28–6.21 (m, 1H, furan), 4.34 (s, 2H, CH_2-furan), 3.38 (t, J = 7.2 Hz, 2H, CH_2–NH–C═N), 2.21 (t, J = 7.4 Hz, 2H, CH_2–C═O), 1.70–1.53 (m, 4H, 2 CH_2), 1.43–1.30 (m, 6H, 3 CH_2). ^{13}C NMR (75.4 MHz, CD_3OD, δ ppm) 176.0 (C═O), 159.2 (C═N), 153.2 (qC, Py), 150.6 (2CH, Py), 148.4 (qC-furan), 143.3 (CH, furan), 117.8 (C≡N), 116.4 (2CH, Py), 111.3 (CH, furan), 108.0 (CH, furan), 43.4 (CH_2–NH–C═N), 37.1 (CH_2-furan), 36.8 (CH_2), 30.2 (CH_2), 30.0 (CH_2), 29.9 (CH_2), 27.6 (CH_2), 26.8 (CH_2). ESI-HRMS *m/z* calcd for $C_{20}H_{27}N_6O_2$ $[M+H]^+$, 383.2186; found, 383.2190.

(E)-N-*(8-(2-Cyano-3-(pyridin-3-yl)guanidino)octyl)-1H-indole-2-carboxamide* ***(41)***. A solution of **21** (48.0 mg, 0.17 mmol), **34b** (44.0 mg, 0.18 mmol) and Et_3N (26.0 μL, 0.18 mmol) in dry CH_2Cl_2:DMF (3:1, 6.6 mL) was stirred at r.t. for 36 h. Then, the solvent was evaporated under reduced pressure and the residue was purified by chromatography column on silica gel (MeOH:EtOAc, 1:40) to yield **41** (15.0 mg, 21%) as a white solid. ^{1}H NMR (300 MHz, CD_3OD, δ ppm) 8.51–8.42 (m, 1H, Py), 8.37–8.29 (m, 1H, 1H, Py), 7.83–7.71 (m, 1H, Py), 7.63–7.53 (m, 1H, indole), 7.45–7.38 (m, 1H Py, 1H indole), 7.24–7.16 (m, 1H, indole), 7.09–7.00 (m, 2H, indole), 3.39 (t, J = 7.1 Hz, 2H, CH_2–NH–C═N), 1.68–1.55 (m, 4H, CH_2–NH, CH_2), 1.44–1.35 (m, 10H, 5 CH_2). ^{13}C NMR (75.4 MHz, CD_3OD, δ ppm) 164.2 (C═O), 160.1 (C═N), 146.8 (CH, Py), 146.1 (CH, Py), 138.3 (qC, Py), 136.3 (qC, indole), 133.7 (CH, indole), 132.4 (qC, indole), 129.1 (qC, indole), 125.5 (CH, indole), 125.4 (CH, indole), 125.0 (CH, Py), 122.7 (CH, indole), 121.1 (CH, indole), 118.7 (CN), 113.0 (CH, Py), 104.2 (CH, indole), 43.2 (CH_2–NH–C═N), 40.6 (CH_2–C═O), 30.6 (CH_2), 30.4 (CH_2), 30.3 (CH_2), 30.2 (CH_2), 28.0 (CH_2), 27.7 (CH_2). ESI-HRMS *m/z* calcd for $C_{24}H_{30}N_7O$ $[M+H]^+$, 432.2507; found, 432.2506.

(E)-1-(4-(1-(1H-Indole-2-carbonyl)piperidin-4-yl)butyl)-2-cyano-3-(pyridin-3-yl)guanidine ***(42)***. A solution of compound **26** (35.0 mg, 0.1 mmol), **34b** (26 mg, 0.1 mmol) and Et_3N (16 μL, 0.1 mmol) in dry MeCN:DMF, 3:1 (4 mL), was stirred at 85 °C for 16 h. The solvent was evaporated under reduced pressure and the residue was purified by chromatography column on silica gel (MeOH:EtOAc:CH_2Cl_2, 1:5:1) to give **42** (34.0 mg, 72%) as a white solid. ^{1}H NMR (300 MHz, Acetone-d_6, δ ppm) 10.62 (s, 1H, NH, indole), 8.68–8.52 (m, 1H, Py), 8.47–8.27 (m, 2H, NH-Py, 1H Py), 7.90–7.73 (m, 1H, Py), 7.69–7.57 (m, 1H, indole), 7.57–7.45 (m, 1H, indole), 7.45–7.31 (m, 1H, Py), 7.31–7.13 (m, 1H, indole), 7.13–6.98 (m, 1H, indole), 6.84–6.76 (m, 1H, indole), 6.77–6.63 (m, 1H, NH–CH_2), 4.70–4.52 (m, 2H, piperidine), 3.49–3.32 (m, 2H, CH_2–NH), 3.01 (br s, 2H, piperidine), 1.93–1.75 (m, 2H, piperidine), 1.72–1.54 (m, 3H, 1H piperidine, CH_2), 1.51–1.08 (m, 6H, 2H piperidine, 2 CH_2). ^{13}C NMR (75.4 MHz, Acetone-d_6, δ ppm) 161.8, 160.1, 146.8, 146.1, 138.3, 136.0, 132.4, 127.5, 123.2, 121.4, 119.8, 118.7, 111.8, 111.7, 103.8, 103.7, 43.3, 41.7, 35.9, 32.4, 29.7, 23.4. ESI-HRMS *m/z* calcd for $C_{25}H_{30}N_7O$ $[M+H]^+$, 444.2501; found, 444.2506.

(E)-1-(6-Azidohexyl)-2-cyano-3-(pyridin-4-yl)guanidine ***(43)***. Reaction of **34a** (762 mg, 3.20 mmol) and 6-azidohexan-1-amine [38] (500 mg, 3.52 mmol) as indicated for **35a**. Chromatography column (MeOH:CH_2Cl_2, 1:8). Yield: 79%, white solid. ^{1}H NMR (300 MHz, $CDCl_3$, δ ppm) 8.48–8.29 (m, 2H, Py), 7.25–7.15 (m, 2H, Py), 6.24–6.04 (m, 1H, NH-Py), 3.37 (q, J = 6.8 Hz, 2H, CH_2–NH), 3.25 (t, J = 6.7 Hz, 2H, CH_2–N_3), 1.69–1.49 (m, 4H, 2 CH_2), 1.49–1.29 (m, 4H, 2 CH_2). ^{13}C NMR (75.4 MHz, $CDCl_3$, δ ppm) 157.7 (C═N), 150.3 (2 CH, Py), 145.6 (Cq, Py), 117.1 (CN), 115.9 (2 CH, Py), 51.4 (CH_2–N_3), 42.6 (CH_2–NH), 29.2 (CH_2), 28.8 (CH_2), 26.4 (CH_2), 26.4 (CH_2). ESI-HRMS *m/z* calcd for $C_{13}H_{19}N_8$ $[M+H]^+$, 287.1729; found, 287.1727.

N-*(Furan-2-ylmethyl)*-N-*(3-morpholinopropyl)prop-2-yn-1-amine* ***(44)***. To a mixture of propargyl bromide (75 μL, 0.84 mmol) and **29d** (377 mg, 1.68 mmol) in dry DMF (6 mL), anh. K_2CO_3 (349 mg, 2.52 mmol) was added, and the reaction mixture was stirred at r.t. for 24 h. The reaction mixture was quenched with ice cold water and dried in vacuo. The residue was dissolved in EtOAc and washed with water (3x). The combined organic layers were dried over Na_2SO_4, the solvent was evaporated, and the crude product was purified by flash chromatography on silica gel (MeOH:EtOAc, 1:20 → 1:10) to yield **44** (140 mg, 64%) as a colourless oil. ^{1}H NMR (300 MHz, $CDCl_3$, δ ppm) 7.36 (dd, J = 1.9, 0.9 Hz, 1H, furan), 6.30 (dd, J = 3.2, 1.9 Hz, 1H, furan), 6.22 (d, J = 3.1 Hz, 1H, furan), 3.76–3.62 (m, 6H, 2 CH_2–O morpholine, CH_2-furan), 3.36 (d, J = 2.4 Hz, 2H, CH_2–C≡CH), 2.58 (t, J = 7.5 Hz, 2H, CH_2), 2.48–2.30 (m, 6H, 2 CH_2 morpholine, CH_2), 2.21 (t, J = 2.4 Hz, 1H, CH≡C), 1.69 (quint, J = 7.4 Hz, 2H, CH_2). ^{13}C NMR (75.4 MHz, $CDCl_3$, δ ppm) 152.1 (qC, furan), 142.3 (CH, Furan), 110.2 (CH, Furan), 108.9 (CH, Furan), 78.4 (C≡CH), 73.3 (CH), 67.1 (2 CH_2–O), 56.9 (CH_2), 53.8 (2 CH_2 morpholine), 51.2 (CH_2), 50.2 (CH_2-furan), 41.9 (CH_2–C≡CH), 24.7 (CH_2). ESI-HRMS *m/z* calcd for $C_{15}H_{23}N_2O_2$ $[M+H]^+$, 263.1753; found, 263.1754.

N-*(Furan-2-ylmethyl)*-N-*(prop-2-yn-1-yl)cyclopentanamine* ***(45)***. Reaction of propargyl bromide (0.55 mL, 5.05 mmol) and **29a** (1.67 g, 10.1 mmol) was performed as indicated for **44**. Chromatography column (Et_2O:Cyclohexane, 1:9). Yield: 99%, yellow oil. ^{1}H NMR (300 MHz, $CDCl_3$, δ ppm) δ 7.41–7.32 (m, 1H, furan), 6.33–6.28 (m, 1H, furan), 6.27–6.22 (m, 1H, furan), 3.76 (s, 2H, CH_2-furan), 3.37 (d, J = 2.4 Hz, 2H, CH_2–C≡CH), 3.01–2.87 (m, 1H, CH), 2.24–2.17 (m, 1H, CH≡C), 2.04–1.87 (m, 2H, CH_2), 1.82–1.67 (m, 2H, CH_2), 1.67–1.39 (m, 4H, 2 CH_2). ^{13}C NMR (75.4 MHz, $CDCl_3$, δ ppm) 152.1 (qC, furan), 142.3 (CH, Furan), 110.2 (CH, Furan), 109.0 (CH, Furan), 78.7 (C≡CH), 73.2 (CH≡C), 63.3 (CH, cyclopentyl), 48.5 (CH_2-furan), 40.7 (CH_2–C≡CH), 31.5 (2 CH_2), 24.1 (2 CH_2). ESI-HRMS *m/z* calcd for $C_{13}H_{18}NO$ $[M+H]^+$,

204.1380; found, 204.1383.

(E)-*2-Cyano-1-(6-(4-(((furan-2-ylmethyl)(3-morpholinopropyl)amino) methyl)-1H-1,2,3-triazol-1-yl)hexyl)-3-(pyridin-4-yl)guanidine* ***(46)***. To a solution of **43** (48.0 mg, 0.17 mmol) in toluene:DMF (8:1, 4.5 mL), **44** (97.0 mg, 0.37 mmol), DIPEA (0.14 mL, 0.81 mmol) and CuI (6.0 mg, 34 μmol) were added, and the solution was stirred at 60 °C for 24 h. After evaporation, the resulting residue was dissolved in EtOAc and washed with a sat. aq. soln. of $NaHCO_3$. The aq. phase was extracted with EtOAc (x2), and the organic phases were collected, dried over Na_2SO_4, filtered, and evaporated. The resulting residue was purified by chromatography column on silica gel (NH_4OH:MeOH:EtOAc, 0.1:1:9) to yield **46** (54.0 mg, 60%) as a white solid. ^{1}H NMR (300 MHz, $CDCl_3$, δ ppm) 8.49–8.30 (m, 2H, Py), 7.48 (s, 1H, triazole), 7.34 (d, J = 1.9 Hz, 1H, furan), 7.30–7.20 (m, 2H, Py), 6.37–6.23 (m, 2H, furan, NH–CH_2), 6.19 (d, J = 3.2 Hz, 1H, furan), 4.32 (t, J = 6.9 Hz, 2H, CH_2-triazole), 3.81–3.54 (m, 8H, CH_2-furan, N–CH_2-triazole, 2 CH_2–O morpholine), 3.38 (q, J = 6.5 Hz, 2H, CH_2–NH), 2.56–2.24 (m, 8H, 2 CH_2 morpholine, 2 CH_2), 1.95–1.81 (m, 2H, CH_2), 1.80–1.64 (m, 2H, CH_2), 1.64–1.50 (m, 2H, CH_2), 1.46–1.20 (m, 4H, 2 CH_2). ^{13}C NMR (75.4 MHz, $CDCl_3$, δ ppm) 157.5 (C═N), 152.1 (qC, furan), 150.6 (2CH, Py), 145.5 (qC, Py), 142.1 (CH, furan), 122.9 (CH, triazole), 116.9 (qC, triazole), 115.6 (2CH, Py), 110.3 (CH, furan), 109.0 (CH, furan), 66.9 (2 CH_2–O morpholine), 56.9 (CH_2), 53.8 (2 CH_2 morpholine), 51.5 (CH_2), 50.1 (CH_2-triazole), 49.9 (N–CH_2-triazole), 48.8 (CH_2-furan), 42.2 (CH_2–NH), 29.9 (CH_2), 29.0 (CH_2), 25.8 (CH_2), 25.7 (CH_2), 24.2 (CH_2). ESI-HRMS *m/z* calcd for $C_{28}H_{41}N_{10}O_2$ $[M+H]^+$, 549.3405; found, 549.3408.

(E)-*2-Cyano-1-(6-(4-((cyclopentyl(furan-2-ylmethyl)amino)methyl)-1H-1,2,3-triazol-1-yl)hexyl)-3-(pyridin-4-yl)guanidine* ***(47)***. Compounds **43** (118.0 mg, 0.41 mmol) and **45** (134 mg, 0.66 mmol) were suspended in a mixture of H_2O/t-butanol (1:1) (4 mL). Sodium ascorbate (16.3 mg, 82.4 μmol) and $CuSO_4{\cdot}5H_2O$ (2.1 mg, 8.2 μmol) were dissolved in H_2O and added to the mixture. The resulting solution was stirred at r.t. for 16 h. The solvent was evaporated, and the residue was purified by flash chromatography on silica gel (NH_4OH:MeOH:EtOAc, 0.1:1:9 → 0.1:1:5) to yield **47** (175.0 mg, 87%) as a white solid. ^{1}H NMR (300 MHz, $CDCl_3$, δ ppm) 8.46–8.34 (m, 2H, Py), 7.49 (s, 1H, triazole), 7.39–7.33 (m, 1H, furan), 7.31–7.23 (m, 2H, Py), 6.37–6.26 (m, 2H, furan, NH–CH_2), 6.22 (d, J = 3.2 Hz, 1H, furan), 4.32 (t, J = 6.9 Hz, 2H, CH_2-triazole), 3.79 (s, 2H, CH_2-furan), 3.66 (s, 2H, N–CH_2-triazole), 3.39 (q, J = 6.7 Hz, 2H, CH_2–NH), 3.02–2.84 (m, 1H, CH cyclopentyl), 1.99–1.79 (m, 4H, 2 CH_2), 1.76–1.39 (m, 8H, 4 CH_2), 1.39–1.22 (m, 4H, 2 CH_2). ^{13}C NMR (75.4 MHz, $CDCl_3$, δ ppm) 157.5 (C═N), 152.2 (qC, furan), 150.6 (2CH, Py), 145.8 (qC, Py), 142.1 (CH, furan), 123.2 (CH, triazole), 117.0 (qC, triazole), 115.5 (2CH, Py), 110.3 (CH, furan), 109.2 (CH, furan), 63.6 (CH, cyclopentyl), 50.0 (CH_2-triazole), 47.8 (N–CH_2-triazole), 46.4 (CH_2-furan), 42.2 (CH_2–NH), 30.6 (2 CH_2), 29.9 (CH_2), 28.9 (CH_2), 25.7 (CH_2), 25.6 (CH_2), 24.3 (2 CH_2). ESI-HRMS *m/z* calcd for $C_{26}H_{36}N_9O$ $[M+H]^+$, 490.3036; found, 490.3037.

N-*(4-((Furan-2-ylmethyl)carbamoyl)phenyl)isoindoline-2-carboxamide* ***(51)***. Compound **50** [39] (45.0 mg, 0.16 mmol), HOBt (32 mg, 0.24 mmol), furfurylamine (19.0 mg, 0.19 mmol) and DIPEA (110 μL, 0.64 mmol) were suspended in DMF (0.5 mL) and EDCI (46.0 mg, 0.24 mmol) was added. The mixture was stirred at r.t. overnight to give a solution that was diluted with 5 mL of ice water. The resulting turbid mixture was stirred at 0 °C for 1 h, then filtered and concentrated to yield **51** (52.0 mg, 90%) as an off-white solid.^{1}H NMR (300 MHz, DMSO-d_6, δ ppm) δ 8.76 (t, J = 5.8 Hz, 1H, NH, amide), 8.58 (s, 1H, NH, urea), 7.81 (d, J = 8.4 Hz, 2H, H–Ar, phenyl), 7.67 (d, J = 8.4 Hz, 2H, H–Ar, phenyl), 7.56 (d, J = 1.8 Hz, 1H, furan), 7.44–7.23 (m, 4H, H–Ar, isoindoline), 6.39 (br t, 1H, furan), 6.26 (br d, 1H, furan), 4.79 (s, 4H, CH_2, isoindoline), 4.45 (d, J = 5.6 Hz, CH_2-furan).^{13}C NMR (75.4 MHz, DMSO-d_6, δ ppm) δ 165.7 (C═O, amide), 153.6 (C═O, urea), 152.7 (qC, furan), 143.3 (C–Ar, isoindoline), 141.9 (CH, furan), 136.7 (qC, Ph), 127.8 (2CH, Ph), 127.3 (Arom. C–H, isoindoline), 127.0 (qC, Ph), 122.7 (2 HC-Ar, isoindoline), 118.2 (2CH, Ph), 110.4 (CH, furan) 106.7 (CH, furan), 51.9 (CH_2, isoindoline), 35.9 (N–CH_2). HRESIMS *m/z* obsd. 384.1313, calc for $C_{21}H_{19}N_3O_3$ $[M+Na]^+$: 384.1324.

N-*(4-(Cyclopentyl(furan-2-ylmethyl)carbamoyl)phenyl)isoindoline-2-carboxamide* ***(52)***. Reaction of **50** and **29a** as indicated for the synthesis of **51**. Yield: 81%, off-white solid. ^{1}H NMR (300 MHz, DMSO-d_6, δ ppm) δ 8.52 (s, 1H, N–H, Urea), 7.65 (d, J = 8.2 Hz, 2H, H–Ar, Phenyl), 7.57 (d, J = 1.9 Hz, 1H, furan), 7.42–7.26 (m, 6H, H–Ar, Ph, isoindoline), 6.40 (t, J = 2.7 Hz, 1H, furan), 6.26 (d, J = 3.2 Hz, 1H, furan), 4.79 (s, 4H, CH_2, Isoindoline), 4.52 (s, 2H, CH_2-furan), 4.21 (br s, 1H, CH, Cyclopentyl), 1.80–1.32 (m, 8H, CH_2, Cyclopentyl). ^{13}C NMR (75.4 MHz, DMSO-d_6, δ ppm) δ 171.4 (C═O, amide), 154.3 (C═O, urea), 152.9 (C–Ar, CH, furan), 142.2 (qC, Ph), 142.0 (CH, furan), 137.2 (C–Ar, isoindoline), 130.6 (qC, Ph), 127.8 (HC-Ar, isoindoline), 127.4 (2CH, Ph), 123.3 (HC-Ar, isoindoline), 119.2 (2CH, Ph), 111.1 (CH, furan), 107.4 (CH, furan), 59.6 (CH, Cyclopentyl), 52.4 (CH_2, Isoindoline), 40.4 (N–CH_2), 29.5 (2C, CH_2, Cyclopentyl), 24.0 (2C, CH_2, Cyclopentyl). HRESIMS *m/z* obsd. 452.1940, calc for $C_{26}H_{27}N_3O_3$ $[M+Na]^+$: 452.1950.

(E)-7-(N′-Cyanoisoindoline-2-carboximidamido)-N-*cyclopentyl*-N-*(furan-2-ylmethyl)heptanamide* ***(53)***. Same procedure as that described for **38a** but starting from **30** (371 mg, 0.95 mmol) and **56** (226.0 mg, 0.86 mmol). Chromatography column (EtOAc:Cyclohexane, 2:1). Yield: 36%, white solid. ^{1}H NMR (300 MHz, $CDCl_3$, δ ppm, mixture of rotamers) 7.42–7.17 (m, 10H, 8H isoindoline, 2H furan), 6.29 (br d, 2H, furan), 6.14 (br s, 2H, furan), 5.36 (br s, 1H, NH–CH_2 rotamer A), 5.25 (br s, 1H, NH–CH_2 rotamer B), 4.90 (s, 8H, 4 CH_2 isoindoline), 4.81–4.61 (m, 1H, CH cyclopentyl rotamer A), 4.48–4.33 (m, 4H, 2 CH_2-furan), 4.27–4.11 (m, 1H, CH cyclopentyl rotamer B), 3.62–3.44 (m, 4H, 2 CH_2–NH), 2.49–2.28 (m, 4H, 2 CH_2–C═O), 1.91–1.28 (m, 32H, 8 CH_2 cyclopentyl, 8 CH_2). ^{13}C NMR (75.4 MHz, $CDCl_3$, δ ppm, mixture of rotamers) 173.8, 173.2, 156.0, 152.7, 152.1, 142.1, 141.1, 135.5, 128.0, 122.7, 118.0, 110.6, 107.3, 107.1, 103.3, 77.6, 77.2, 76.7, 58.8, 56.3, 53.7, 43.0, 42.7, 41.9, 38.5, 33.7, 33.5, 30.1, 29.9, 29.1, 28.7, 28.4, 26.4, 26.0, 25.1, 23.9. ESI-HRMS *m/z* calcd for $C_{27}H_{36}N_5O_2$ $[M+H]^+$, 462.2860; found, 462.2864.

(E)-N-*(4-Chlorobenzyl)-7-(N′-cyanoisoindoline-2-carboximidamido)*-N-*(furan-2-ylmethyl)heptanamide* ***(54)***. Same procedure as described for **53** starting from **37b**. Yield: 42%, white solid. ^{1}H NMR (300 MHz, $CDCl_3$, δ ppm, mixture of rotamers) 7.40–7.02 (m, 18H, 8H Ph, 8H isoindoline, 2H furan), 6.41–6.25 (m, 2H, furan), 6.25–6.11 (m, 2H, furan), 5.17–5.01 (m, 2H, NH–CH_2), 4.89 (s, 8H, 4 CH_2 isoindoline), 4.58–4.29 (m, 8H, 2 CH_2-Ph, 2 CH_2-furan), 3.66–3.44 (m, 4H, CH_2–NH), 2.55 (t, J = 7.3 Hz, 2H, CH_2–C═O rotamer A), 2.35 (t, J = 7.3 Hz, 2H, CH_2–C═O rotamer B), 1.83–1.27 (m, 16H, 8 CH_2). ^{13}C NMR (75.4 MHz, $CDCl_3$, δ ppm, mixture of rotamers) 173.4, 156.0, 150.9, 150.0, 142.9, 142.4, 136.1, 135.4, 135.3, 133.6, 133.3, 129.6, 129.2, 128.9, 128.1, 127.9, 122.7, 117.9, 110.5, 108.9, 108.5, 77.6, 77.2, 76.7, 53.7, 50.1, 47.7, 43.8, 43.1, 41.6, 33.0, 30.0, 28.8, 28.6, 26.4, 26.3, 25.0. ESI-HRMS *m/z* calcd for $C_{29}H_{33}ClN_5O_2$ $[M+H]^+$, 518.2314; found, 518.2317.

(E)-7-(N′-Cyanoisoindoline-2-carboximidamido)-N-*(furan-2-ylmethyl)-N-(3)-morpholinopropyl)heptanamide* ***(55)***. Same procedure as described for **53** starting from **37d**. Chromatography column (NH_4OH:MeOH: EtOAc, 0.1:1:10). Yield: 52%, colourless oil. ^{1}H NMR (300 MHz, $CDCl_3$, δ ppm, mixture of rotamers) 7.42–7.22 (m, 10H, 8H isoindoline, 2H furan), 6.36–6.26 (m, 2H, furan), 6.26–6.15 (m, 2H, furan), 5.15–4.99 (m, 2H, 2 NH–CH_2), 4.90 (s, 8H, isoindoline), 4.56 (s, 2H, CH_2-furan rotamer A), 4.45 (s, 2H, CH_2-furan rotamer B), 3.77–3.64 (m, 8H, 4 CH_2 morpholine), 3.62–3.49 (m, 4H, 2 CH_2–NH), 3.44–3.29 (m, 4H, 2 CH_2), 2.54–2.23 (m, 16H, 4 CH_2 morpholine, 4 CH_2), 1.78–1.53 (m, 8H, 4 CH_2), 1.52–1.30 (m, 8H, 4 CH_2). ^{13}C NMR (75.4 MHz, $CDCl_3$, δ ppm, mixture of rotamers) 173.2, 173.0, 156.0, 151.5, 150.7, 142.7, 142.1, 135.4, 128.1, 122.8, 117.8, 110.6, 108.4, 108.1, 77.6, 77.2, 76.7, 67.1, 67.0, 56.3, 55.6, 53.8, 53.7, 50.9, 45.4, 45.2, 44.5, 43.1, 43.0, 41.6, 33.1, 32.9, 30.0, 29.9, 28.7, 26.3, 26.3, 25.6, 25.1, 25.0, 24.5. ESI-HRMS *m/z* calcd for $C_{29}H_{41}N_6O_3$ $[M+H]^+$, 521.3339; found, 521.3235.

(E)-7-(2-Cyano-3-phenylguanidino)-N-*cyclopentyl*-N-*(furan-2-ylmethyl)heptanamide* ***(57)***. Same procedure as described for **38a**

starting from **30** and **61a**. Chromatography column (EtOAc:Cyclohexane, 1:2 → 1:1). Yield 80%, white solid. ^{1}H NMR (300 MHz, $CDCl_3$, δ ppm, mixture of rotamers) 7.60–7.16 (m, 14H, 10H Ph, 2H furan, 2 NH-Ph), 6.29 (br d, 2H, furan), 6.13 (br s, 2H, furan), 5.02 (s, 2H, 2 NH–CH_2), 4.80–4.60 (m, 1H, CH cyclopentyl rotamer A), 4.38 (br d, 4H, 2 CH_2-furan), 4.28–4.06 (m, 1H, CH cyclopentyl rotamer B), 3.33–3.17 (m, 4H, 2 CH_2–NH), 2.47–2.23 (m, 4H, 2 CH_2–C═O), 1.89–1.15 (m, 32H, 8 CH_2 cyclopentyl, 8 CH_2). ^{13}C NMR (75.4 MHz, $CDCl_3$, δ ppm, mixture of rotamers) 173.7, 173.0, 158.8, 152.7, 152.2, 142.1, 141.0, 135.6, 130.2, 127.4, 125.5, 118.0, 110.6, 107.5, 107.0, 77.6, 77.2, 76.7, 58.7, 56.2, 41.9, 41.8, 38.4, 33.7, 33.5, 30.0, 29.1, 29.0, 28.7, 26.4, 25.0, 23.9. ESI-HRMS *m/z* calcd for $C_{25}H_{34}N_5O_2$ $[M+H]^+$, 436.2707; found, 436.2707.

*(E)-6-(2-Cyano-3-phenylguanidino)-*N*-cyclopentyl-*N*-(furan-2-ylmethyl)hexane-1-sulfonamide (**58**).* Same procedure as that described for **35a** starting from **32** and **61a**. Column chromatography EtOAc: Cyclohexane, 1:1 → 2:1. Yield: 96%, white solid. ^{1}H NMR (300 MHz, $CDCl_3$, δ ppm) 7.52–7.16 (m, 7H, 5H Ph, 1H furan, NH-Py), 6.41–6.21 (m, 2H, furan), 4.89 (t, J = 5.8 Hz, 1H, NH–CH_2), 4.35 (s, 2H, CH_2-furan), 4.13 (quint, J = 8.3 Hz, 1H, CH cyclopentyl), 3.31–3.18 (m, 2H, CH_2–NH), 2.80–2.67 (m, 2H, CH_2SO_2), 1.95–1.41 (m, 12H, 8H cyclopentyl, 2 CH_2), 1.41–1.17 (m, 4H, 2 CH_2). ^{13}C NMR (75.4 MHz, $CDCl_3$, δ ppm) 158.9 (C═N), 151.5 (qC, furan), 142.2 (CH, furan), 135.4 (qC, Ph), 130.3 (2CH, Ph), 127.8 (CH, Ph), 125.8 (2CH, Ph), 118.0 (CN), 110.8 (CH, furan), 109.2 (CH, furan), 59.3 (CH, cyclopentyl), 53.3 (CH_2SO_2), 41.8 (CH_2–NH), 40.0 (CH_2-furan), 30.0 ($2CH_2$, cyclopentyl), 29.1 (CH_2), 27.9 (CH_2), 26.2 (CH_2), 23.6 ($2CH_2$, cyclopentyl), 23.3 (CH_2). ESI-HRMS *m/z* calcd for $C_{24}H_{33}N_5O_3SNa$ $[M+Na]^+$, 494.2196; found, 494.2196.

*Ethyl (E)-4-(2-cyano-3-(6-(*N*-cyclopentyl-*N*-(furan-2-ylmethyl)sulfamoyl)hexyl)guanidino)benzoate (**59**).* Same procedure as described for **58** starting from **61b**. Column chromatography EtOAc:Cyclohexane, 1:2 → 1:1. Yield: 95%, pale-yellow solid. ^{1}H NMR (300 MHz, $CDCl_3$, δ ppm) 8.06 (d, J = 8.6 Hz, 2H, Ph), 7.88 (s, 1H, NH-Ph), 7.38–7.34 (m, 1H, furan), 7.30 (d, J = 8.6 Hz, 2H, Ph), 6.36–6.25 (m, 2H, furan), 5.24 (br s, 1H, NH–CH_2), 4.43–4.30 (m, 4H, CH_2CH_3, CH_2-furan), 4.13 (quint, J = 8.4 Hz, 1H, CH cyclopentyl), 3.30 (q, J = 6.8 Hz, 2H, CH_2–NH), 2.79–2.70 (m, 2H, CH_2SO_2), 1.92–1.45 (m, 12H, 8H cyclopentyl, 2 CH_2), 1.45–1.20 (m, 7H, CH_3CH_2, 2 CH_2). ^{13}C NMR (75.4 MHz, $CDCl_3$, δ ppm) 165.7 (C═O), 158.2 (C═N), 151.4 (qC, furan), 142.2 (CH, furan), 140.2 (qC, Ph) 131.5 (2CH, Ph), 128.5 (qC, Ph), 123.5 (2CH, Ph), 110.8 (CH, furan), 109.2 (CH, furan), 61.4 (CH_2CH_3), 59.3 (CH, cyclopentyl), 53.2 (CH_2SO_2), 42.1 (CH_2–NH), 40.0 (CH_2-furan), 30.0 ($2CH_2$, cyclopentyl), 29.0 (CH_2), 27.8 (CH_2), 26.2 (CH_2), 23.6 ($2CH_2$, cyclopentyl), 23.3 (CH_2), 14.4 (CH_3CH_2). ESI-HRMS *m/z* calcd for $C_{27}H_{37}N_5O_3SNa$ $[M+Na]^+$, 566.2400; found, 566.2408.

*(E)-6-(3-(4-Azidophenyl)-2-cyanoguanidino)-*N*-cyclopentyl-*N*-(furan-2-ylmethyl)hexane-1-sulfonamide (**60**).* Same procedure as described for **58** starting from **61c**. Chromatography column (EtOAc:Cyclohexane, 1:2 → 1:1). Yield: 84%, light-red solid. ^{1}H NMR (300 MHz, $CDCl_3$, δ ppm) 7.64 (s, 1H, NH-Ph), 7.35 (dd, J = 1.9, 0.9 Hz, 1H, furan), 7.23 (d, J = 8.7 Hz, 2H, Ph), 7.06 (d, J = 8.7 Hz, 2H, Ph) 6.40–6.16 (m, 2H, furan), 4.89 (br s, 1H, NH–CH_2), 4.35 (s, 2H, CH_2-furan), 4.13 (quint, J = 8.5 Hz, 1H, CH, cyclopentyl), 3.24 (q, J = 6.8 Hz, 2H, CH_2–NH), 2.80–2.69 (m, 2H, CH_2SO_2), 1.95–1.41 (m, 12H, 8H cyclopentyl, CH_2), 1.41–1.08 (m, 6H, 3 CH_2). ^{13}C NMR (75.4 MHz, $CDCl_3$, δ ppm) 159.0 (C═N), 151.5 (qC, furan), 142.2 (CH, furan), 139.6 (C≡N), 132.1 (qC, Ph), 127.4 (2CH, Ph), 120.7 (2CH, Ph), 118.0 (qC, Ph), 110.8 (CH, furan), 109.2 (CH, furan), 59.3 (CH, cyclopentyl), 53.2 (CH_2SO_2), 41.9 (CH_2–NH), 40.0 (CH_2-furan), 30.0 ($2CH_2$, cyclopentyl), 29.8 (CH_2), 29.1 (CH_2), 27.9 (CH_2), 26.2 (CH_2, cyclopentyl), 23.6 (CH_2, cyclopentyl), 23.3 (CH_2). ESI-HRMS *m/z* calcd for $C_{24}H_{32}N_8O_3SNa$ $[M+Na]^+$, 535.2209; found, 535.2210.

4.2. Biological evaluation

Cell lines and reagents

MiaPaCa-2 and MDA-MB-231 were purchased from ATCC (LGC Standards S.r.l., Milan, Italy) and maintained in RPMI1640 medium supplemented with 10% FBS, penicillin (50U/mL) and streptomycin (50 μg/mL) (Thermofisher, Italy). Five hematological cell lines (ML2 – Acute myeloid leukemia, Jurkat – Acute lymphoblastic leukemia, Namalwa – Burkitt lymphoma, RPMI8226 – Multiple Myeloma and NB4 – acute myeloid leukemia M3) were purchased from DSMZ (German Collection of Microorganisms and Cell Cultures) or ATCC. The cell lines were cultured in RPMI medium (Invitrogen AG, 61870-01) supplemented with 10% heat inactivated fetal calf serum (Amimed, 2-01F30–I) and 1% penicillin/streptomycin at 37 °C (Amimed, 4-01F00–H) in a humidified atmosphere of 95% air and 5% CO_2. FK866 was obtained from the NIMH Chemical Synthesis and Drug Supply Program.

Cell viability assay

2×10^3 MiaPaCa-2 or MDA-MB-231 cells were plated in 96 well plates and let adhere overnight. 24 h later cells were treated with the analogues of FK866. Viability was determined 72 h after. The culture plates were fixed with cold 3% trichloroacetic acid at 4 °C for 30 min, washed with cold water and dried overnight. Finally, the plates were stained with 0.4% sulforodhamine B (SRB) in 1% acetic acid, washed four times with 1% acetic acid to remove unbound dye, dried overnight and then the stain was extracted with 10 mM Tris Base and the absorbance was read at 560 nm.

Measurement of intracellular NAD$^+$ levels

MiaPaCa-2 or MDA-MB-231 cells were plated at a density of 3×10^4 cells/well in 24-well plates. After 24 h, cells were treated (or not) with the different compounds and cultured for further 24 h (in the time course experiments, cells were cultured for further 24 h, 48 h and 72 h). Cells were harvested and lysed in 0.1 ml 0.6 M perchloric acid. Intracellular NAD^+ levels were determined as previously reported [40] and ATP levels were quantified by a commercially available ATP determination kit (Invitrogen, Carlsbad, CA) following the manufacturer's instruction. Luminescence was measured using a FLUOstar OPTIMA (BMG Labtech, Ortenberg, Germany) and ATP concentrations in the samples were calculated from the ATP standard curve.

Immunoblotting

For protein lysate generation from cultured cells, 2.5×10^5 MiaPaCa-2 cells were plated in 100 mm Petri dishes. After 24 h, cells were treated with compound **47** and **35a** for 48 h. Thereafter, cells were washed and protein lysates were generated in the presence of 50–200 μL lysis buffer (25 mM Tris-phosphate, pH 7.8; 2 mM DTT; 2 mM 1,2-diaminocyclohexane-*N,N,N',N'*-tetraacetic acid; 10% glycerol; 1% Triton X-100). Cell lysates were incubated on ice for 15 min with 10 s vortex shaking every 5 min. Finally, lysates were spun at 10.000 g for 2 min at 4 °C. Supernatants were recovered and either used immediately or stored for subsequent use. Proteins (35 μg) were separated by SDS-PAGE, transferred to a PVDF membrane (Immobilon-P, Millipore S.p. A.), and detected with the following antibodies: PARP (Cell Signaling #9542) and Vinculin (Santa Cruz/sc-5573). Band intensities were quantified by Quantity One SW software (Bio-Rad Laboratories, Inc.) using standard enhanced chemiluminescence.

Determination of NAMPT inhibition

NAMPT inhibition was determined as previously reported [41]. Briefly, 10 ng of recombinant human NAMPT protein (#ab198090, Abcam, Cambridge, UK) were incubated in 40 μL reaction buffer (0.4 mM PRPP, 2 mM ATP, 0.02% BSA, 2 mM DTT, 12 mM $MgCl_2$ and 50 mM Tris-HCl) in eppendorf tubes, in the presence or absence of the different compounds. After a 5 min incubation at 37 °C, 9.0 μL of NAM (0.2 μM final concentration) were added and the reaction was stopped after 15 min, by heating samples at 95 °C for 1 min. Samples were then cooled to 0 °C and NMN was detected by adding 20 μL of 20% acetophenone and 20 μL KOH (2 M) into each tube. The mixture was vortexed and kept at 0 °C for 3 min; 90 μL of 88% formic acid were then added and the tubes

were incubated at 37 °C for 10 min. Finally, 100 μL of the mixture was transferred into a flat-bottom 96-well plate and the fluorescence (excitation 382 nm, emission 445 nm) was measured using a CLARIOstar®^{Plus} (BMG Labtech).

Flow cytometry analyses

The cytotoxic and cellular effects of **35a**, **39a** and **47** on malignant cell lines were evaluated using a Beckman Coulter Cytomics FC500 flow cytometer (Beckman Coulter International S.A.). The measured parameters included cell death, MMP assessments and ROS production.

Cell death analysis

To assess cell death, cells were stained with ANNEXIN-V (ANXN, eBioscience, BMS306FI/300) and 7-aminoactinomycin D (7AAD, Immunotech, A07704) as described by the manufacturer and analyzed using flow cytometry. Dead cells were identified as $7AAD^+$ and early apoptotic cells as $ANXN^+$ $7AAD^-$.

Assessment of mitochondrial membrane potential (MMP)

ML2, Jurkat and RPMI8226 cells were incubated with NAMPT inhibitors for up to 96 h. At each time point, cells were stained with Tetramethylrhodamine, methyl ester (TMRM, ThermoFisher Scientific, T668) according to the manufacturer's protocol. TMRM is a cell-permeant dye that accumulates in the active mitochondria, showing red-orange fluorescence, detected by flow cytometer. The amount of the dye is directly proportional to the amount of live cells with active mitochondria. The graphs depict the percentage of cells losing MMP over time.

Detection of cellular and mitochondrial ROS

Intracellular levels of H_2O_2, mitochondrial and cytosolic superoxide anions were determined in NAMPT inhibitor-treated and control hematological cell lines by flow cytometry. The cell permeant specific fluorescent probes were used, i.e. dihydroethidium (DHE, Marker Gene Technologies, M1241), MitoSOX (Molecular Probes, M36008) and 6-carboxy-2′,7′-dichlorodihydrofluorescein diacetate ester (carboxy-H2DCFDA; Molecular Probes, C-400). DHE is oxidized intracellularly to ethidium by superoxide anions giving bright red fluorescence. MitoSOX, is selectively targeted to mitochondria, where it is oxidized by ROS and exhibits red fluorescence. Instead, carboxy-H2DCFDA is hydrolyzed yielding a polar non-fluorescent product (DCFH), which in the presence of hydrogen peroxide is then oxidized to green fluorescent dichlorofluorescein (DCF). Cells were stained separately with 5 μM of TMRM and H2DCFDA dyes and 10 μM of DHE in PBS, incubated in the dark at 37 °C for 15 min. Then, the cell suspension was analyzed using flow cytometry.

Determination of intracellular NAD^+ and ATP contents

Cells (1×10^6/mL) in log growth phase were seeded in 6-well plate in presence or absence of NAMPT inhibitors. At each time point 800 μL of cells was centrifuged at 900 g (2000 rpm) for 5 min and washed with cold PBS. Then, supernatant was discarded and cells were re-suspended in 300 μL of lysis buffer ($NaHCO_3$ 20 mM and NA_2CO_3 100 mM) and kept at −80 °C for at least 4 h before analysis.

Total NAD^+ content was measured in cell lysates using a biochemical assay described previously [42]. Briefly, cell lysates (20 μL) were plated in a 96-well flat bottom plate. A standard curve was generated using a 1:3 serial dilution in lysis buffer of a β-NAD stock solution. Cycling buffer (160 μL) was added into each well and the plate was incubated for 5 min at 37 °C. After, pre-warmed at 37 °C ethanol (20 μL) was added into each well and the plate was incubated for an additional 5 min at 37 °C. The absorbance was measured in a kinetic mode at 570 nm after 5, 10, 15, 20, and 30 min at 37 °C on a spectrophotometer. The amount of NAD+ in each sample was normalized to the protein content for each test sample at each time point.

Total ATP cell content was quantified using the ATP determination Kit (Life Technologies, A22066) according to manufacturer's instructions.

Declaration of competing interest

The authors declare that they have no known competing financial interests or personal relationships that could have appeared to influence the work reported in this paper.

Data availability

Data will be made available on request.

Acknowledgements

This work has received funding from the European Union's Horizon 2020 research and innovation programme under the Marie Sklodowska-Curie grant agreement No671881 (INTEGRATA). This work was also supported by the Ministerio de Ciencia e Innovación (Grant PID2020-116460RB-100 funded by MCIN/AEI/10.13039/501100011033), the Associazione Italiana per la Ricerca sul Cancro (AIRC; IG#22098, to A. Nencioni) and the Italian Ministry of Health (PE-2016-02362694 and PE-2016-02363073). We also thank CITIUS-Universidad de Sevilla for MS and NMR services. The authors acknowledge Carlos G. Newburn for technical assistance.

Appendix A. Supplementary data

Supplementary data to this article can be found online at https://doi.org/10.1016/j.ejmech.2023.115170.

References

[1] L.E. Navas, A. Carnero, NAD^+ metabolism, stemness, the immune response, and cancer, Signal Transduct. Targeted Ther. 6 (2021) 1–20.
[2] a) A. Chiarugi, C. Dölle, R. Felici, M. Ziegler, The NAD metabolome—a key determinant of cancer cell biology, Nat. Rev. Cancer 12 (2012) 741–752;
b) S. Chowdhry, C. Zanca, U. Rajkumar, T. Koga, Y. Diao, R. Raviram, F. Liu, K. Turner, H. Yang, E. Brunk, J. Bi, F. Furnari, V. Bafna, B. Ren, P.S. Mische, NAD metabolic dependency in cancer is shaped by gene amplification and enhancer remodelling, Nature (2019) 570–575.
[3] M.S. Ghanem, F. Monacelli, A. Nencioni, Advances in NAD-lowering agents for cancer treatment, Nutrients 13 (2021) 1665.
[4] Wei, Y.; Xiang, H.; Zhang, W. Review of various NAMPT inhibitors for the treatment of cancer. Front. Pharmacol. 13:970553.
[5] J.A. Khan, X. Tao, L. Tong, Molecular basis for the inhibition of human NMPRTase, a novel target for anticancer agents, Nat. Struct. Mol. Biol. 13 (2006) 582–588.
[6] K. Holen, L.B. Saltz, E. Hollywood, K. Burk, A.R. Hanauske, The pharmacokinetics, toxicities, and biologic effects of FK866, a nicotinamide adenine dinucleotide biosynthesis inhibitor, Invest. N. Drugs 16 (2008) 45–51.
[7] A. von Heideman, A. Berglund, R. Larsson, P. Nygren, Safety and efficacy of NAD depleting cancer drugs: results of a phase I clinical trial of CHS 828 and overview of published data, Cancer Chemother. Pharmacol. 65 (2010) 1165–1172.
[8] T.S. Zabka, J. Singh, P. Dhawan, B.M. Liederer, J. OeH, M.A. Kauss, Y. Xiao, M. Zak, T. Lin, B. McCray, N. La, T. Nguyen, J. Beyer, C. Farman, H. Uppal, P. S. Dragovich, T. O'Brien, D. Sampath, D.L. Misner, Retinal toxicity, in vivo and in vitro, associated with inhibition of nicotinamide phosphoribosyltransferase, Toxicol. Sci. 144 (2015) 163–172 (and references therein).
[9] a) O.A. Aboud, C.-H. Chen, W. Senapedis, E. Baloglu, C. Argueta, R.H. Weiss, Dual and specific inhibition of NAMPT and PAK4 by KPT- 9274 decreases kidney cancer growth, Mol. Cancer Therapeut. 15 (2016) 2119–2129;
b) N. Li, M.A. Lopez, M. Linares, S. Kumar, S. Oliva, J. Martinez-Lopez, L. Xu, Y. Xu, T. Perini, W. Senapedis, E. Baloglu, M.A. Shammas, Z. Hunter, K. C. Anderson, S.P. Treon, N.C. Munshi, M. Fulciniti, Dual PAK4-NAMPT inhibition impacts growth and survival, and increases sensitivity to DNA-damaging agents in waldenstrom macroglobulinemia, Clin. Cancer Res. 25 (2019) 369–377;
c) S.R. Mitchell, K. Larkin, N.R. Grieselhuber, T.-H. Lai, M. Cannon, S. Orwick, P. Sharma, Y. Asemelash, P. Zhang, V.M. Goettl, L. Beaver, A. Mims, V.K. Puduvalli, J.S. Blachly, A. Lehman, B. Harrington, S. Henderson, J.T. Breitbach, K.E. Williams, S. Dong, E. Baloglu, W. Senapedis, K. Kirschner, D. Sampath, R. Lapalombella, J. C. Byrd, Selective targeting of NAMPT by KPT-9274 in acute myeloid leukemia, Blood Adv 3 (2019) 242–255.
[10] G.B. Mpilla, Md H. Uddin, M.N. al Al-Hallak, A. Aboukameel, Y. Li, S.H. Kim, R. Beydoun, G. Dyson, E. Baloghlu, W.T. Senapedis, Y. Landesman, K.-U. Wagner, N.T. Viola, B.F. El-Rayes, P.A. Philip, R.M. Mohammad, A.S. Azmi, Neuroendocrine tumors to everolimus, Mol. Cancer Therapeut. 20 (2021) 1836–1845.
[11] L. Korotchkina, D. Kazyulkin, P.G. Komarov, A. Polinsky, E.L. Andrianova, S. Joshi, M. Gupta, S. Vujcic, E. Kononov, I. Toshkov, Y. Tian, P. Krasnov, M.V. Chernov, J. Veith, M.P. Antoch, S. Middlemiss, K. Somers, R.B. Lock, M.D. Norris, M. J. Henderson, M. Haber, O.B. Chernova, A.V. Gudkov, OT-82, a novel anticancer

drug candidate that targets the strong dependence of hematological malignancies on NAD biosynthesis, Leukemia 34 (2020) 1828–1839.
[12] C. Travelli, S. Aprile, R. Rahimian, A.A. Grolla, F. Rogati, M. Bertolotti, F. Malagnino, R. di Paola, D. Impellizzeri, R. Fusco, V. Mercalli, A. Massarotti, G. Stortini, S. Terrazzino, E. del Grosso, G. Fakhfouri, M.P. Troiani, M.A. Alisi, G. Grosa, G. Sorba, P.L. Canonico, G. Orsomando, S. Cuzzocrea, A.A. Genazzani, U. Galli, G.C. Tron, Identification of novel triazole-based nicotinamide phosphoribosyltransferase (NAMPT) inhibitors endowed with antiproliferative and antiinflammatory activity, J. Med. Chem. 60 (2017) 1768–1792.
[13] M.K. Christensen, K.D. Erichsen, U.H. Olesen, J. Tjørnelund, P. Fristrup, A. Thougaard, S.J. Nielsen, M. Sehested, P.B. Jensen, E. Loza, I. Kalvinsh, A. Garten, W. Kiess, F. Björkling, Nicotinamide phosphoribosyltransferase inhibitors, design, preparation, and structure−activity relationship, J. Med. Chem. 56 (2013) 9071–9088.
[14] X. Zheng, P. Bauer, T. Baumeister, A.J. Buckmelter, M. Caligiuri, K.H. Clodfelter, B. Han, Y.-C. Ho, N. Kley, J. Lin, D.J. Reynolds, G. Sharma, C.C. Smith, Z. Wang, P. S. Dragovich, A. Oh, W. Wang, M. Zak, J. Gunzner-Toste, G. Zhao, P.-W. Yuen, K. W. Bair, Structure-based identification of ureas as novel nicotinamide phosphoribosyltransferase (NAMPT) inhibitors, J. Med. Chem. 56 (2013) 4921–4937.
[15] J. Bai, S.R. Majjigapu, B. Sordat, S. Poty, P. Vogel, P. Elías-Rodriguez, A.J. Moreno-Vargas, A.T. Carmona, I. Caffa, M. Ghaneme, A. Khalifa, I. Robina, C. Gajate, F. Mollinedo, A. Nahimana, M. Duchosal, A. Nencioni, Identification of new FK866 analogues with potent anticancer activity against pancreatic cancer, Eur. J. Med. Chem. 239 (2022), 114504.
[16] G. Zhao, C.F. Green, Y.-H. Hui, L. Prieto, R. Shepard, S. Dong, T. Wang, B. Tan, X. Gong, L. Kays, R.L. Johnson, W. Wu, S. Bhattachar, M. Del Prado, J.R. Gillig, M. C. Fernandez, K.D. Roth, S. Buchanan, M.-S. Kuo, S. Geeganage, T.P. Burkholder, Discovery of a highly selective NAMPT inhibitor that demonstrates robust efficacy and improved retinal toxicity with nicotinic acid coadministration, Mol. Cancer Therapeut. 16 (2017) 2677–2688.
[17] C.J. Higginson, M.R. Eno, S. Khan, M.D. Cameron, M.G. Finn, Albumin-oxanorbornadiene conjugates formed *ex vivo* for the extended circulation of hydrophilic cargo, ACS Chem. Biol. 11 (2016) 2320–2327.
[18] C.A. Sanhueza, M.M. Baksh, B. Thuma, M.D. Roy, S. Dutta, C. Préville, B. A. Chrunyk, K. Beaumont, R. Dullea, M. Ammirati, S. Liu, D. Gebhard, J.E. Finley, C.T. Salatto, A. King-Ahmad, I. Stock, K. Atkinson, B. Reidich, W. Lin, R. Kumar, M. Tu, E. Menhaji-Klotz, D.A. Price, S. Liras, M.G. Finn, V. Mascitti, Efficient liver targeting by polyvalent display of a compact ligand for the asialoglycoprotein receptor, J. Am. Chem. Soc. 139 (2017) 3528–3536.
[19] M. Duchosal, N. Aimable, P. Vogel, I. Robina, F. Mollinedo, A. Nencioni, A."Piperidine Derivatives for Use in the Treatment of Pancreatic Cancer", 2018. WO 2018/024907 A1, International Application nº PCT/EP2017/069870.
[20] R. Ronchetti, G. Moroni, A. Carotti, A. Gioiello, E. Camaion, Recent advances in urea- and thiourea-containing compounds: focus on innovative approaches in medicinal chemistry and organic synthesis, RSC Med. Chem. 12 (2021) 1046–1064.
[21] X. Zheng, P. Bauer, T. Baumeister, A.J. Buckmelter, M. Caligiuri, K.H. Clodfelter, B. Han, Y.-C. Ho, N. Kley, J. Lin, D.J. Reynolds, G. Sharma, C.C. Smith, Z. Wang, P. S. Dragovich, A. Oh, W. Wang, M. Zak, J. Gunzner-Toste, G. Zhao, P. Yuen, K. W. Bair, Structure-based identification of ureas as novel Nicotinamidephosphoribosyltransferase (Nampt) inhibitors, J. Med. Chem. 56 (2013) 4921–4937.
[22] Compound **31** Was Prepared Following an Alternative Procedure by *N*-Chlorosuccinimide-Mediated Oxidation (See Supplementary Material) that Showed to Be More Efficient than the One Previously Described in Reference 13.
[23] J. O'Brien-Brown, A. Jackson, T.A. Reekie, M.L. Barron, E.L. Werry, P. Schiavini, M. McDonnell, L. Munoz, S. Wilkinson, B. Noll, S. Wang, M. Kassiou, Discovery and pharmacological evaluation of a novel series of adamantyl cyanoguanidines as P2X7 receptor antagonists, Eur. J. Med. Chem. 130 (2017) 433–439.
[24] J.A. Khan, X. Tao, L. Tong, Molecular basis for the inhibition of human NMPRTase, a novel target for anticancer agents, Nat. Struct. Mol. Biol. 13 (2006) 582–586, https://doi.org/10.1038/nsmb1105.
[25] J.L. Wilsbacher, M. Cheng, D. Cheng, S.A.J. Trammell, Y. Shi, J. Guo, S.L. Koeniger, P.J. Kovar, Y. He, S. Selvaraju, H.R. Heyman, B.K. Sorensen, R.F. Clark, T. M. Hansen, K.L. Longenecker, D. Raich, A.V. Korepanova, S. Cepa, D.L. Towne, V. C. Abraham, H. Tang, P.L. Richardson, S.M. McLoughlin, I. Badagnani, M.L. Curtin, M.R. Michaelides, D. Maag, F.G. Buchanan, G.G. Chiang, W. Gao, S.H. Rosenberg, C. Brenner, C. Tse, Discovery and characterization of novel nonsubstrate and substrate NAMPT inhibitors, Mol. Cancer Therapeut. 16 (2017) 1236–1245.
[26] A. Oh, Y.-C. Ho, M. Zak, Y. Liu, X. Chen, P.-W. Yuen, X. Zheng, Y. Liu, P. S. Dragovich, W. Wang, Structural and biochemical analyses of the catalysis and potency impact of inhibitor phosphoribosylation by human nicotinamide phosphoribosyltransferase, Chembiochem 15 (2014) 1121–1130.
[27] U. Galli, G. Colombo, C. Travelli, G.C. Tron, A.A. Genazzani, A.A. Grolla, Recent advances in NAMPT inhibitors: a novel immunotherapic strategy, Front. Pharmacol. 11 (2020) 656.
[28] Z. Moore, G. Chakrabarti, X. Luo, A. Ali, Z. Hu, F.J. Fattah, R. Vemireddy, R. J. DeBerardinis, R.A. Brekken, D.A. Boothman, NAMPT inhibition sensitizes pancreatic adenocarcinoma cells to tumor-selective, PAR-independent metabolic catastrophe and cell death induced by β-lapachone, Cell Death Dis. 6 (2015) e1599.
[29] A. Nahimana, A. Attinger, D. Aubry, P. Greaney, C. Ireson, A.V. Thougaard, J. Tjørnelund, K.M. Dawson, M. Dupuis, M.A. Duchosal, The NAD biosynthesis inhibitor APO866 has potent antitumor activity against hematologic malignancies, Blood 113 (2009) 3276–3286.
[30] M. Hasmann, I. Schemainda, FK866, a highly specific noncompetitive inhibitor of nicotinamide phosphoribosyltransferase, represents a novel mechanism for induction of tumor cell apoptosis, Cancer Res. 63 (2003) 7436–7442.
[31] V. Ginet, J. Puyal, C. Rummel, D. Aubry, C. Breton, A.J. Cloux, S.R. Majjigapu, B. Sordat, P. Vogel, S. Bruzzone, A. Nencioni, M.A. Duchosal, A. Nahimana, A critical role of autophagy in antileukemia/lymphoma effects of APO866, an inhibitor of NAD biosynthesis, Autophagy 10 (2014) 603–617.
[32] A.J. Cloux, D. Aubry, M. Heulot, C. Widmann, O. ElMokh, F. Piacente, M. Cea, A. Nencioni, A. Bellotti, K. Bouzourène, M. Pellegrin, L. Mazzolai, M.A. Duchosal, N. Aimable, Reactive oxygen/nitrogen species contribute substantially to the antileukemia effect of APO866, a NAD lowering agent, Oncotarget 10 (2019) 6723–6738.
[33] O. David, W.J.N. Meester, H. Bieräugel, H.E. Schoemaker, H. Hiemstra, J.H. Van Maarseveen, Intramolecular staudinger ligation: a powerful ring-closure method to form medium-sized lactams, Angew. Chem. Int. Ed. 42 (2003) 4373–4375.
[34] P.N.H. Trinh, D.J.W. Chong, K. Leach, S.J. Hill, J.D.A. Tyndall, L.T. May, A. J. Vernall, K.J. Gregory, Development of covalent, clickable probes for adenosine A1 and A3 receptors, J. Med. Chem. 64 (2021) 8161–8178.
[35] M. Giroud, J. Ivkovic, M. Martignoni, M. Fleuti, N. Trapp, Inhibition of the cysteine protease human cathepsin L by triazine nitriles : amide ··· heteroarene p -stacking interactions and chalcogen bonding in the S3 pocket, ChemMedChem 12 (2017) 257–270.
[36] C.M. Jakobsen, S.R. Denmeade, J.T. Isaacs, A. Gady, C.E. Olsen, S.B. Christensen, Design, synthesis, and pharmacological evaluation of thapsigargin analogues for targeting apoptosis to prostatic cancer cells, J. Med. Chem. 44 (2001) 4696–4703.
[37] M.K. Christensen, K.D. Erichsen, U.H. Olesen, J. Tjørnelund, P. Fristrup, A. Thougaard, S.J. Nielsen, M. Sehested, P.B. Jensen, E. Loza, I. Kalvinsh, A. Garten, W. Kiess, F. Bjo, Nicotinamide phosphoribosyltransferase inhibitors, design, preparation, and structure – activity relationship, J. Med. Chem. 56 (2013) 9071–9088.
[38] C. Romuald, E. Busseron, F. Coutrot, Very contracted to extended Co -conformations with or without oscillations in two- and three-station ['2]Daisy chains, J. Org. Chem. 75 (2010) 6516–6531.
[39] M.L. Curtin, H.R. Heyman, R.F. Clark, B.K. Sorensen, G.A. Doherty, T.M. Hansen, R.R. Frey, K.A. Sarris, A.L. Aguirre, A. Shrestha, N. Tu, K. Woller, M.A. Pliushchev, R.F. Sweis, M. Cheng, J.L. Wilsbacher, P.J. Kovar, J. Guo, D. Cheng, K. L. Longenecker, D. Raich, A.V. Korepanova, N.B. Soni, M.A. Algire, P. L. Richardson, V.L. Marin, I. Badagnani, A. Vasudevan, F.G. Buchanan, D. Maag, G. G. Chiang, C. Tse, M.R. Michaelides, SAR and characterization of non-substrate isoindoline urea inhibitors of nicotinamide phosphoribosyltransferase (NAMPT), Bioorg. Med. Chem. Lett. 27 (2017) 3317–3325.
[40] G. Sociali, A. Grozio, I. Caffa, S. Schuster, P. Becherini, P. Damonte, L. Sturla, C. Fresia, M. Passalacqua, F. Mazzola, N. Raffaelli, A. Garten, W. Kiess, M. Cea, A. Nencioni, S. Bruzzone, SIRT6 deacetylase activity regulates NAMPT activity and NAD(P)(H) pools in cancer cells, Faseb. J. 33 (2019) 3704–3717.
[41] R.Y. Zhang, Y. Qin, X.Q. Lv, P. Wang, T.Y. Xu, L. Zhang, C.Y. Miao, A fluorometric assay for high-throughput screening targeting nicotinamide phosphoribosyltransferase, Anal. Biochem. 412 (2011) 18–25.
[42] A. Rongvaux, F. Andris, F. Van Gool, O. Leo, Reconstructing eukaryotic NAD metabolism, Bioessays 25 (2003) 683–690.